8-2017

Petrogenesis of Pleisto-Holocene Basalts and Basaltic Andesites from Newberry Volcano, Oregon

John Mitchell Clay

ABSTRACT

Newberry Volcano (43.7°N, 121.3°W) is a Cascade rear arc volcano in central Oregon that covers nearly 2,000 km^2 and represents a volume of roughly 200 km^3 of mostly mafic magmas. This composite shield dramatically exceeds the volume of all other Cascade volcanoes, except for Medicine Lake Volcano in Northern California. Newberry began forming about 400 ka with the last eruption ending at 1.3 ka (Donnelly-Nolan et al., 2011). Proposed tectonic models that explain the origin of the volcano are as follows: 1. Mantle decompression melting from lithospheric extension (Xue and Allen, 2006); 2. Slab window or tear in the lithosphere (Tian and Zhao, 2012); 3. Subduction-induced counterflow of the Yellowstone plume (Jordan et al., 2004). The research goal of this study is to test these models to better understand the mantle processes and petrogenetic origin of Newberry Volcano by analyzing the mafic lavas from sequential eruptions ranging in age from ~400 ka to 7 ka. Thirty-five (35) samples were collected and whole-rock geochemical data has been obtained by inductively coupled plasma mass spectrometry (ICP-MS) for major and trace elements. Isotopic analyses of eight (8) samples were conducted via TIMS and MC-ICPMS. Petrographic analyses of rock thin sections exhibit olivine and plagioclase phenocrysts throughout the sample majority. Major element classification on a silica-alkali diagram shows that basalts, trachybasalt, basaltic andesites, basaltic trachyandesites and andesite (SiO_2=48.2-57.0%; Na_2O+K_2O=3.2-6.3%) provide evidence for crystal fractionation within the Newberry mafic suite and potentially a positive trend in SiO_2 over time. Enrichments in LREE (La/Yb=3-9), LILE (Sr/La=19-60; Ba/La=13-31) and depletions in HFSE (Ba/Ta=147-1064; La/Ta=11-36) indicate a role for subduction related processes and the possible addition of slab-derived fluids and/or sediments to the mantle source. $^{87}Sr/^{86}Sr$ (0.7031-0.7036), $^{143}Nd/^{144}Nd$ (0.5129-0.5130), $^{206}Pb/^{204}Pb$ (18.82-19.08), $^{207}Pb/^{204}Pb$ (15.56-15.60) and $^{208}Pb/^{204}Pb$ (38.43-38.61) indicate a slightly depleted, E-MORB-like asthenospheric source region beneath Newberry. The data presented report that Newberry basalts and basaltic andesites are chemically similar to calc-alkaline basalts from Medicine Lake Volcano (Donnelly-Nolan et al., 2008) and

other arc basalts from the central Cascade Range (Bacon et al., 1997) and are most likely produced by rear-arc flux melting of the E-MORB-like asthenospheric wedge from dehydration of the subducting Juan de Fuca Plate.

MONTCLAIR STATE UNIVERSITY

Petrogenesis of Pleisto-Holocene basalts and basaltic andesites from Newberry Volcano, Oregon

by

JOHN MITCHELL CLAY

A Master's Thesis Submitted to the Faculty of

Montclair State University

In Partial Fulfillment of the Requirements

For the Degree of

Master of Science

August 2017

School: College of Science and Mathematics

Department: Earth and Environmental Studies

Thesis Committee:

[redacted]

Thesis Sponsor:

Dr. Matthew Gorring

[redacted]

Committee Member:

Dr. Tanya Blacic

[redacted]

Committee Member:

Dr. Stefanie Brachfeld

PETROGENESIS ORIGIN OF PLEISTO-HOLOCENE BASALTS AND BASALTIC ANDESITES FROM NEWBERRY VOLCANO, OREGON

A THESIS

Submitted in partial fulfillment of the requirements

For the degree of Master of Science

by

JOHN MITCHELL CLAY

Montclair State University

Montclair, NJ

2017

ACKNOWLEDGEMENTS

I would first like to thank my thesis advisor Dr. Matthew Gorring of the Department of Earth and Environmental Studies at Montclair State University. With his guidance, persistence and sheer knowledge, I was able to achieve goals that I never thought were possible. As a teacher, Matt was patient and understanding and as an advisor, he was always there for me for academic issues and virtually everything else. My travels with Matt around the western United States were some of the most valuable experiences I have received in my life and I would not trade them for anything. I would also like to thank Dr. Tanya Blacic and Dr. Stefanie Brachfeld for being extremely supportive as committee members and as two people who have taught me an immense amount about geology and so much more. I thank the Margaret and Herman Sokol Foundation for supporting my research through the Summer Graduate Research Fellowship; without such funds, sample collection would have been impossible. I would like to thank Dr. Mark Feigenson and Dr. Linda Godfrey of the Department of Earth and Planetary Sciences at Rutgers University for their countless hours assisting me with the isotope analyses. Thank you to the many students and friends that I spent my time studying, learning and, occasionally, having fun with at my time at Montclair State University. Of those students, I would especially like to thank my two great friends and colleagues, Norjmaa Khosbaatar and Shane Nichols-O'Neill, for being two of the most dependable and intelligent people I have ever befriended. The endless amount of time that the three of us have spent laughing, working hard, listening to music and, of course, rock climbing is an unforgettable memory that I will take with me for the rest of my life. Thank you to Dr. Loretta Dickson, who gave me the strongest foundation in geology that I could ask for and who urged me to continue my studies. I thank Joe Schisselbauer and Eric Zoleski for standing by me for the past ten years and for being true friends. Finally, I express my sincerest gratitude to my family, John and Cheryl Clay, Frank and Jacalyn Sharp and Gretchen Clay, for encouraging me and wholeheartedly supporting everything that I do.

TABLE OF CONTENTS **PAGE**

LIST OF FIGURES

LIST OF TABLES

1. INTRODUCTION

The Cascade Range is a continental arc of stratovolcanoes and other active centers. The volcanism is produced by the subduction of the Juan de Fuca plate underneath the North American plate that causes fluid flux melting of the asthenospheric mantle wedge between plates. The volcanic activity of the Cascades has made the Pacific Northwestern United States a potentially threatening and notoriously active region, with the inclusion of volcanoes like Mount St. Helens, Mount Rainier and Mount Hood. Newberry Volcano is a lesser known volcano, but poses a significant hazard, which last erupted a rhyolite-obsidian flow at 1.3 ka, is located just 25 miles south of the major city of Bend with a population of 200,000 people (Donnelly-Nolan, 2011). Newberry lies at the confluence of several geologic regions with the main arc of the Cascades to the west, the nearby Oregon High Lava Plains to the east and the Basin and Range province to the southeast. The origin of Newberry and its eruptions has been at the forefront of a tectonic controversy for decades. A commonly proposed model for the origin of the volcano involves the mantle decompression melting that typically occurs during the extension of the lithosphere, set in the rear of a continental volcanic arc combined with the extensional rifting due to the basin and range region (Xue and Allen, 2006; Donnelly-Nolan et al., 2008). Another model suggests that the volcano formed simultaneously with a slab window in the lithosphere that was generated during the subduction of the Juan de Fuca plate. Upon the probable asthenospheric upwelling through this tear, stoping mechanics caused blocks of continental crust to assimilate with the upper mantle, thus producing calc-alkaline basalts, high alumina olivine tholeiites (HAOT) and basaltic andesites (Beachly et al., 2012; Tian and Zhao, 2012). Yet another model indicates that volcanism at Newberry is related to the subduction-induced western counterflow of the rising plume head of the Yellowstone hotspot to the east (Jordan et al., 2004). In this model, the relationship between the westward track of the Oregon High Lava Plains (HLP), the Columbia River Basalt Group (CRBG) and the northeastward track of the Yellowstone-Snake River Plain (YSRP) is linked directly to the tectonics of the region. At Newberry, counterflow

suction, coupled with mantle decompression, is thought to have produced large volumes of mafic lavas that erupted to create the volcano (Jordan et al., 2004).

The overall purpose of this paper is to investigate the mantle source region of the mafic eruptions of Newberry Volcano in the High Cascade rear-arc region and its changing aspects over time from 400 ka to the present day. The goal of this study is to understand the tectonic origin of Newberry Volcano by interpreting geochemical, isotopic and age data collected from basaltic lavas from several eruptions. By comparing Newberry with more heavily studied volcanic centers in the Cascade volcanic arc, like Medicine Lake Volcano in California, further evidence may be found for the expansion of Newberry Volcano and its recent mafic to felsic alternating style of eruption (Grove et al., 1997; Donnelly-Nolan et al., 2008). The appropriate tectonic models were tested by collecting samples for whole-rock geochemical analysis of major and trace elements, along with Sr-Nd-Pb isotopes of sequential basaltic eruptions. There are many geophysical studies of Newberry Volcano, including P-wave tomography and waveform modeling, that capture the crustal structure of the volcanic plumbing system (Fig. 1) (Catchings and Mooney, 1988; Beachly et al., 2012). However, there is a lack of whole-rock geochemical and isotopic data for many of the mafic flow units from Newberry. It is difficult to determine a tectonic origin with geophysical and major element data alone; therefore, a more comprehensive geochemical analysis of Newberry volcanics is necessary. The key to understanding the pending threat and eruptive style of Newberry Volcano is to determine its origin, and consequently, it is very important to constrain the petrogenesis of the mafic lavas and their relationship to the Cascadia geology and volcanology.

2. REGIONAL TECTONIC AND GEOLOGIC SETTING

Newberry Volcano (43.7°N, 121.3°W) is in the rear arc setting of the southern Cascade Mountain Range in central Oregon, USA. It lies on the western edge of the Oregon High Lava

Plains (HLP), between the Columbia River Basalt Group (CRBG) large igneous province to the east and the main volcanic arc of the Cascades to the west (Fig. 2). The volcanic center also resides on the extreme northwestern corner of the Basin and Range Province of the western United States. Newberry also lies ~300-400 km west of the edge of the North American craton (i.e., west of the $^{87}Sr/^{86}Sr = 0.706$ line) where the continental crust retains less ^{87}Rb and consists of oceanic terranes accreted during the Mesozoic (Ernst, 1988) (Figs. 2 and 3). Much of the tectonic influence on this arc region is due to the subduction of the Juan de Fuca plate (~17 km/Ma NE) beneath the North American plate (~14-26 km/Ma SSW) (Jordan et al., 2004). The combined subduction of the Juan de Fuca plate and the Gorda and Explorer microplates is a remnant of the relict Farallon plate subduction which began ~150 Ma and resulted in both the Sevier and Laramide orogenies (Liu et al., 2008). The southern Cascades consist of centers such as Lassen Peak, Mount Shasta, Medicine Lake Volcano, Crater Lake (Mount Mazama), Newberry Volcano, Three Sisters volcanic cluster, Mount Jefferson and Mount Hood; all of which have produced volcanic rocks within the last 2 Ma until as recently as 100 years ago with the eruption of Lassen Peak, CA which began in 1917. Amongst these rather violent stratovolcanoes, Newberry Volcano, OR and Medicine Lake Volcano, CA are comparable voluminous composite shields containing roughly 400 km^3 and 600 km^3 of total material, respectively.

There are older units near the volcano, like the Dry River Canyon basalts (Fig. 4a) and it is generally thought that these basaltic flows are pre-Newberry caldera in age (~8 Ma) (McKee et al., 1976; Fiebelkorn et al., 1983; Linneman, 1990; Donnelly-Nolan et al., 2004; Donnelly-Nolan et al., 2011; Jensen, 2015). The modern Newberry volcanic setting (Fig. 4b) began forming between ~700 and 400 ka, with a proto-caldera formation at 300 ka after the eruption of the 350-ka basalt of Crooked River Gorge and before the 90-ka basalt of Lunabess Hill (Figs. 4c, 4d and 4e) (Macleod et al., 1982; Jensen et al., 2009; Jensen, 2015). The most recent caldera was formed at 75 ka in between the eruptions of the 78-ka basalt of Bend and the 75-ka basalt of Lava Top

Butte (Donnelly-Nolan, 2011; Jensen, 2015). Intermittent eruptions and fissure ruptures persisted after the formation of Newberry Caldera, however, all was buried at ~7.7 ka by ash from the nearby catastrophic Mount Mazama caldera collapse event where Crater Lake, OR (Fig. 4f) now resides (Bacon, 1983; Hallett et al., 1997). Relative and ^{14}C age dates place only the ~7 ka Northwest Rift Zone lavas and the 1.3 ka Big Obsidian flow as younger than the ashfall deposits from Mazama (Peterson and Groh, 1969; Chitwood et al., 1977; Robinson and Trimble, 1981). The Northwest Rift Zone lavas are the youngest mafic flows to occur on the flanks of Newberry; they began erupting with the formation of Lava Butte (Figs. 4g and 4h) (1,529 m) and subsequently vented through large fissures just SW of present-day Bend, OR, thus creating the sampled Lava Butte flow, Mokst Butte flow, South Kelsey flow, Forest Road flow and Lava Cast Forest flow (Fig. 4i) (McKay et al., 2009). The Big Obsidian flow (Fig. 4j) is considered to be the last degassed magma brought forth from the central vent of the volcano that erupted as a mixture of rhyolite and obsidian at ~73-74% SiO_2 (MacLeod and Sherrod, 1988).

The 6-8 km wide central vent of the system, aptly named Newberry Caldera, is surrounded by a series of concealed caldera ring faults and filled in by both mafic and felsic lava flows that encase East and Paulina Lakes (MacLeod et al., 1995). The hydrologic system of the caldera is interesting as Paulina Creek is the only outlet flowing west from Paulina Lake; meteoric water is the only inlet and the lakes are not interconnected (Chitwood and Jensen, 2000). An alpine glacier existed inside Newberry Caldera during the last regional glacial advance at ~24 ka, during which time deposits such as glacial erratics, tills, moraines and outwash plains have been found to be evident on the flanks of the volcano (Scott, 1977; Scott and Gardner, 1992; Donnelly-Nolan, 2004; Donnelly-Nolan and Jensen, 2009). The massive 83 ka Paulina Peak rhyolite domes stand at 2,343 m and overlook the entire caldera as well as a majority of the southern Cascades (Donnelly-Nolan et al., 2004; Jensen, 2015).

3. SAMPLE COLLECTION, PREPARATION AND METHODOLOGY

3.1. Sample Naming and Classification

Sample location coordinates and the ages of thirty-five (35) samples collected at Newberry Volcano are reported in Tables 1 and 2 and represented in Fig. 5. Rock samples were collected from five major volcanic units: 350 ka basalt of Crooked River Gorge (CRGB), 90 ka basalt of Lunabess Hill (LHB), 78 ka basalt of Bend (BB), 75 ka basalt of Lava Top Butte (LTBB) and 7 ka basalt of the Northwest Rift Zone (NWRZ, notated as Qyb) (Figs. 6 and 7) (Jensen et al., 2009). Other minor rock units consist of: 7.6 Ma basalt of Dry River Canyon (Tb-DRC), 188 ka basaltic andesite of Pilot Butte (Qba-PB), 600 ka basalt of McKay Butte (Qer), 11.2 ka basalt of East Lake Resort (Qbce), 10 ka basalt of the Crater Wall (Qcw), basalt of Sheep's Rump (Qbcs), basalt of Paulina Lake flow (Qbcp), 39 ka basalt of Klawhop Butte (Qba-KH), basalt of Abbott Butte (Qba-ABB) and basalt of Grade Butte (Qba-GRB). The older volcanic units were dated using the potassium-argon (K-Ar) method, whilst the younger Holocene units were dated using carbon-14 (^{14}C) dating on fallen trees encased in lava flows (Peterson et al., 1969; McKee et al., 1976; Chitwood et al., 1977; Robinson et al., 1981; Fiebelkorn et al., 1983; Donnelly-Nolan et al., 2000; Champion et al., 2004; Donnelly-Nolan et al., 2004; Donnelly-Nolan et al., 2011; Jensen, 2015). Note that the prefixes Tb and Q refer to Tertiary (Neogene) age and Quaternary age rock samples. These rock unit names were assigned by Jensen (2015) and are based upon previous nomenclature in the literature.

3.2. Field Observations and Collection Methods

Sampling was conducted at Newberry Volcano from the days of 25 June 2016 to 02 July 2016. Rock ages and collection locations are listed in Table 2 and field notes are present in this paper in Appendix A. The current available geologic map of Newberry Volcano is 1:62,500; however, the map only includes the Northwest Rift Zone lavas in its frame of reference so a combination of previous studies was required to plan exact collecting locations (Macleod et al., 1995; Jensen et al., 2009). A schematic field map was adapted by hand from the *Roadside Guide*

to the Geology of Newberry National Volcanic Monument, A Field Guide to Newberry Volcano, and a series of thirty (30) topographic maps from the US Geological Survey (USGS) and the US Department of Agriculture (USDA) (Jensen et al., 2009; Jensen, 2015). Thirty-five (35) samples were collected from the aforementioned rock units and other various exposures and flow edges. Field excursions were staged from camp sites at Cinder Hill Campground, Deschutes County, OR and LaPine State Park, LaPine, OR.

Samples were collected from sites in the Deschutes National Forest, the Crooked River National Grassland and the Newberry National Volcanic Monument as permitted by the U.S. Department of the Interior (DOI). Many of the sample sites were located in challenging terrain on unpaved and sometimes un-maintained national forest roads. Much of the collection was done on foot through thick underbrush and forested areas. Blocks of basalt of approximately 125 cm^3 and 1,000 g were collected for thin section preparation. Samples were dislodged using 2 lb and 4 lb sledgehammers and chisel. Nearly 100 g of fresh, unweathered rock chips were also collected from each sample site for geochemical analyses. Rocks with vesicles, caliche and excessive oxidation were avoided. Hand samples exhibit some visible plagioclase feldspar and olivine phenocrysts. The overall sample color shows varying degrees of light to dark gray. The Northwest Rift Zone lavas tended to be a darker color with more vesicles, resembling the classic a'a lava flow type, while the older flows to the north exhibit a lighter gray with more phenocrysts and weathering present.

3.3. Petrographic Preparations

In order to perform a petrographic analysis, rock thin sections were prepared from all thirty-five (35) hand samples. The samples were individually cut into thin slabs and subsequently trimmed into rectangular billets of dimensions 2 cm x 4 cm x 1 cm using a water (H_2O) assisted MK 10-inch BD-2014 diamond blade tile/rock saw. The billets were shipped to Spectrum Petrographics, Inc. in Vancouver, WA for preparation of standard 30 µm thin sections. No cover

slips were applied to the thin sections to anticipate possible analysis using a Hitachi S3400N Scanning Electron Microscope (SEM) accompanied by a Bruker X-Flash energy dispersive x-ray spectrometer (EDS). The thin sections were analyzed on a Zeiss Axioskop petrographic microscope and photomicrographed by an AxioCam digital camera with Axiovision software.

3.4. Geochemical Preparations

3.4.1. Major and Trace Elements

Sample preparation for the analysis of major and trace elements were conducted inside the laboratories of the Center for Environmental and Life Sciences (CELS) within the Department of Earth and Environmental Studies (EAES) at Montclair State University. 50 g of rock chips were weighed from thirty-five (35) samples using a OHAUS balance and gently crushed with a hardened steel mortar and pestle. The resultant grains were sent through a set of U.S.A. Standard Testing Sieves (a No. 4 with 4.75 mm openings and a No. 20 with 0.85 mm openings) and ground to a powder using a Spex CertiPrep 8500-115 V alumina ceramic shatterbox. Whole rock geochemical analysis for major and trace elements was conducted through inductively coupled plasma mass spectrometry (ICP-MS) on a Thermo Fisher Scientific iCap Q quadrapole inductively coupled plasma mass spectrometer with Qtegra software.

Rock powders were prepared for major and trace element analysis for all 35 samples collected. Approximately 0.1000 g of powdered rock sample and 0.4000 g of lithium metaborate ($LiBO_2$) flux agent were weighed, recorded exactly and mixed. Flux fusion occurred in a high temperature Lindberg muffle furnace using graphite (C) crucibles at 1,050 °C for ~30 minutes with a stirring period at the 15-minute mark. The fused molten bead was dissolved in 50 mL of 7% trace metal grade nitric (HNO_3) acid. The HNO_3 was magnetically stirred and the mixture was filtered into a 60 mL Nalgene bottle using Whatman filter paper and a Nalgene funnel. The filtered solution produced was a "master" solution with a dilution factor of ~500x. A 2.5-mL aliquot of the "master" solution was diluted by 50 mL of 2% trace metal grade HNO_3 to produce

a final solution with a dilution factor of 10,000x for ICP-MS analysis. Seven (7) USGS rock standard solutions (DNC-1, BHVO-2, G-2, W-2, BCR-2, AGV-2 and BIR-1) and three (3) blank solutions of pure $LiBO_2$ were also prepared for the purposes of blank correction and sample calibration. These solutions were prepared in the same manner as the samples, with the exception of 5-mL aliquots of "master" solution diluted by 100 mL of 2% trace metal grade HNO_3. A drift solution spiked with known concentrations of several elements was measured every sixth sample to correct for variations in ICP-MS instrument operating conditions during a 3-hour run.

Major and trace element data are presented within this thesis as the average of 3 replicate runs (Table 1) on the ICP-MS. Analytical precision and accuracy of the instrument is demonstrated by a reproducibility experiment, in which one basalt sample (BB-1) was prepared eight (8) separate times and measured as an unknown. One USGS rock standard (BCR-2) was also prepared eight (8) separate times and measured. Analytical results and accuracies are presented in Table 3. ICP-MS instrument precision (%RSD; $\pm 1\sigma$) for major elements is ±3-8% based on the reproducibility of BB-1 and BCR-2. The accuracy is ±2-8% based on the reported USGS values for BCR-2. ICP-MS instrument precision (%RSD; $\pm 1\sigma$) for trace elements is ±5-8% based on the reproducibility of BB-1 and BCR-2, with the exceptions of Nb, Cs, Ta and Pb which are ±10-20%. Trace element accuracy is ±1-4% for most elements based on the reported USGS values for BCR-2, with the exceptions of Ga, Zr and Cs (±10%) and Cr and Pb (±20-50%).

3.4.2. Sr-Nd-Pb Istopes

Sample preparations for the isotopic analyses of key samples, Qyb7-1; Qyb3-1; Qcw-1; Qba-4KH; LTBB-3; BB-1; LHB-1; CRGB-3, were conducted in facilities of the Wright Geological Laboratory within the Department of Earth and Planetary Sciences at Rutgers University. Isotopic geochemical analysis for strontium (Sr) was conducted through VG Sector thermal ionization mass spectrometry (TIMS). Isotopic geochemical analysis for neodymium (Nd) and lead (Pb) was conducted through Neptune Plus high resolution multicollector

inductively coupled plasma mass spectrometry (MC-ICPMS). 50 mg of chips from each sample were processed for the analyses. This amount of material was estimated based on calculations relating to neodymium (Nd) as the limiting factor. According to trace element geochemical analysis, the eight samples ranged from 15-25 ppm Nd and the instrumentation at Rutgers University required at least 200 ng of Nd. This meant that 10 mg of rock chips from each sample were needed to carry out the analysis, however, an additional 40 mg were collected to account for potential loss of material.

Approximately 50 mg of sample was placed in a 15 mL Savillex Teflon beaker. 2 mL of Aristar Ultra BDH 100% hydrofluoric (HF) acid were added in 1 mL aliquots, along with 10 drops (~0.5 mL) of pure 100% HNO_3. HF is a weak acid, therefore HNO_3 is required for complete rock dissolution and ion dissociation. The Savillex beaker was capped and dried on a temperature-controlled hot plate overnight at 135° C. The dry-down process continued for another night at 135° C after 1 mL of pure 100% hydrobromic (HBr) acid was added. 2 mL of H_2O were added to the bromide material and dried at 95° C until a light brown solid remained.

Lead (Pb) separation was conducted using 50 µL AG-X8-200-400 mesh (anion) resin columns. The columns were back-flushed with H_2O and filled with resin. The resin was cleaned with 0.5 mL 0.5 N HNO_3, 15 drops of 6 N hydrochloric (HCl) acid, and 15 drops of H_2O and, subsequently, primed by eluting 0.5 mL 0.5 N HBr. The samples were loaded in columns with a Savillex collection beaker underneath them for collection of rare earth elements (REE) with 0.5 mL 0.5 N HBr. Major elements were eluted by adding 0.2 mL 0.5 N HBr, 1 mL 0.5 N HBr and 0.5 mL 0.5 N HBr. Pb was collected in a Savillex beaker with 1 mL 0.5 N HNO_3 and left in solution for analysis. The resultant REE solution was prepared for further elemental separation.

Strontium (Sr) separation was conducted using 200 mL AG 50WX8 200-400 mesh (cation) resin columns. The columns were back-flushed with 1.5 N HCl and rinsed with 1.5 N HCl to conserve all resin. 1 mL of REE sample solution was loaded in each column and rinsed

twice with 1 mL 1.5 N HCl. REE were eluted by adding 50 mL 1.5 N HCl and 50 mL 2.3 N HCl. Sr was collected in a Savillex collection beaker with 9 mL 7.3 N HCl and the concentrated REE were collected in a large Savillex collection beaker with 14 mL 7.3 N HCl. The Sr solution was placed on a temperature-controlled hot plate and left in solid for analysis. The REE solution was also placed on the same hot plate and dried for neodymium (Nd) separation.

Neodymium (Nd) separation was conducted using 25 mL reverse phase HDEHP on Teflon powder resin columns. Before the loading of REE sample solids, 0.25 mL 0.23 N HCl was added to dried samples. The columns were rinsed twice with 0.25 mL 0.23 N HCl. Any remaining REE were eluted by adding the following: 3.8 mL 0.23 N HCl, 3.6 mL 0.23 N HCl, 3.4 mL 0.23 N HCl, and 3.2 mL 0.23 N HCl. Nd was collected in a Savillex collection beaker with 4.5 mL 0.23 N HCl and left in solution for analysis.

Isotopic data are presented within this thesis (Table 4) were obtained using the TIMS and the MC-ICPMS. Analytical results and accuracies are presented in Table 5. Standard analyses, accepted values and uncertainties are presented in Table 6. TIMS instrument precision ($\pm 2\sigma$) for $^{87}Sr/^{86}Sr$ isotope ratios is ±0.000004. MC-ICPMS instrument precision ($\pm 1\sigma$) is reported as: $^{143}Nd/^{144}Nd$ = ±0.000003, $^{206}Pb/^{204}Pb$ = ±0.00101, $^{207}Pb/^{204}Pb$ = 0.0008 and $^{208}Pb/^{204}Pb$ = 0.0021.

4. ANALYSES OF LAVA FLOWS AT NEWBERRY VOLCANO

4.1. Petrography

The samples collected at Newberry Volcano consist of a series of calc-alkaline basalt and basaltic andesite, with a fine to medium-grained aphanitic and occasionally porphyritic texture. Hand sample and thin section analysis was conducted to determine the sample mineralogy. The samples contain plagioclase feldspar, pyroxene (orthopyroxene and clinopyroxene) and olivine, with accessory Fe-Ti oxides. Plagioclase feldspar and orthopyroxene account for a large majority of the mineralogy of all samples and are present as matrix and phenocrystic phases.

Clinopyroxene is almost exclusively seen as large phenocrysts in some of the older basalt flows. Olivine phenocrysts exist primarily in rock units from 350 to 75 ka with oxidative weathering present. Other volcanic features such as flow alignment of crystals, vesicles, and microscopic pressure ridges were also noted and are presented in Figs. 8 and 9.

Upon inspection of the major element data, it is clear that the plagioclase feldspar in the sample suite is a mixture of albite ($NaAlSi_3O_8$) and anorthite ($CaAl_2Si_2O_8$) and is probably a calcic plagioclase (labradorite or bytownite). The grains are triclinic prisms with lengths varying from several micrometers to 2,000 µm with average length to width ratios of 3:1 to 5:1 (Figs. 10 and 11). The plagioclase form is generally individual euhedral to anhedral tabular or elongate; however, some bladed aggregates exist in the more phenocrystic samples. The crystals are colorless in plain polarized light (PPL) with low relief. In cross polarized light (XPL), they are biaxial (+ or -) with a birefringence (δ) of 0.010-0.013; their interference color is 1st order gray to white. Twinning is very evident and identified to be simple Carlsbad to complex lamellar albite. Cleavage is not apparent in thin section. The plagioclase tends to be the least altered mineral in the plagioclase-pyroxene-olivine complex with occasional relative pitted textures but no oxidation (Deer et al., 1992; Nesse, 2012).

The orthopyroxene is a mixture of enstatite ($MgSiO_3$) and ferrosilite ($FeSiO_3$) and is almost certainly Mg-rich orthopyroxene which is common in mafic rocks. The grains are orthorhombic prisms with lengths varying from 500 µm to 2,000 µm with average length to width ratios of 1:1 to 2:1 (Fig. 12). The crystal form is euhedral to anhedral stubby prismatic. The crystals are colorless to pale orange and green in PPL with moderately high relief. In XPL, they are biaxial (+ or -) with a birefringence (δ) of 0.007-0.020; their interference color is 1st order white to 2nd order blue. Twinning does not occur, however exsolution lamellae is seen in some grains and cleavage is good in two directions intersecting at ~88°. The orthopyroxene can be

quite altered by oxidation as it is often surrounded by orange and red iron staining and can have a heavily broken, hackly texture (Deer et al., 1992; Nesse, 2012).

The observed lower birefringence of clinopyroxene in the slides determines that it is mostly a calcic clinopyroxene, with augite $(Ca,Mg,Fe^{2+},Fe^{3+},Al)_2(Si,Al)_2O_6$) being the most likely candidate in Newberry lavas. The grains are monoclinic prisms with lengths varying from 500 µm to 2,000 µm with average length to width ratios of 1:1 to 3:1 (Fig. 13). The crystal form is generally euhedral to anhedral stubby prismatic, but other massive forms are apparent as well. The crystals are colorless to pale green in PPL with high relief. In XPL, they are biaxial (+) with a birefringence (δ) of 0.018-0.034; their interference color is 2nd order blue to pink. Simple Carlsbad twinning exists along with exsolution lamellae and cleavage is good in two directions intersecting at ~87°. The clinopyroxene is relatively unaltered aside from fractured crystal edges (Deer et al., 1992; Nesse, 2012).

The olivine in the samples is a mixture of forsterite (Mg_2SiO_4) and fayalite (Fe_2SiO_4) and is almost certainly Mg-rich olivine which is common in mafic rocks. The grains are orthorhombic aggregates with lengths varying from 10 µm to 1,000 µm with 1:1 length to width ratios (Figs. 14 and 15). The crystal form is typically anhedral and equant, however some euhedral grains can be seen in older flows. The crystals are colorless to pale yellow in PPL with high relief. In XPL they are biaxial (+ or -) with a birefringence (δ) of 0.035-0.052; their interference color is 2nd order pink to 4th order pink. Twinning and cleavage are not found on any olivine grains, however curving fractures can be seen well in PPL. The olivine is the most weathered of the minerals in Newberry rocks; it is highly fractured and oxidized in all sections that it exists (Deer et al., 1992; Nesse, 2012).

4.2. Whole Rock Geochemical Analyses

4.2.1. Major Element Analysis and Fractional Crystallization

Major element results are reported as un-normalized values in Table 1. All samples are characterized as mafic or intermediate by a Total Alkali Silica diagram (TAS) (Fig. 16), referencing Na_2O+K_2O against SiO_2. The mafic rocks from Newberry Volcano can be classified as basalts (48.2-51.3 wt.% SiO_2 and 3.2-5.4 wt.% Na_2O+K_2O) with one trachybasalt sample (Qcw-1; 51.3 wt.% SiO_2 and 5.5 wt.% $Na_2O + K_2O$). The intermediate rocks collected can be classified as basaltic andesites (52.2-56.4 wt.% SiO_2 and 4.2-5.4 wt.% $Na_2O + K_2O$) and basaltic trachyandesites (51.3-56.8 wt.% SiO_2 and 5.2-6.3 wt.% $Na_2O + K_2O$) with one andesite sample (Qba-3PB; 57.0 wt.% SiO_2 and 5.4 wt.% $Na_2O + K_2O$). The complete suite of mafic to intermediate samples from Newberry show a crude positive trend of increasing SiO_2 (48.2-57.0 wt.%) and Na_2O+K_2O (3.2-6.3 wt.%) through time from 7.6 Ma to 7 ka (Fig. 16).

Broad negative trends on Harker diagrams (oxides vs. SiO_2) of MgO, Fe_2O_3, CaO and TiO_2 as well as positive trends in Na_2O and K_2O vs. SiO_2 are consistent with magma differentiation via crystal fractionation of an assemblage consisting of plagioclase + orthopyroxene + clinopyroxene + olivine ± Fe-Ti oxides (Fig. 17). Based on this data, it is interpreted that secondary processes of fractional crystallization occurred in the magma chamber after the initial ponding of mantle-derived parental basalts beneath Newberry Volcano.

4.2.2. Trace Element Analysis of Mafic Rocks

Trace element analyses of eighteen (18) mafic samples collected at Newberry Volcano are reported in Table 1 and are represented on multi-element diagrams and rare earth element (REE) diagrams normalized by N-MORB and Leedy chondrite, respectively (Figs. 18, 19, 20 and 21). The mafic rocks all have smooth, parallel LREE-enriched and slightly HREE-depleted patterns (La/Yb = 2.9-8.9) consistent with a slightly enriched mantle source region samples (Figs. 18a, 19a, 20a and 21a). Mafic REE patterns also show very slight positive Eu anomalies (Eu/Eu*

= 1.0-1.1) indicating plagioclase feldspar crystallization and accumulation sometimes occurred which corresponds well with the number of phenocrysts seen in the petrographic analyses of these samples (Figs. 18a, 19a, 20a and 21a).

The mafic suite of rocks from Newberry Volcano show an affinity to the incompatible trace element signature expected from calc-alkaline arc basalts produced by subduction processes. This signature is characterized by enrichments in fluid soluble, large ion lithophile elements (LILE - Sr, Ba, K) and light rare earth elements (LREE – La, Ce, Nd), as well as depletions in high field strength elements (HFSE – Nb, Ta, Hf, Ti) that are evident in Figures 18b, 19b, 20b and 21b. The relative high concentrations for Ba, Sr, K and LREE are consistent with the addition of slab-derived fluids and subducted sediments to the mantle source region. Strong depletions in Nb and Ta represent insolubilities in slab-derived fluids coupled with the presence of residual accessory minerals like rutile (TiO_2) and/or Fe-Ti oxides during partial melting of the mantle source.

Mafic samples (Qba-1, -2, -5ABB, -6GRB and -7) that are thought to represent the earliest shield-building stage of Newberry Volcano (700-600 ka) are quite variable geochemically, however, they do conform well to the fields of calc-alkaline basalts from Medicine Lake Volcano and mafic rocks from the Cascade Volcanic arc (Figs. 18a and 18b) (Bacon et al., 1997; Donnelly-Nolan et al., 2008). These samples contain large amounts of Sr and Ba, with Qba-7 being the most striking, thus relating to the subduction influence on the region during the early development of Newberry Volcano. Sample Qba-5ABB, from a dike crosscutting the Abbott Butte cinder pit, shows a stronger relative depletion in incompatible trace elements, particularly U, Th, La and Ce, compared to other older samples.

The early stages (350-90 ka; Fig. 19) of Newberry Volcano are dominated by mafic rocks with the eruption of the Crooked River Gorge basalt and the Lunabess Hill basalt from which samples collected were strictly classified as basalt. Samples CRGB-1, -2 and -3 and LHB-1 and -

2 are generally more depleted than other collected samples, however REE patterns show that heavy rare earth elements (HREE) are more variable and enriched than mafic rocks from the southern Cascade arc and Medicine Lake (Fig. 19a). Sample CRGB-1 and CRGB-3 are notable as the samples with the strongest depletions in such elements as U, Nb and Hf and the "flattest" REE patterns (La/Yb = 2.97 and 2.91, respectively) of the entire Newberry suite. CRGB-3 shows subtle HREE enrichment with some of the highest chondrite normalized values for Er (15.1), Yb (14.5) and Lu (13.9). The Lunabess Hill samples have mid-range REE concentrations, relatively low La/Yb ratios of (3.9-4.0) and show less dramatic enrichments and depletions in trace elements compared to all other samples.

The mid-stage of the volcano (78-39 ka) (Fig. 20) is composed of the Bend basalt unit, from which all samples collected are classified as basalt, and the Lava Top Butte basalt, where three (out of five) samples are basalt. Samples BB-1, -2, -3 and -4 show a subtle difference in trace element composition based on sampling location. BB-1 and -2 were collected to the north within the city of Bend, OR and have slightly more enriched multi-element patterns, higher concentrations of LREE and have steeper REE patterns (La/Yb = 5.7) than BB-3 and -4 (La/Yb = 3.6-3.9) which were taken to the south, nearby the Northwest Rift Zone lavas and Benham Falls (Fig. 5). The multi-element and REE patterns of the LTBB-2, -3 and -5 samples are parallel and very closely packed almost to the point of indiscernibility indicating no significant differences between these samples.

There was only one mafic rock sample recovered from the late stages (11.2-6.8 ka) (Fig. 21; Qcw-1) of Newberry from the basalt of the Crater Wall collected within the caldera. Sample Qcw-1 is a trachybasalt as it is more alkaline than other mafic samples in the geochemical survey. The multi-element pattern indicates that this sample is relatively depleted in Th and U (Fig. 21b) and enriched in MREE and HREE compared to intermediate rocks of a similar age (Fig. 21a).

4.2.2. Trace Element Analysis of Intermediate Rocks

Trace element analyses of seventeen (17) intermediate samples collected at Newberry Volcano are reported in Table 1. All samples are represented on multi-element diagrams and rare earth element (REE) diagrams normalized by N-MORB and Leedy chondrite, respectively (Figs. 18, 19, 20 and 21).

The intermediate suite of rocks from Newberry Volcano show trace element signatures that are similar to that of the mafic rocks, however they are more enriched in incompatible trace element concentrations overall. Chondrite normalized rare earth element diagrams are somewhat steeper, parallel and slightly more LREE-enriched (La/Yb = 4.4-8.6) than the mafic suite (Figs. 18a, 19a, 20a and 21a). They also have very slight negative Eu anomalies (Eu/Eu* = 0.9-1.0) indicating that less plagioclase feldspar accumulation occurred in these samples than the mafic suite (Figs. 18a, 19a, 20a and 21a). Similar to the mafic suite, N-MORB normalized multi-element diagrams of intermediate rocks show enrichments in fluid soluble, large ion lithophile elements (LILE – Sr, Ba, K) and light rare earth elements (LREE – La, Ce, Nd), as well as depletions in high field strength elements (HFSE – Nb, Ta, Hf, Ti) that are evident in Figures 18b, 19b, 20b and 21b. The relative high concentrations for Ba, Sr, K and LREE are consistent with the addition of slab-derived fluids and subducted sediments to the mantle source region. Strong depletions in Nb and Ta represent insolubilities in slab-derived fluids coupled with the presence of residual accessory minerals like rutile (TiO_2) and/or Fe-Ti oxides during partial melting of the mantle source.

Two intermediate samples predate the modern Newberry shield phase (Tb-1DRC, Tb-2DRC; Fig. 18). These samples are 7.6 ± 0.08 Ma basaltic trachyandesites collected from the Dry River Canyon locality to the northeast of Newberry Caldera. They are the most arc-like rocks in the sample suite with enrichments in LREE and LILE concentrations and strong depletions in HFSE (Ba/Ta = 797-1064; La/Ta = 27-36; Sr/La = 44-58). Samples Qer-1 and -2 are basaltic

trachyandesites west of the caldera, near McKay Butte, that represent the earliest shield-building stage of Newberry Volcano (~600 ka; McKee et al., 1976). These samples have similar LILE and LREE enrichments and HFSE depletions as mafic rocks of a similar age, but generally have higher overall concentrations and are more enriched in MREE and HREE (Figs. 18a and b).

The early stages of the volcano (350-90 ka) are dominated by basalts from CRGB and LHB, however, Qba-3PB, is an andesite collected on the flank of Pilot Butte dated at ~188 ka (the only andesite collected from this survey). A comparison of data from Qba-3PB to the Cascade Volcanic arc field shows that it is more enriched in Ba, Th, U and K than most Cascade arc basalts and to the Crooked River Gorge and Lunabess Hill basalts (Fig. 19b). The REE pattern of Qba-3PB is also steeper (La/Yb = 5.7) than the Crooked River Gorge and Lunabess Hill basalts.

Intermediate samples collected from the mid stage of Newberry (78-39 ka) were retrieved from both the west and the east Lava Top Butte flows and from the Klawhop Butte flow (Fig. 20). Samples LTBB-1 and -4 are basaltic andesites with trace elements that differ from each other significantly. LTBB-1 is a slightly oxidized block of a flow from the southeast flank of Bessie Butte, which is a part of the western Lava Top Butte unit. This rock has very drastic HFSE depletions with the lowest absolute concentrations of Nb and Ta in the entire study. Qba-4KH is a basaltic andesite collected from a flow out of Klawhop Butte to the southwest that erupted at 39 ka. The trace element signature of Qba-4KH is strikingly similar to the andesite of Pilot Butte (Qba-3PB) with enrichments of Ba, Th, U and K relative to most Cascade arc basalts and to the Newberry mafic rocks of similar age.

The late forming stage of Newberry Volcano (11.2-6.8 ka) is dominated by intermediate lavas that have similar LILE and LREE enrichments and HFSE depletions as the mafic rocks but have distinctly higher overall concentrations (Figs. 21a and b). Three intra-caldera rocks, samples Qbce-1, Qbcs-1 and Qbcp-1, have the highest concentrations of incompatible trace elements while the Northwest Rift Zone intermediate lavas (Qyb samples) mirror the intra-caldera

rocks but at a slightly lower concentration. The NWRZ lavas fit into the upper limit of the calc-alkaline basaltic field from Medicine Lake Volcano of which many erupted between 7.1-6.8 ka, and thus are well synchronized with the Northwest Rift Zone eruptions (Donnelly-Nolan et al., 2008). This trace and REE comparison is crucial in relating the two volcanic centers as well as others in the Cascade Range.

4.2.3. Sr-Nd-Pb Isotopic Analysis

Isotopic analyses of eight (8) samples collected at Newberry Volcano are reported in Table 3. Samples Qyb7-1, Qyb3-1, Qcw-1, Qba-4KH, LTBB-3, BB-1, LHB-1 and CRGB-3 are represented on isotope differentiation diagrams of $^{143}Nd/^{144}Nd$ against $^{87}Sr/^{86}Sr$ (Fig. 22), $^{207}Pb/^{204}Pb$ against $^{206}Pb/^{204}Pb$ (Fig. 23) and $^{208}Pb/^{204}Pb$ against $^{206}Pb/^{204}Pb$ (Fig. 24). The isotope data support the interpretation that the trace elements provide, which is that Newberry Volcano is related more to subduction processes than to a plume source.

$^{87}Sr/^{86}Sr$ ratios of 0.70309-0.70359 indicate a mantle source that is slightly depleted in ^{87}Rb (Fig. 25). Because of the slight deviation from primordial mantle evolution, it has been interpreted that these Newberry samples are produced by the melting of shallow mantle. $^{143}Nd/^{144}Nd$ ratios of 0.52892-0.513001 also indicated a slightly depleted mantle source (Fig. 26). The relatively high values for Nd ratios show that more ^{144}Nd than ^{147}Sm has been removed, indicating that the samples are derived from a slightly depleted mantle source with a distinct lack of crustal influence. When these two ratios are plotted against one another, the analyzed samples are represented as being isotopically similar to mid-ocean ridge basalts (MORB) (Fig. 22). BB-1 ($^{87}Sr/^{86}Sr$ = 0.70309 and $^{143}Nd/^{144}Nd$ = 0.513001) is an excellent example of one of these MORB-like samples that can provide evidence for the production of Newberry lavas. The Sr-Nd isotope results are comparable to other Cascade arc basalt isotopic data from nearby Mount Adams, Simcoe Mountains, Mount Shasta, Crater Lake, Lassen Peak and Medicine Lake Volcano shown in Fig. 22 (Bacon et al., 1997). Other rocks from island arc settings like Japan and New Zealand

can be considered similar or, at the very least, the more depleted examples of these localities share a likeness to Newberry. The analyses are also akin to some of the available isotope data from the CRBG which include the units: Grande Ronde basalt, Wanapum basalt, Imnaha basalt and Picture Gorge basalt (McDougall, 1976; Carlson et al., 1981; Carlson, 1984; Hooper, 1988; Brandon et al., 1993; Hooper and Hawkesworth, 1993). The Picture Gorge basalts, which erupted simultaneously with the Grande Ronde basalts at ~15 ka, model extremely well with Newberry lavas (Reidel et al., 1989). Picture Gorge seems to have a consistently depleted mantle source that is comparable to basalts analyzed from Newberry Volcano. Fields produced by data collected from Graham, (2009) provide that the source of Newberry Volcano is only slightly more N-MORB-like than HLP lavas, but is vastly different than the continentally influenced Snake River Plain basalt field that is related to the Yellowstone hotspot track (YSRP) which has much higher $^{87}Sr/^{86}Sr$ (0.704-0.708) ratios (Graham et al., 2009).

$^{206}Pb/^{204}Pb$ ratios are 18.820-19.083, $^{207}Pb/^{204}Pb$ ratios are 15.561-15.601 and $^{208}Pb/^{204}Pb$ ratios are 38.426-38.609. The Newberry source plots as slightly more enriched than the northern hemisphere reference line (NHRL), a linear approximation between a depleted Pb mantle reservoir (DM) and a high μ mantle reservoir where $\mu = {}^{238}U/^{204}Pb$ (HIMU) (Hart, 1984; Winter, 2010). The interpretation that these eight Newberry samples are somewhat MORB-like is well corroborated with represented Pb variations that show them residing in the enriched half of the Atlantic and Pacific MORB field (Figs. 23 and 24). The samples also correspond with Cascade Pb data collected by Bacon, (1997) and Mitchell and Asmerom, (2011) with the exception of Qyb3-1 and BB-1, which lie on the ^{206}Pb enriched end of the suite with $^{206}Pb/^{204}Pb$ ratios of 19.022 and 19.083, respectively (Bacon et al., 1997; Graham et al., 2009; Mitchell and Asmerom, 2011). The Newberry suite plots as more Pb enriched than an oceanic volcanic prevalent mantle source (PREMA), but it avoids the indication of crustal components that a completely enriched mantle source (EMI and EMII) would involve. Although the CRBG are not represented on Pb

figures here, preexisting $^{208}Pb/^{204}Pb$ and $^{206}Pb/^{204}Pb$ ratio data derive that Picture Gorge basalts cluster just above the NHRL in a similar fashion to the mixing of both DM and HIMU reservoirs as the Newberry mantle source (Fig. 24) (McDougall, 1976; Carlson et al., 1981; Carlson, 1984; Staudigel et al., 1984; Hamelin et al., 1986; Zindler and Hart, 1986; Hooper, 1988; Wilson, 1989; Brandon et al., 1993; Hooper and Hawkesworth, 1993; Winter, 2010).

5. DISCUSSION OF PETROGENESIS

5.1. Origin of Magmas

Newberry Volcano, being a producer of vast volumes of compositionally variable lavas, has magmatic origins that have been interpreted several times using different tectonic models. The analytical outcomes provided in this thesis suggest a depleted upper mantle as a possible source of magma generation by recognizing evident mantle source characteristics shown in newly acquired geochemical data.

The suggested counterflow suction and mantle plume impingement model has been supported primarily by age progression data and the moderate geochemical resemblance to the CRBG (Jordan et al., 2004; Baksi, 2013; Barry, 2013; Camp et al., 2013). The Newberry-HLP volcanic track, the CRBG magma timing and YSRP track do show relative age progressions, however, it is not made clear that there is a direct geochemical symbiosis between the three regions. The proposition states that the rising hot mantle of the Yellowstone plume, which created the YSRP silicic lavas, flattened upon ascendance to the lithosphere, and was drawn westward by the subduction of the Juan de Fuca plate (Pierce and Morgan, 1992; Pierce et al., 2002; Shervais et al, 2008; Coble and Mahood, 2012; Camp, 2013). While traveling west, the plume head is considered to have generated pulses of magmatic activity through extensional fractures and faults that resulted in the CRBG and HLP lavas. The timing and age progression of the HLP makes this model plausible since the rhyo-dacites clearly show a trend of age decreasing

from east to west, but the bimodal volcanism presents an issue here since there is very little to no age progression in any of the HLP mafic flows (Hooper et al., 2007; Leeman et al., 2008; Ford et al., 2013). The movement of the North American plate is also problematic as it does not correspond with the age progression of silicic rocks of the HLP, thus defying the ability to call upon simple motion of the tectonic plate over the plume head. Trace element data from Newberry basalts and basaltic andesites presented in this paper indicate a consistent arc-like trend of HFSE depletion and LILE enrichment as well as LREE enrichment and slight HREE depletion, however Sr, Nd and Pb isotopic results show a fairly depleted, E-MORB-like mantle source which is significantly different from the isotopic composition of plume-related basalts of most of the CRBG (particularly the Grande Ronde and Wanapum units) and the SRP basalts (Fig. 22). These geochemical differences between Newberry and the CRBG and SRP mafic lavas from the Yellowstone plume raise uncertainty regarding the plume entrainment model.

A slab-window or tear in the lithosphere is a solution to magma generation that has been utilized in regions of South America, especially at the Chile Triple Junction (CTJ) where the Nazca, South American and Antarctic plates interact with one another (Gorring and Kay, 2001; Gorring et al., 2003; DaSilva, 2009). This model can be an explanation at Newberry as well because of the many microplates and tectonic stresses at odds. Although there was no geophysical evidence collected by this study, the subsurface has been explored by several seismic tomography surveys in past research (Bisdorf, 1983; Fitterman, 1983; Fitterman et al., 1985; Dawson and Stauber, 1986; Fitterman et al., 1988; Catchings and Mooney, 1988; Beachly, 2011; Beachly et al., 2012). Low velocity anomalies and absent deep earthquake data found at Newberry may depict rising hot mantle through a lithospheric tear underneath the Cascades (Tian and Zhao, 2012). Tian and Zhao, (2012) suggest that consistent and continuous heat from the deep mantle has caused the Juan de Fuca plate to be thermally weakened east of the main Cascade arc. This would imply that magma generation is occurring at depth in the mantle and

arriving to the surface relatively unopposed by continental crust. Sr and Nd isotopic data from this survey support the slab-window model by placing Newberry samples at or near MORB depletion levels, however Pb data are indicative of possible E-MORB. Trace element data generally support a lithospheric tear, but they do not show any MORB-like or HAOT trends which might be expected instead. If this model proves to be accurate, the subducting tear in the Juan de Fuca plate should have produced a crude eastward age progression of mafic lavas, which has yet to be documented.

The trends in multi-element diagrams and REE plots presented in this paper are most like those of the classic arc signature, with high concentrations of Ba, Th, K and Sr and low concentrations of Nb, Ta and Ti. This, along with the ability to categorize Newberry isotopic results with other Cascade arc basalts, lends itself to a preferred model that involves subduction-related flux melting of the asthenospheric wedge coupled with decompression melting produced by extensional lithosphere-controlled processes. The extension in the rear arc is caused primarily by subduction with an added component of Basin & Range extension to the southeast. The subduction process can explain the HFSE and LILE anomalies by the addition of slab-derived fluids to the mantle source (Long et al., 2012). The LREE enrichment and lack of severe HREE depletion shows that partial melting occurred without the presence of garnet at relatively shallow depths which is corroborated by E-MORB-like isotopic data.

5.2. Implications for Petrogenetic Timeline

The prevalent rear arc subduction argument can be made for primary magma generation and fractional crystallization is the secondary process considered. Since shallow melting through thinning lithosphere occurred, there is already limited continental crust influence so assimilation of any large amount of North American craton would be improbable for this scenario. Major element analysis does however provide evidence for crystal fractionation of Newberry's magma chamber by a trend of increasing SiO_2 and $Na_2O + K_2O$ through time. The silica trend is also

bolstered by a series of silicic eruptions at Newberry, which ended with the Big Obsidian flow of 1.3 ka; the volcanic plumbing system has clearly changed from mafic to intermediate. By viewing trace element data, it can be determined that subtly increasing concentrations overall also support fractionation over time. Further major element modeling is necessary in order to document the details of secondary petrogenetic processes at Newberry Volcano.

6. CONCLUSIONS

The mapping, sample collection, preparation and geochemical analyses of the mafic flows of Newberry Volcano during this research allow for a possible petrogenetic origin of magma generation to be made. Newberry Volcano, set in the rear arc region of the central High Cascade Range, is a true rear arc volcano. The magma chamber contains massive volumes of material that has erupted several times over with the capability to produce compositionally variable lavas that make up the modern Newberry shield, which has existed for at least 400 ka. Mafic samples collected on this shield and inside the caldera have been geochemically analyzed and were found to be basalts, trachybasalts, basaltic andesites, basaltic trachyandesites and andesites. Several published K-Ar and ^{14}C ages place major voluminous eruptions at 350 ka (CRGB), 90 ka (LHB), 78 ka (BB), 75 ka (LTBB) and 7 ka (NWRZ, Qyb) that have all been characterized by this research. A thirty-five (35) sample suite of major and trace element data are provided as well as a suite of eight (8) new isotopic analyses. These data indicate that Newberry Volcano has a petrogenetic origin linked to the rear arc extension of the lithosphere caused by the subduction of the Juan de Fuca plate underneath the North American plate. Magma generation at this location is produced by flux melting of the asthenospheric wedge coupled with decompression melting produced by lithospheric extension and the of the addition of subducted slab-derived fluids.

A variety of lavas ranging from mafic (48.2-51.3 wt.% SiO_2) to intermediate (51.3-57.0 wt.% SiO_2) were collected in order to summarize the chemical signature of each flow appropriately. Lava flows became increasingly more silicic through time until the last large eruption of the Northwest Rift Zone at 7 ka, of which all lavas were basaltic andesites. The trend of increasing silica content shows quite clearly the impact of crystal fractionation on the Newberry magma system. All samples have modest arc signatures with enrichments in LREE (La/Yb = 3-9), LILE (Sr/La = 19-60; Ba/La = 13-31) and depletions in HFSE (Ba/Ta = 147-1064; La/Ta = 11-36) that indicate an important role for subduction related processes and the possible addition of slab-derived fluids and/or sediments to the mantle source. $^{87}Sr/^{86}Sr$ ratios (0.70309-0.70359) and $^{143}Nd/^{144}Nd$ ratios (0.52892-0.513001) show that there is a slightly depleted, E-MORB-like mantle source that is similar to most mafic rocks form the Oregon HLP. Pb isotope data ($^{206}Pb/^{204}Pb$ =18.820-19.083, $^{207}Pb/^{204}Pb$ = 15.561-15.601 and $^{208}Pb/^{204}Pb$ = 38.426-38.609) further affirms that the mantle region is like that of an enriched MORB at an average of DM and HIMU mantle reservoirs comparative to the rest of the Cascade arc, the HLP and some portions of the CRBG (e. g., Picture Gorge). The data presented indicate that Newberry basalts and basaltic andesites are chemically similar to calc-alkaline basalts from the central Cascade Range (Bacon et al., 1997) and are most likely produced by rear-arc flux melting of the E-MORB-like asthenospheric wedge from dehydration of the subducting Juan de Fuca plate. The geochemical evidence represented does not support the need for the involvement of a mantle plume or a slab window/tear at Newberry Volcano. The importance of this study is that geochemical/geophysical analyses and monitoring continue to occur at Newberry Volcano to understand its tectonic origin, bimodal styles of eruption and potential threat posed to the Pacific Northwestern United States.

7. REFERENCE CITED

Arculus, R. J. and Powell, R. (1986). Source component mixing in the regions of arc magma generation. *Journal of Geophysical Research: Solid Earth*, *91*(B6), 5913-5926.

Bacon, C. R. (1983). Eruptive history of Mount Mazama and Crater Lake caldera, Cascade Range, USA. *Journal of Volcanology and Geothermal Research*, *18*(1-4), 57-115.

Bacon, C.R., Bruggman, P.E., Christiansen, R.L., Clynne, M.A., Donnelly-Nolan, J.M. and Hildreth, W. (1997). Primitive Magmas at Five Cascade Volcanic Fields: Melts from Hot, Heterogenous Sub-Arc Mantle. *The Canadian Mineralogist, Vol. 35, pp. 397-423.*

Baksi, A.K. (2013). Timing and duration of volcanism in the Columbia River Basalt Group: a review of existing radiometric data and new constraints on the age of the Steens through Wanapum Basalt extrusion. *Geol. Soc. Am. Spec. Pap., 497*(3), 67–85. Retrieved from http://dx.doi.org/10.1130/2013.2497(03).

Barry, T.L., Kelley, S.P., Reidel, S.P., Camp, V.E., Self, S., Jarboe, N.A., Duncan, R.A. and Renne, P. R. (2013). Eruption chronology of the Columbia River Basalt Group. *Geol. Soc. Am. Spec. Pap., 297*, 45–66. Retrieved from http://dx.doi.org/10.1130/2013.2497(02).

Beachly, M. W. (2011). The upper crustal P-wave velocity structure of Newberry volcano, Central Oregon. *A Master's Thesis.* University of Oregon.

Beachly, M. W., Hooft, E. E. E., Toomey, D. R. and Waite, G. P. (2012). Upper crustal structure of Newberry Volcano from P-wave tomography and finite difference waveform modeling, *J. Geophys. Res., 117, B10311*., 17 pp. doi:10.1029/2012JB009458.

Bisdorf, R.J. (1983). Schlumberger Soundings near Newberry Caldera, Oregon. *U.S. Geol. Surv. Open File Rep., 83-825.*

Brandon, A. D., Hooper, P. R., Goles, G. G. and Lambert, R. S. J. (1993). Evaluating crustal contamination in continental basalts: the isotopic composition of the Picture Gorge Basalt of the Columbia River Basalt Group. *Contributions to Mineralogy and Petrology*, *114*(4), 452-464.

Camp, V.E. (2013). Origin of Columbia River Basalt: passive rise of shallow mantle, or active upwelling of a deep-mantle plume? *Geol. Soc. Am. Spec. Pap., 497*(7), 181–199. Retrieved from http://dx.doi.org/10.1130/2013.2497(07).

Camp, V.E., Ross, M.E., Duncan, R.A., Jarboe, N.A., Coe, R.S., Hanan, B.B. and Johnson, J.A. (2013). The Steens Basalt: Earliest lavas of the Columbia River Basalt Group., *in Reidel, S.P., Camp, V.E., Ross, M.E., Wolff, J.A., Martin, B.S., Tolan, T.L., and Wells, R.E., eds., The Columbia River Flood Basalt Province: Geol. Soc. Am. Spec. Pap., 497,* 87–116. doi:10.1130/2013.2497(04).

Carlson, R. W., Lugmair, G. W. and Macdougall, J. D. (1981). Columbia River volcanism: the question of mantle heterogeneity or crustal contamination. *Geochimica et Cosmochimica Acta*, *45*(12), 2483-2499.

Carlson, R. W. (1984). Isotopic constraints on Columbia River flood basalt genesis and the nature of the subcontinental mantle. *Geochimica et Cosmochimica Acta*, *48*(11), 2357-2372.

Catchings, R. and Mooney, W. (1988). Crustal structure of east central Oregon: Relation between Newberry Volcano and regional crustal structure, *J. Geophys. Res., 93*(B9), 10081–10094. doi:10.1029/JB093iB09p10081.

Champion, D. E., Donnelly-Nolan, J. M., Lanphere, M. A. and Ramsey, D. W. (2004). Magnetic excursion recorded in basalt at Newberry Volcano, central Oregon, *Transactions, American Geophysical Union*, v. 85, no. 47, abstract GP43B-0861.

Chitwood, L. A., Jensen, R. A. and Groh, E. A. (1977). The age of Lava Butte. *Ore Bin*, *39*, 157-164.

Chitwood, L.A. and Jensen, R.A. (2000). Large Prehistoric Flood Along Paulina Creek, Newberry Volcano, Oregon, *in Jensen, R.A., and Chitwood, L.A., eds, What's New at Newberry Volcano, Oregon: Guidebook for the Friends of the Pleistocene Eighth Annual Pacific Northwest Cell Field Trip*, pp. 32-40.

Coble, M.A. and Mahood, G.A. (2012). Initial impingement of the Yellowstone plume located by widespread silicic volcanism contemporaneous with Columbia River flood basalts. *Geology*, *40*(7), 655–658. Retrieved from http://dx.doi.org/10.1130/G32692.1.

DaSilva, M. J. (2009). Ridge Subduction Volcanism in the Zeballos Complex, Southern Patagonian Andes. *A Master's Thesis*. Montclair State University

Dawson, P. B. and Stauber, D. A. (1986). Data report for a three-dimensional high-resolution P-velocity structural investigation of Newberry Volcano, Oregon, using seismic tomography. *U.S. Geol. Surv. Open File Rep.,* 86-352.

Deer, W. A., Howie, R. A. and Zussman, J. (1992). *An Introduction to the Rock-forming Minerals, 2nd edition.* Harlow, Essex, England: Pearson Education Limited.

Donnelly-Nolan, J. M., Champion, D. E. and Lanphere, M. A. (2000). North flank stratigraphy revealed by new work at Newberry volcano, Oregon , *in Jensen, R.A., and Chitwood, L.A., eds, What's New at Newberry Volcano, Oregon: Guidebook for the Friends of the Pleistocene Eighth Annual Pacific Northwest Cell Field Trip*, pp. 177-180.

Donnelly-Nolan, J. M., Champion, D. E., Lanphere, M. A. and Ramsey, D. W. (2004). New thoughts about Newberry Volcano, central Oregon USA. In *AGU Fall Meeting Abstracts*.

Donnelly-Nolan, J. M., Grove, T. L., Lanphere, M. A., Champion, D. E. and Ramsey, D. W. (2008). Eruptive history and tectonic setting of Medicine Lake Volcano, a large rear-arc volcano in the southern Cascades. *J. Volcanol. Geotherm. Res., 177*, 313-328. doi:10.1016/j.jvolgeores.2008.04.023.

Donnelly-Nolan, J. M. and Jensen, R. A. (2009). Ice and water on Newberry Volcano, central Oregon. *Field Guides*, *15*, 81-90.

Donnelly-Nolan, J. M., Stovall, W. K., Ramsey, D. W., Ewert, J. W. and Jensen, R. A. (2011). Newberry Volcano-Central Oregon's Sleeping Giant. *U. S. Dep. In., U. S. Geol. Surv. Fact Sheet 2011-3145*., 6 pp.

Duncan, R. A. and Richards, M. A. (1991). Hotspots, mantle plumes, flood basalts, and true polar wander. *Reviews of Geophysics*, *29*(1), 31-50.

Dupré, B. and Allègre, C. J. (1983). Pb–Sr isotope variation in Indian Ocean basalts and mixing phenomena. *Nature*, *303*(5913), 142-146.

Ernst, W. G. (1988). Metamorphic terranes, isotopic provinces, and implications for crustal growth of the western United States. *Journal of Geophysical Research: Solid Earth*, *93*(B7), 7634-7642.

Fiebelkorn, R. B., Walker, G. W., MacLeod, N. S., McKee, E. H. and Smith, J. G. (1983). Index to K-Ar Determinations for the State of Oregon: Isochron/West, no. 37, p. 3-60.

Fitterman, D. V. (1983). Time-Domain Electromagnetic Soundings of Newberry Volcano, Deschutes County, Oregon. *U.S. Geol. Surv. Open File Rep., 1-63.*

Fitterman, D.V., Neev, D.K., Bradley, J.A. and Grose, C.T. (1985). More Time-Domain Electromagnetic Soundings of Newberry Volcano, Deschutes County, Oregon. *U.S. Geol. Surv. Open File Rep., 85-451.*

Fitterman, D., Stanley, W. and Bisdorf, R. (1988). Electrical structure of Newberry volcano, Oregon, *J. Geophys. Res.*, *93*(B9), 10119–10134. doi:10.1029/JB093iB09p10119.

Ford, M.T., Grunder, A.L. and Duncan, R.A. (2013). Bimodal volcanism of the High Lava Plains and Northwestern Basin and Range of Oregon: distribution and tectonic implications of age-progressive rhyolites. *Geochem. Geophys. Geosyst. 14* (8), 2836–2857.

Gill, J. B. (1981). Geophysical setting of volcanism at convergent plate boundaries. In *Orogenic andesites and plate tectonics* (pp. 44-63). Springer, Berlin, Heidelberg.

Google. (2017). Google Earth computer software Vers. 7.1.8.3036. *Google, Inc.*

Gorring, M. L. and Kay, S. M. (2001). Mantle processes and sources of Neogene slab window magmas from southern Patagonia, Argentina. *Journal of petrology*, *42*(6), 1067-1094.

Gorring, M., Singer, B., Gowers, J. and Kay, S. M. (2003). Plio–Pleistocene basalts from the Meseta del Lago Buenos Aires, Argentina: evidence for asthenosphere–lithosphere interactions during slab window magmatism. *Chemical Geology*, *193*(3), 215-235.

Graham, D. W., Reid, M. R., Jordan, B. T., Grunder, A. L., Leeman, W. P. and Lupton, J. E. (2009). Mantle source provinces beneath the Northwestern USA delimited by helium isotopes in young basalts. *J. Volcanol. Geotherm. Res.*, *188*, 128-140. doi:10.1016/j.jvolgeores.2008.12.004.

Grove, T. L., Donnelly-Nolan, J. M. and Housh, T. (1997). Magmatic processes that generated the rhyolite of Glass Mountain, Medicine Lake volcano, N. California. *Contrib. Mineral. Petrol., 127,* 205-223.

Gripp, A. E. and Gordon, R. G. (2002). Young tracks of hotspots and current plate velocities. *Geophysical Journal International*, *150*(2), 321-361.

Hallett, D. J., Hills, L. V. and Clague, J. J. (1997). New accelerator mass spectrometry radiocarbon ages for the Mazama tephra layer from Kootenay National Park, British Columbia, Canada. *Canadian Journal of Earth Sciences*, *34*(9), 1202-1209.

Hamelin, B. and Allègre, C. J. (1985). Large-scale regional units in the depleted upper mantle revealed by an isotope study of the South-West Indian Ridge. *Nature*, *315*(6016), 196-199.

Hamelin, B., Dupré, B. and Allègre, C. J. (1986). PbSrNd isotopic data of Indian Ocean ridges: new evidence of large-scale mapping of mantle heterogeneities. *Earth and Planetary Science Letters*, *76*(3-4), 288-298.

Hart, S. R. (1984). A large-scale isotope anomaly in the Southern Hemisphere mantle. *Nature*, *309*(5971), 753-757.

Hooper, P. R. (1988). Crystal fractionation and recharge (RFC) in the American Bar flows of the Imnaha basalt, Columbia River Basalt Group. *Journal of Petrology*, *29*(5), 1097-1118.

Hooper, P. R. and Hawkesworth, C. J. (1993). Isotopic and geochemical constraints on the origin and evolution of the Columbia River Basalt. *Journal of Petrology*, *34*(6), 1203-1246.

Hooper, P.R., Camp, V.E., Reidel, S.P. and Ross, M.E. (2007). The origin of the Columbia River flood basalt province: Plume versus nonplume models, *in Foulger, G.R., and Jurdy, D.M., eds., Plates, plumes, and planetary processes: Geological Society of America Special Paper 430*, p. 635–668, doi: 10.1130/2007.2430(30).

Jensen, R., J. Donnelly-Nolan and D. Mckay (2009). A field guide to Newberry Volcano, Oregon, in Volcanoes to Vineyards: Geologic Field Trips Through the Dynamic Landscape of the Pacific Northwest. *Geol. Soc. of Am., Boulder, Colo. Field Guide, 15,* 53–79. doi:10.1130/2009.fld015(03).

Jensen, R. A. (2015). Roadside Guide to the Geology of Newberry National Volcanic Monument. *CenOreGeoPub*.

Jordan, B.T., Grunder, A.L., Duncan, R.A. and Deino, A.L. (2004). Geochronology of age-progressive volcanism of the Oregon High Lava Plains: implications for the plume interpretation of Yellowstone. *J. Geophys. Res. 109*(B10202). Retrieved from http://dx.doi.org/10.1029/2003JB002776.

Le Bas, M., Maitre, R. L., Streckeisen, A., Zanettin, B. and IUGS Subcommission on the Systematics of Igneous Rocks. (1986). A chemical classification of volcanic rocks based on the total alkali-silica diagram. *Journal of petrology*, *27*(3), 745-750.

Leeman,W.P., Annen, C. and Dufek, J., 2008. Snake River Plain–Yellowstone silicic volcanism: implications for magma genesis and magma fluxes. *Geol. Soc. Lond. Spec. Publ. 304*(1), 235–259. Retrieved from http://dx.doi.org/10.1144/SP304.12.

Le Maitre, R. W., Streckeisen, A., Zanettin, B., Le Bas, M. J., Bonin, B., Bateman, P. and Lameyre, J. (2002). Igneous rocks: A classification and glossary of terms; Recommendations of the International Union of Geological Sciences. In *Subcommission on the Systematics of Igneous rocks*. Cambridge University Press.

Linneman, S. R. (1990). The petrologic evolution of the Holocene magmatic system of Newberry volcano, central Oregon: Laramie, Univeristy of Wyoming, Ph. D. dissertation, 293 p.

Liu, L., Spasojević, S. and Gurnis, M. (2008). Reconstructing Farallon plate subduction beneath North America back to the Late Cretaceous. *Science*, *322*(5903), 934-938.

Long, M. D., Till, C. B., Druken, K. A., Carlson, R. W., Wagner, L. S., Fouch, M. J., James, D. E., Grove, T. L., Schmerr, N. and Kincaid, C. (2012). Mantle dynamics beneath the Pacific Northwest and the generation of voluminous back-arc volcanism, *Geochem. Geophys. Geosyst., 13*(Q0AN01). doi:10.1029/2012GC004189.

MacLeod, N. S., Sherrod, D. F. and Chitwood, L. A. (1982). Geologic map of Newberry Volcano, Deschutes, Klamath, and Lake Counties, Oregon. *U.S. Geol. Surv. Open-File Report 82-847*.

MacLeod, N. S. and Sherrod, D. R. (1988). Geologic evidence for a magma chamber beneath Newberry Volcano, Oregon. *Journal of Geophysical Research: Solid Earth*, *93*(B9), 10067-10079.

MacLeod, N., Sherrod, D., Chitwood, L. and Jensen, R. (1995). Geologic map of Newberry volcano, Deschutes, Klamath, and Lake Counties, Oregon, *U.S. Geol. Surv. Misc. Invest. Ser., Map I-2455, 2 sheets, scale 1:62,500*.

Masuda, A., Nakamura, N. and Tanaka, T. (1973). Fine structures of mutually normalized rare-earth patterns of chondrites. *Geochimica et Cosmochimica Acta*, *37*(2), 239-248.

May, W., Parris, R., Beck, C., Fassett, J., Greenberg, R., Guenther, F. and Gettings, R. (2000). Definitions of terms and modes used at NIST for value-assignment of reference materials for chemical measurements. *NIST special publication*, *260*, 136.

McCulloch, M. T. and Bennett, V. C. (1994). Progressive growth of the Earth's continental crust and depleted mantle: geochemical constraints. *Geochimica et Cosmochimica Acta*, *58*(21), 4717-4738.

McDougall, I. (1976). Geochemistry and origin of basalt of the Columbia River Group, Oregon and Washington. *Geological Society of America Bulletin*, *87*(5), 777-792.

McKay, D., Donnelly Nolan, J., Jensen, R. and Champion, D. (2009). The post-Mazama northwest rift zone eruption at Newberry Volcano, Oregon, in Volcanoes to Vineyards: Geologic Field Trips Through the Dynamic Landscape of the Pacific Northwest. *Geol. Soc. of Am., Boulder, Colo. Field Guide, 15, edited by J. E. O'Connor et al.*, 91–110. doi:10.1130/2009.fld015(05).

McKee, E. H., MacLeod, N. S. and Walker, G. W. (1976). Potassium-argon ages of late Cenozoic silicic volcanic rocks, southeast Oregon: Isochron/West, no. 15, p. 37-41.

Menzies, M. A. (1983). Mantle ultramafic xenoliths in alkaline magmas: evidence for mantle heterogeneity modified by magmatic activity. *Continental basalts and mantle xenoliths*, *272*, 92-110.

Moore, L. J., Murphy, T. J., Barnes, I. L. and Paulsen, P. J. (1982). Absolute isotopic abundance ratios and atomic weight of a reference sample of strontium. *Journal of Research of the National Bureau of Standards*, *87*(1), 1-8.

Mitchell, E. C. and Asmerom, Y. (2011). U-series isotope systematics of mafic magmas from central Oregon: Implications for fluid involvement and melting processes in the Cascade arc. *Earth Plan. Sci. Let., 312,* 378-389. doi:10.1016/j.epsl.2011.09.060.

Müller, R. D., Royer, J. Y. and Lawver, L. A. (1993). Revised plate motions relative to the hotspots from combined Atlantic and Indian Ocean hotspot tracks. *Geology*, *21*(3), 275-278.

Nesse, W.D. (2012). *Introduction to Mineralogy, 2nd Edition*. New York, NY: Oxford University Press, Inc.

Peterson, N. V. and Groh, E. A. (1969). The ages of some Holocene volcanic eruptions in the Newberry Volcano area, Oregon. *Ore Bin*, *31*(4), 73-87.

Pierce, K. L. and Morgan, L. A. (1992). The track of the Yellowstone hot spot: Volcanism, faulting, and uplift. *Geological Society of America Memoirs*, *179*, 1-54.

Pierce, K.L., Morgan, L.A. and Saltus, R.W. (2002). Yellowstone plume head: postulated tectonic relations to the Vancouver slab, continental boundaries, and climate *in Bonnichsen, Bill, White, C.M., McCurry, Michael (Eds.), Tectonic and Magmatic Evolution of the Snake River Plain Volcanic Province. Idaho Geological Survey Bulletin, 30,* 5–33.

Reidel, S. P., Tolan, T. L., Hooper, P. R., Beeson, M. H., Fecht, K. R., Bentley, R. D. and Anderson, J. L. (1989). The Grande Ronde Basalt, Columbia River Basalt Group; Stratigraphic descriptions and correlations in Washington, Oregon, and Idaho. *Geological Society of America Special Papers*, *239*, 21-54.

Robinson, S. W. and Trimble, D. A. (1981). US Geological Survey, Menlo Park, California, radiocarbon measurements II. *Radiocarbon*, *23*(2), 305-321.

Rollinson, H. R. (1993). Discriminating between tectonic environments using geochemical data. *Using Geochemical Data: Evaluation, Presentation, Interpretation. Longman Scientific & Technical, Essex, UK*, 171-214.

Schilling, J. G., Zajac, M., Evans, R., Johnston, T., White, W., Devine, J. D. and Kingsley, R. (1983). Petrologic and geochemical variations along the Mid-Atlantic Ridge from 29 degrees N to 73 degrees N. *American Journal of Science*, *283*(6), 510-586.

Scott, W. E. (1977). Quaternary glaciation and volcanism, Metolius River area, Oregon. *Geological Society of America Bulletin*, *88*(1), 113-124.

Scott, W. E. and Gardner, C. A. (1992). *Geologic map of the Mount Bachelor volcanic chain and surrounding area, Cascade Range, Oregon* (No. 1967).

Staudigel, H., Zindler, A., Hart, S. R., Leslie, T., Chen, C. Y. and Clague, D. (1984). The isotope systematics of a juvenile intraplate volcano: Pb, Nd, and Sr isotope ratios of basalts from Loihi Seamount, Hawaii. *Earth and Planetary Science Letters*, *69*(1), 13-29.

Sun, S. S. and McDonough, W. S. (1989). Chemical and isotopic systematics of oceanic basalts: implications for mantle composition and processes. *Geological Society, London, Special Publications*, *42*(1), 313-345.

Tanaka, T., Togashi, S., Kamioka, H., Amakawa, H., Kagami, H., Hamamoto, T. and Kunimaru, T. (2000). JNdi-1: a neodymium isotopic reference in consistency with LaJolla neodymium. *Chemical Geology*, *168*(3), 279-281.

Tian, Y. and Zhao, D. (2012). P-wave tomography of the western United States: Insight into the Yellowstone hotspot and the Juan de Fuca slab. *Phys. Earth Plan. Int., 200-201,* 72-84. Retrieved from http://dx.doi.org/10.1016/j.pepi.2012.04.004.

Vidal, P., Chauvel, C. and Brousse, R. (1984). Large mantle heterogeneity beneath French Polynesia. *Nature*, *307*(5951), 536-538.

White, W. M., Dupré, B. and Vidal, P. (1985). Isotope and trace element geochemistry of sediments from the Barbados Ridge-Demerara Plain region, Atlantic Ocean. *Geochimica et cosmochimica acta*, *49*(9), 1875-1886.

Wilson, M. (1989). Igneous Petrogenesis. A Global Tectonic Approach.

Wilson, S. A. (1997). The collection, preparation, and testing of USGS reference material BCR-2, Columbia River, Basalt: U.S. Geological Survey Open-File Report 98-xxx.

Winter, J. D. (2010). *Principles of Igneous and Metamorphic Petrology, 2nd Edition*. Upper Saddle River, NJ: Prentice Hall.

Xue, M. and Allen, R. M. (2006). Origin of the Newberry Hotspot Track: Evidence from shear-wave splitting. *Earth Plan. Sci. Let., 244,* 315-322. doi:10.1016/j.epsl.2006.01.066.

Yuan, H., Yuan, W., Cheng, C., Liang, P., Liu, X., Dai, M. and Lai, S. (2016). Evaluation of lead isotope compositions of NIST NBS 981 measured by thermal ionization mass spectrometer and multiple-collector inductively coupled plasma mass spectrometer. *Solid Earth Sciences*, *1*(2), 74-78.

Zindler, A., Jagoutz, E. and Goldstein, S. (1982). Nd, Sr and Pb isotopic systematics in a three-component mantle: a new perspective. *Nature*, *298*(5874), 519-523.

Zindler, A. and Hart, S. (1986). Chemical geodynamics. *Annual review of earth and planetary sciences*, *14*(1), 493-571.

8. APPENDICES

8.1. Appendix A: Field Notations and Relationships

All samples were collected from Newberry Volcano, OR (43.7°N, 121.3°W) in the Newberry National Volcanic Monument, the Crooked River National Grassland and the Deschutes National Forest.

Site 1: 06/25/2016

- Bessie Butte, ENE face of butte with relatively small massive flow interjecting towards Rd. 1810
- Flow is massive on bottom and increasingly more vesicular to top, flow is roughly 2-3 m thick
- Bessie Butte is highly altered, top of butte is yellowish-red (altered scoria)
- LTBB-1 collected (basaltic andesite) with large plagioclase phenocrysts
- Several (6 or 7 inch diameter) boreholes, potentially for paleomagnetism dating research
- Flow is possibly in a NE direction from previous older flow

Site 2:

- North of Rd. 18 on 4,421 ft. knob, essentially center of Kelsey Butte quadrangle
- On outcrop of mostly vesicular weathered basalt, but found what looks like some massive columnar jointed basalt
- Flow seems to have moved in a NE direction from the south and continues to fan out, flow is 4-5 m thick
- Seems to be sitting on top of a layer of vesicular basalt or scoria
- LHB-1 collected (basalt, generally homogenous crystalline structure)
- Knob seems to overlook another flow headed NNW, somewhat in the direction of Coyote Butte, flows are visible from Rd. 18 across open field

Site 3:

- North of site 2 by ~1 mi. off of bike path on Rd. 1819
- Outcrop is part of the same flow as site 2
- LHB-2 collected (basalt, light gray with white specks, possibly plagioclase phenocrysts), rock seems harder than LHB-1
- Site next to small pile of basalt talus, overlooking a basalt ridge to the NW
- 0.5 mi. on bike path from the Skeleton Cave

Site 4: 06/26/2016

- East of Rd. 20 as it heads south through the Horse Ridge quadrangle
- Roughly 20 mi. E of Bend, OR
- Down the chasm from the historic site pull-off, sign reads “Prehistoric River – Oregon Geology”
- Site overlooks the Dry River Canyon glacial outlet that was barred by lava flows
- Lava flows dammed nearby lake and created glacial outlet, river has since dried up
- Canyon shows several exposed flows that were downcut by the Dry River
- Basalt flow sampled is quite massive, 3 m thick
- Basalt is very fine grained, darker than yesterday’s samples, no phenocrysts
- Tb-1DRC collected, indicated as tertiary age basalt from the Horse Ridge, older than all units in study

Site 5:

- About a mile NW of site 4 on Rd. 20, we turned around and are headed back to Bend through Horse Ridge
- Still adjacent to Dry River Canyon at NW end of basalt outcrop, sitting on ridge overlooking canyon opening up to the north
- In ESE section of Horse Ridge quadrangle
- Tb-2DRC collected, tertiary basalt is lighter in color than site 4, same grain size but harder
- Site seems to be at higher elevation than foreground to the north, section of basalt seems much thicker than nearby flows ~6-8 m

Site 6:

- Traveled ~3 mi. from site 5 up Rd. 20
- Dry River Canyon has turned to the east from our location
- In central E region of Horse Ridge quadrangle
- LTBB-2 collected, some basalt is more vesicular, darker in color than last two sites and coarser grained, contains olivine phenocrysts
- Flow is roughly 2 m thick
- Site btw two signs: Oregon Badlands and Flatiron Rock Trailhead at mile post 16

Site 7:

- Headed ~1.5 mi WNW on Rd. 20 from site 6 at mile post 14.2
- Moving towards western portion of Horse Ridge
- LTBB-3 collected, massive basalt, looks very similar to LTBB-2, however less vesicular and olivine phenocrysts are not visible
- Flow is roughly 1.5 m thick

Site 8:

- About 2 miles NW on Rd. 20 from site 7, mile post 12.3
- We have just passed Stookey Rd. intersection with Rd. 20
- In NW corner of Horse Ridge quadrangle where LHB strip should exist, however rocks are not much different so named Qba-1
- Outcrop is about 3 m thick, vesicular basalt, large olivine phenocrysts abundant, caliche ($CaCO_3$) on some rocks
- We found vents from a lava tube cave at this site
- Possibly older basalts from Newberry

Site 9:

- Traveled about 3 miles up Rd. 20 from site 8, mile post 9.8
- In btw Rickard Rd. and Dodds Rd. in SE corner of Bend Airport quadrangle
- Gone past LTBB on map of flows so interpreted as different flow, Qba-2 collected, fine-grained gray basalt, very small olivine crystals that were part of rock matrix, not phenocrysts
- Flow is 2-3 m thick from road level

Site 10: 06/27/2016

- Back on Rd. 20 on basalt flows of Horse Ridge
- At mile post 13, less than a mile SE of site 8, just south of Stookey Rd.
- According to Jensen 2009, this site is the end of Lava Top Butte basalt on Rd. 20
- LTBB-4 collected, fine-grained gray basalt, olivine phenocrysts visible with hand lens only
- Outcrop is 4-5 m high from road level

Site 11:

- Drove W into Bend quadrangle, turned right off Rd. 20 and parked at Juniper School
- Walked east up Pilot Butte, behind Pilot Butte Middle School and stopped at about 3,800 ft on cinder pit
- Took several samples of well put-together cinders (low vesicle amount) named Qba-3PB, 188 ka

Site 12:

- Drove W on Norton Ave. and turned right on 3rd St. to get on Olney Ave., driving W towards Hwy. 97, parked at Wendy's
- Roadcut is along railroad intersection with Olney Ave., just before Hwy. 97
- Collected BB-1, Bend basalt sample is lighter in color, few olivine crystals, much lighter gray

Site 13:

- Drove S on Hwy. 97 through Bend to Bend basalt outcrops, took exit 139 Reed Market Rd. and made a left, parked at McDonald's
- Walked down to SE corner of cloverleaf exit ramp to outcrop with prominent ditch for discretion
- Collected BB-2, light gray, slightly larger olivine phenocrysts

Site 14:

- Continued S on Hwy 97. to Newberry Crater access Rd. 21 traveling ESE, almost to the end of Finley Butte quadrangle
- Found outcrop of basalt at mile post 5.9 on Rd. 21 headed towards Cinder Hill Campsite
- Basalt is very fine grained and very hard, unsure of flow name, probably one of Newberry's older flows, named Qer-1

Site 15: 06/28/2016

- On our way to Crater Lake, OR today, stopped along Rd. 21 westbound towards Hwy. 97 where we viewed a small flow yesterday while returning to Cinder Hill camp at mile post 7.1, passed gate to caldera
- Basalt flow is near caldera in Paulina Peak quadrangle on WNW corner on Rd. 21
- Qer-2, basalt is an older flow from Newberry, very fine grained, no phenocrysts visible to eye, some blocks have been detached in a small talus

Site 16: 06/29/2016

- Sampling caldera basalts today, traveled form LaPine State Park camp on Rd. 21
- Outcrop is on Rd. 21, just south of RV park and East Lake Resort
- Parked at Newberry Crater trailhead and walked around on trail, looking at float deposits but no outcrops other than roadcut, walked on rhyolite/obsidian flow as well
- Qbce-1, basalt of East Lake Resort

Site 17:

- Large outcrop visible from Cinder Hill camp and eastern shore of East Lake
- Drove north on Rd. 21 up the east shore of East Lake and parked at boat ramp nearest base camp 1, walked up talus slope to tree line, bush wacking up steep talus
- Collected Qcw-1, basalt of the Crater Wall, probably an old eastern flank of Mt. Newberry composite shield volcano
- Site in btw East Lake Resort and 1st camp

Site 18:

- End of a basalt flow on the NE corner of the caldera, past the last boat ramp in Cinder Hill campsite and went onto Newberry Crater trail from fishing parking lot, walked ~0.5 mi N
- Basalt is very dark like East Lake Resort basalt but slightly lighter gray, this basalt is probably part of a flow from Sheep's Rump to NE of crater Qbcs-1

Site 19:

- Drove west on Rd. 21 and turned right into Little Crater campground and drove to the end of camp road 570 to intersection of Little Crater trail and Pauline Lakeshore Loop trail, took Paulina trail
- Collected basalt from Paulina Lake flow which makes up the eastern shore Qbcp-1, olivine phenocrysts and unknown black minerals

Site 20: 06/30/2016

- Sampling Northwest Rift Zone lavas today, left LaPine camp and drove north on Hwy. 97, exited 151 exit to Lava Lands Visitor Center, walked up to the end of the Trail of the Molten Lands to Phil Brogan Viewpoint
- Walked back down trail ~50 ft to wall of joint sets in slightly massive basalt, picked up several fallen blocks
- Qyb1-1, basalt of the Lava Butte flow is very dark in color w/some plagioclase phenocrysts

Site 21:

- Made right out of Lava Lands Visitor Center onto Rd. 9702 towards Benham Falls trailhead, seeing several outcrops of older basalt flows, probably Bend basalt, just SW of NWRZ flows
- BB-3 collected, coarse grained, seems to be part of a thick flow, columnar jointed, outcrop has been cored heavily for paleomagnetism studies

Site 22:

- Drove NW on Rd. 9702 to Benham Falls East trailhead, took Sun-Lava bike path up to Black Rock trail and turned left, walked on trail almost to train tracks
- Took sample of Qyb1-2, north end of Lava Butte flow basalt, first sample is much better, no massive blocks at toe of flow, all A'a lava with caliche filled vesicles

Site 23:

- Walked back down Black Rock trail and onto Sun-Lava bike path
- Picked up block of Bend basalt BB-4, coarser-grained, light gray
- Location is south of Deschutes River and gaging station in center of Benham Falls quadrangle

Site 24:

- Went on Hwy. 97 N, turned right onto North Paulina Rd. 9710 and SSE to topographic feature, Klawhop Butte
- Klawhop Butte is heavily forested and lumps of basalt stick out of ground, resistant blocks
- Sample was highly weathered and oxidized, some parts are vesicular Qba-4KH

Site 25:

- Walked across Rd. 9710 to A'a flow from Mokst Butte to the south, walked across knob to flow
- Most pieces were vesicular and frothy but some were massive, took sample Qyb3-1 in south of Lava Butte quadrangle

Site 26: 07/01/2016

- On the way to Lava Cast Forest, got on Hwy. 97 N and exited at exit 153 Lava Cast Forest Rd. 9720, stopped ~1.0 mi from 97 at cinder pit of Abbott Butte
- Cinders are vibrantly multi-colored blues, purples, golds and reds
- Sampled dike cross-cutting pit in N-S direction Qba-5ABB

Site 27:

- In Lava Cast Forest, drove ~9.0 mi to the end of Rd. 9720, sampled basalt of Lava Cast Forest flow, best samples were tree casts, sampled Qyb8-1 along Lava Cast Forest trail, near center of Lava Cast Forest

Site 28:

- Walked through Lava Cast parking lot to an adjacent flow across form Rd. 9720
- Sampled few massive basalt chunks in flow called Forest Road flow Qyb7-1, basalt was from toe of a small flow on the larger one, very fine-grained, large olivine phenocrysts

Site 29:

- Returning to Hwy. 97 from Lava Cast Forest Rd. 9720, driving WNW
- Several outcrops of older basalt flow are sticking up along road
- Sampled Qba-6GRB, basalt from the Grade Butte flow, much older than NWRZ lavas, no date constrained
- Basalt is light gray w/numerous plagioclase and olivine phenocrysts

Site 30:

- Got on Hwy. 97 N, turned right onto Rd. 18 China Hat Rd, then made right on Rd. 1810 at Bessie Butte
- Sampled basalt flow in between section of road where Rd. 1814 comes in left and Rd. 9714 comes in right, while driving S on Rd. 1810, walked up slope past small road with sharp left turn Qba-7, basalt looks very similar to basalt of Bessie Butte, red stripes in it from oxidation
- Extremely large plagioclase phenocrysts and olivine

Site 31:

- While driving S on Rd. 1810, turned right onto Rd. 9714 and left onto the merge of Rds. 700 and 710, walked diagonally through forest to A'a lava flow across from Rd. 800
- Basalt is dark, fine-grained from NWRZ flow called South Kelsey flow Qyb4-1, quite a small lava flow compared to other NWRZ flows

Site 32: 07/02/2016

- On our way back to Portland, drove up Hwy. 97 from base 2 and went through Bend and Redmond, turned right onto Hwy. 126 E, drove to low topography and parked at SW Twin Lakes Rd. in O'Neil quadrangle south
- Collected CRGB-1, basalt is part of the flow edge of the Crooked River Gorge basalt flow, large olivine and plagioclase phenocrysts, moderately coarse
- Site in btw M. P. 6.0 and 7.0

Site 33:

- Turned back around on Hwy. 126, now traveling west towards Redmond and Hwy. 97
- Collected sample of CRGB-2, basalt of Crooked River Gorge, just east of Jackson Rd. intersection on Hwy. 126 in Redmond quadrangle SE corner, basalt looks very similar to CRGB-1 and also resembles Bend basalt

Site 34:

- Went back on Hwy. 97 N and then turned right onto Rd. 370 NW O'Neil Hwy, passed Overland Ranch Rd. going off right, stopped at outstanding outcrop of CRGB
- Collected CRGB-3, sample looks identical to CRGB-1
- Site is in western O'Neil quadrangle with a nice overlook of the Crooked River basin

Site 35:

- Returned to Hwy. 97 and then left onto Lower Bridge Way past the town of Terrebonne, drove west to the Deschutes River at Buckhorn Canyon, drove just past Steamboat Rock and parked
- Outcrop is basalt on top of very white rock unknown (could be volcanic) with underlying light brown layer (also volcanic)
- Basalt is Lava Top Butte basalt according to Jensen flow map LTBB-5
- Site is in northeast corner of Cline Falls quadrangle and overlooks Deschutes River canyon
- Made rough strat section of volcaniclastic roadcut

8.2. Appendix B: Figures and Tables

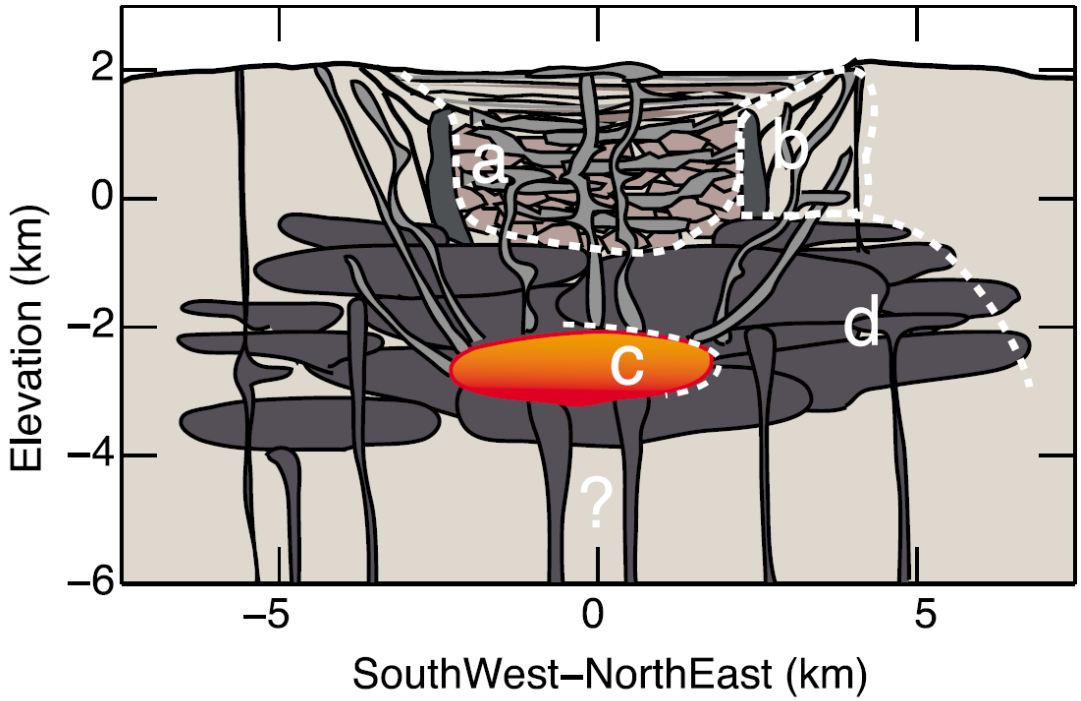

Figure 1. An interpretation of the shallow structure of Newberry Volcano based on tomographic and finite difference waveform modeling from (Beachly et al., 2012). The region a shows the caldera-fill zone. The region b shows the ring dike and fault system surrounding the caldera zone. The region c is the magma body. The region d shows remnants of old magma chambers, dikes and sills. (After Beachly et al., 2012).

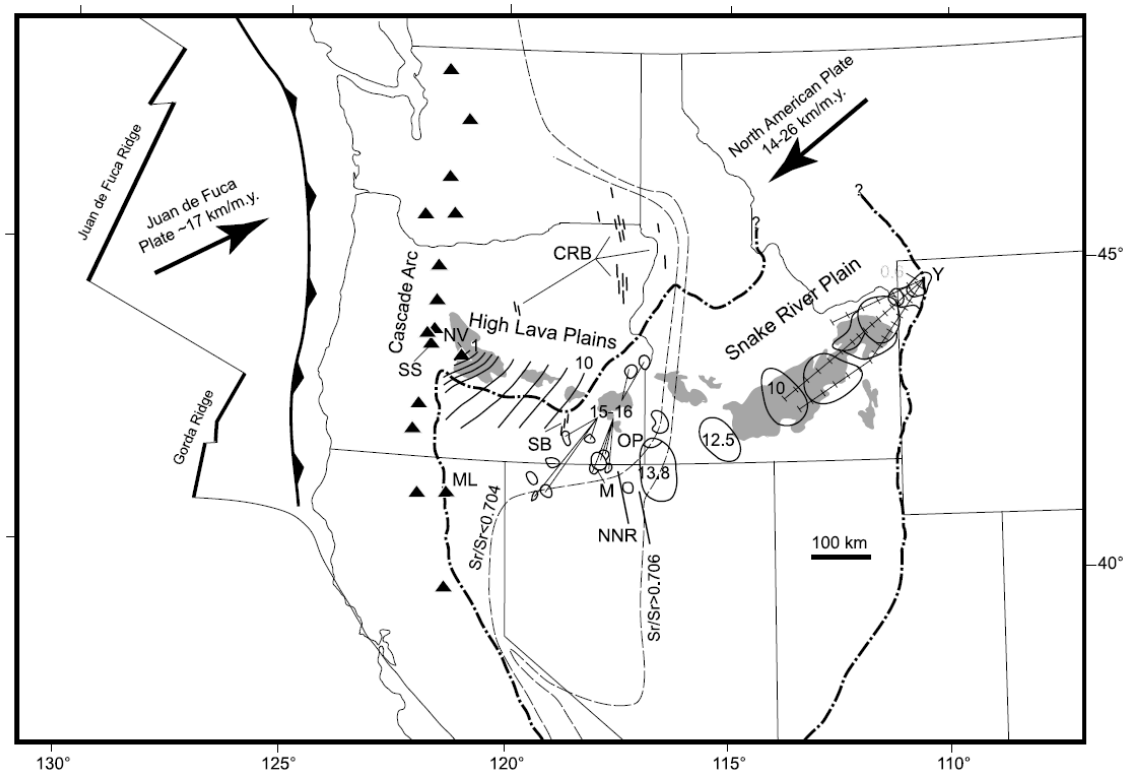

Figure 2. The tectonic setting of the Oregon High Lava Plains (HLP) and Snake River Plain. Yellowstone (Y); McDermitt volcanic field (M); Owyhee Plateau (OP); Newberry volcano (NV); South Sister (SS); Medicine Lake volcano (ML). Pliocene and younger basalts of the HLP and YSRP are shaded. The bold dash-dotted line shows the limit of Basin and Range extension. Curved lines cutting across the HLP and northwestern Basin and Range are isochrons of silicic volcanism 10 Ma and 1 Ma are labeled. Circled areas are volcanic centers of the Yellowstone-Snake River Plain (YSRP) and Owyhee region (After Pierce and Morgan, 1992); ages are given for some calderas to indicate age progression, with many volcanic centers identified in the range 15–16 Ma. Also shown are dike complexes that fed middle Miocene flood basalts; Columbia River basalt dikes (CRB); Steens Basalt dikes (SB); Northern Nevada Rift (NNR). Ticked lines (ticks represent 1 m.y. intervals) across the YSRP are back-projected from Yellowstone to show the lengths of hot spot tracks predicted by global plate motion models plus extension (the northern line is based on the model of Gripp and Gordon, 2002) which extends only to 6 Ma, the period of the model; line middle is based on the model of (Müller et al., 1993), and the southern line is based on the model of (Duncan and Richards, 1991). The light dashed lines indicate approximate positions of the Sr isotope discontinuities (After Ernst, 1988). (After Jordan et al., 2004).

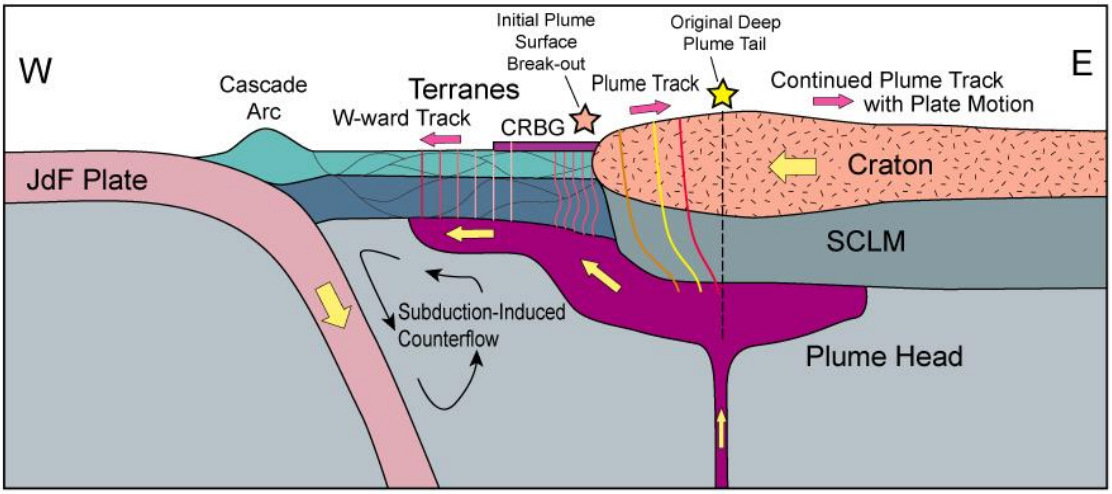

Figure 3. A cross sectional diagram across southern Oregon and Idaho, illustrating the possible westward impingement of the Yellowstone plume head by subduction-induced counterflow to the thinner accreted plate margin and hotspot track migration. JdF is the Juan de Fuca plate, CRBG is the Columbia River Basalt Group and SCLM is Subcontinental lithospheric mantle (After Jordan et al., 2004; Winter, 2010).

Figure 4. Photographic images of Newberry Volcano Field Study 25 June 2016 to 02 July 2016. **(a)** the Dry River Canyon basalt outcrop of the Horse Ridge-Badlands Volcano (7.6 Ma) at sites 4 and 5 **(b)** Newberry Volcano view from the top of Pilot Butte (188 ka), Bend, OR **(c)** columnar basalt of LHB (90 ka) flow at sites 2 and 3 **(d)** roadcut of Crooked River Gorge (350 ka) basalt flow overlooking Crooked River basin at site 34 **(e)** railroad bridge spanning the Crooked River Gorge.

Figure 4 (cont.). Photographic images of Newberry Volcano Field Study 25 June 2016 to 02 July 2016. **(f)** Crater Lake and Wizard Island at the site of the former Mount Mazama caldera collapse eruption (7.7 ka) **(g)** A'a lava flow at the base of Lava Butte (7 ka) at site 20 **(h)** view of Lava Butte from the north end of the same lava flow at site 22 **(i)** tree cast in lava at the Lava Cast Forest flow (7.2 ka) at site 27 **(j)** Newberry Caldera view from the top of Paulina Peak (83 ka); East Lake, Paulina Lake, the Big Obsidian flow (1.3 ka), the Interlake Obsidian flow (7.3 ka), the Central Pumice Cone and the Game Hut Obsidian flow can be seen from this point. All photographs taken by J. M. Clay.

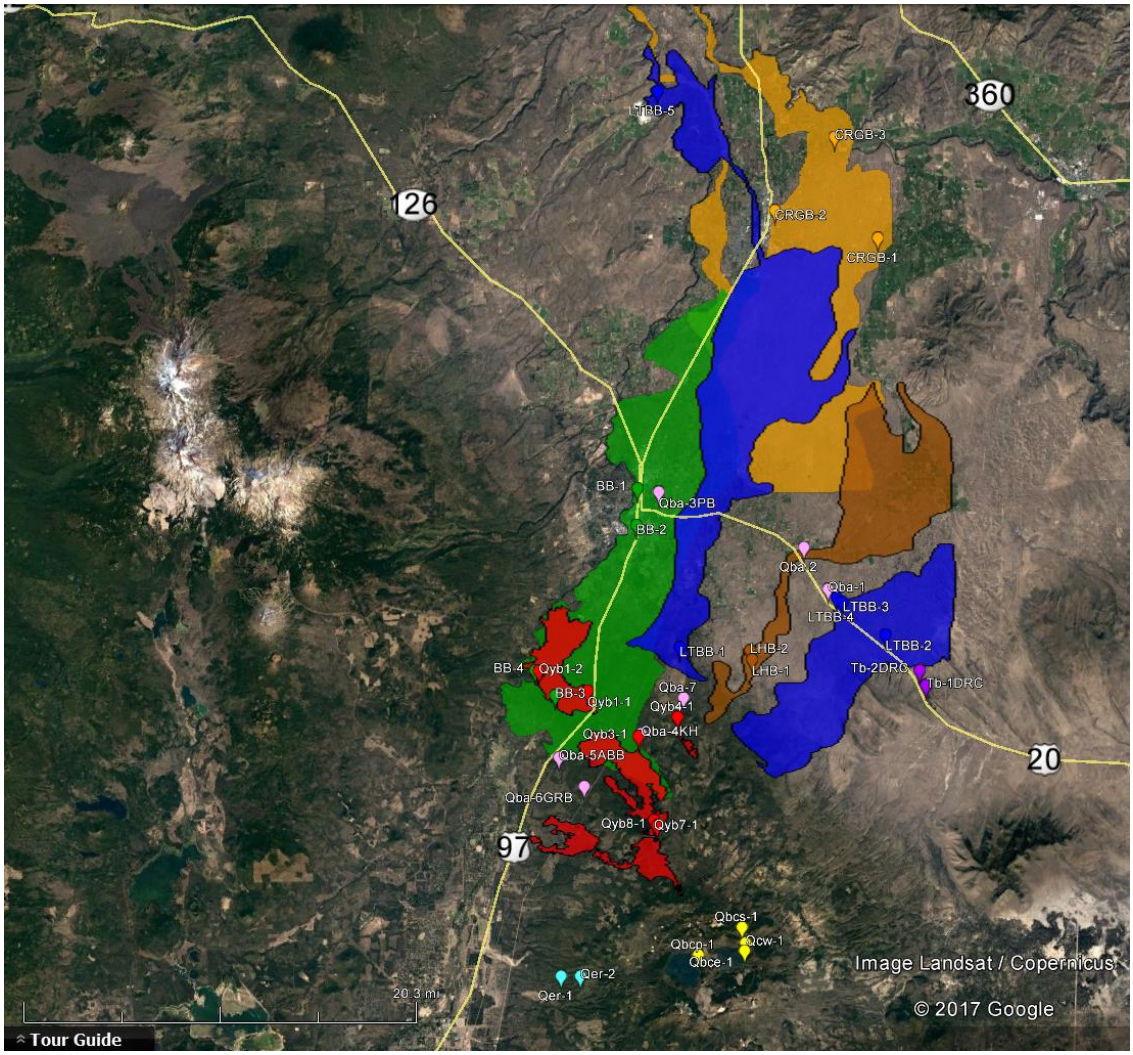

Figure 5. Newberry Volcano, Oregon and sample locations. Purple = Tb (7.6 Ma), Light blue = Qer (600 ka), Pink = Qba (700-39 ka), Orange = CRGB (350 ka), Brown = LHB (90 ka), Green = BB (78 ka), Dark blue = LTBB (75 ka), Red = Qyb (7.2-6.8 ka), Yellow = Qc (11.2-10 ka). Orange shaded depicts CRGB flow, Brown shaded depicts LHB flow, Green shaded depicts BB flow, Dark blue shaded depict LTBB flows, Red shaded depict NWRZ, Qyb flows (After Jensen et al., 2009; Google, 2017).

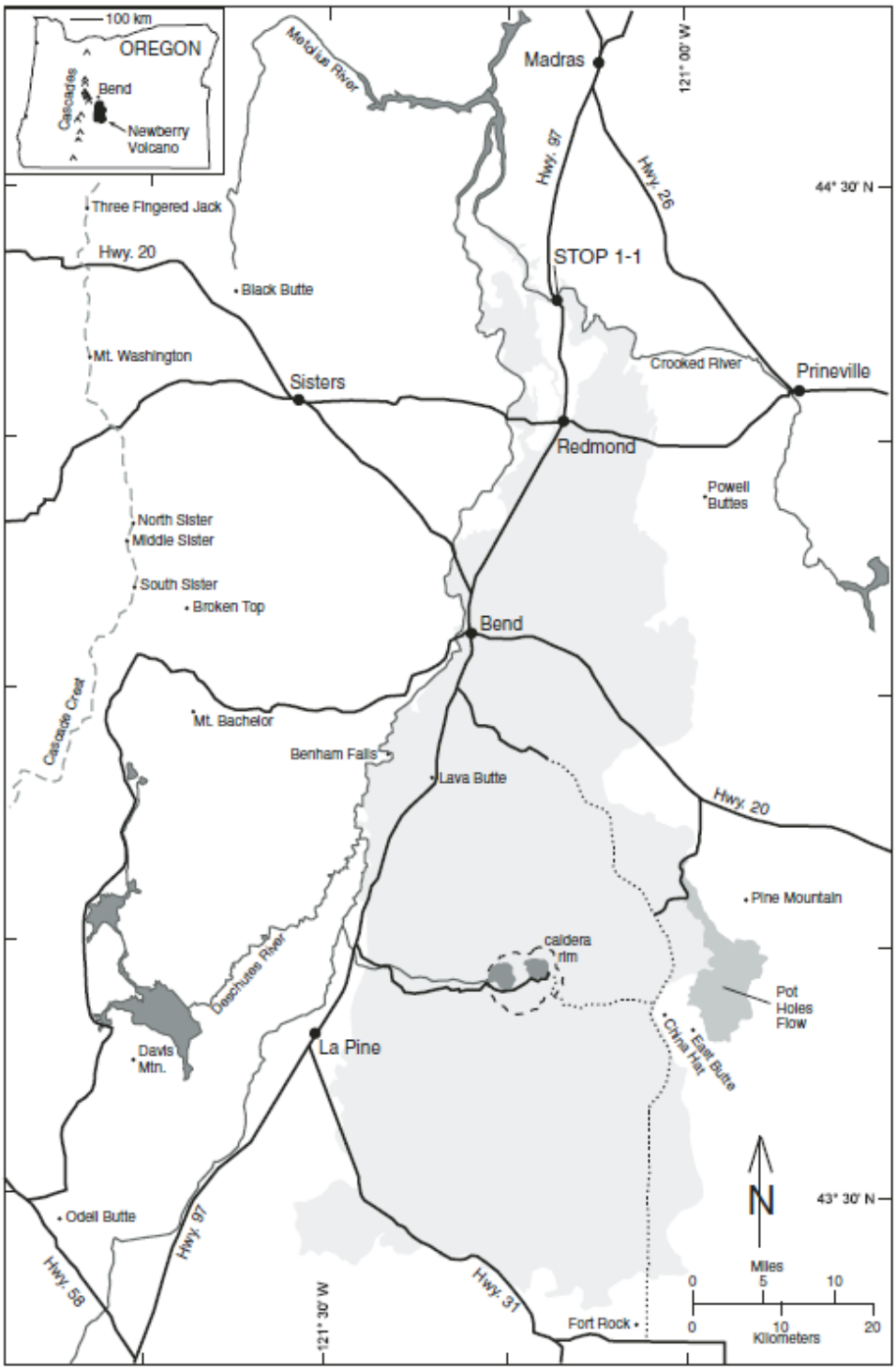

Figure 6. Simplified map of Newberry Volcano. Light gray region shows approximate distribution of lavas from the volcano. (after Jensen et al., 2009).

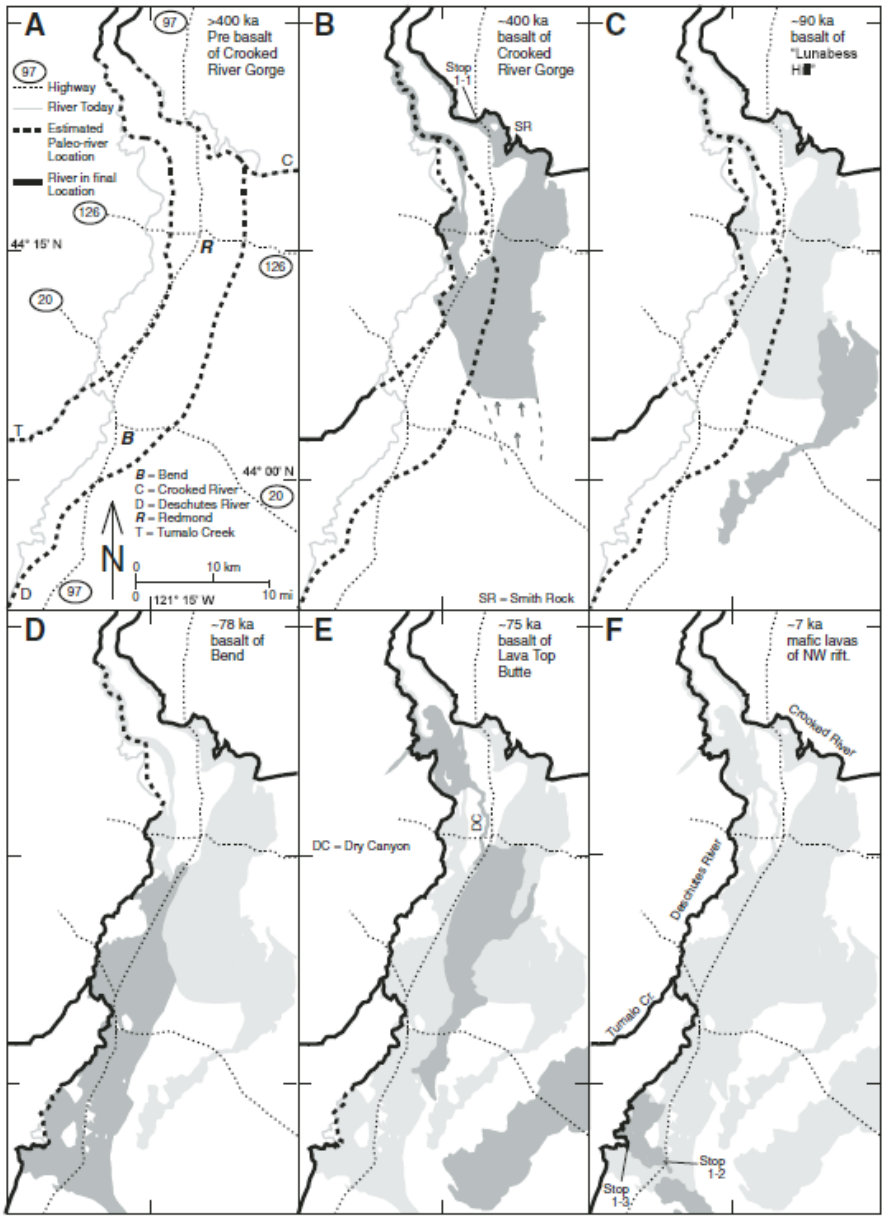

Figure 7. Panels A through F show the progression of lava flows from Newberry Volcano through time. Dark gray region is shown in that panel, while light gray regions are flows from previous panels. (After Jensen et al., 2009).

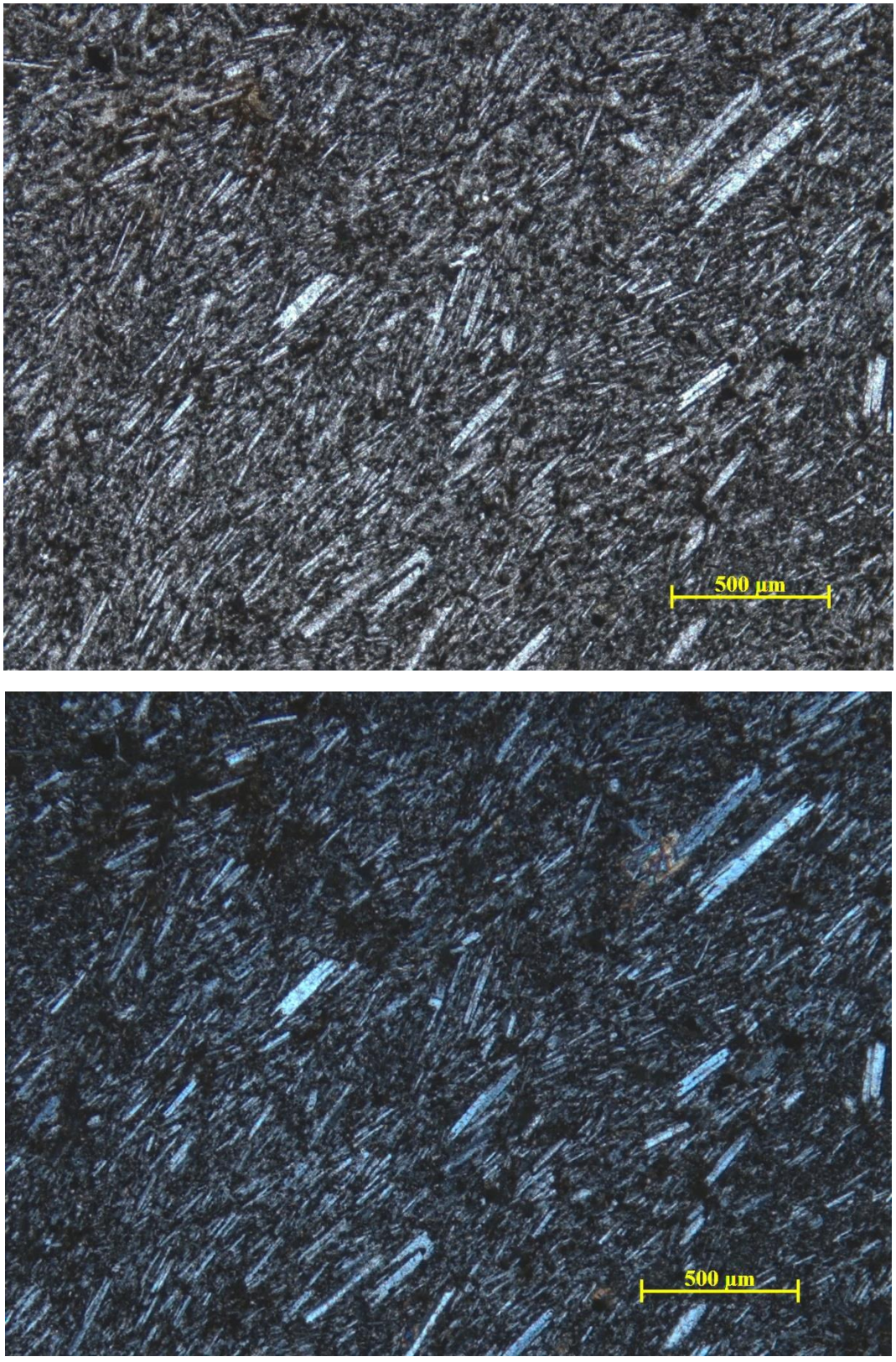

Figure 8. A photomicrograph of thin section view of sample Qer-2 (600 ka) showing plagioclase crystals aligned with the direction of lava flow. (Above: PPL, Below: XPL).

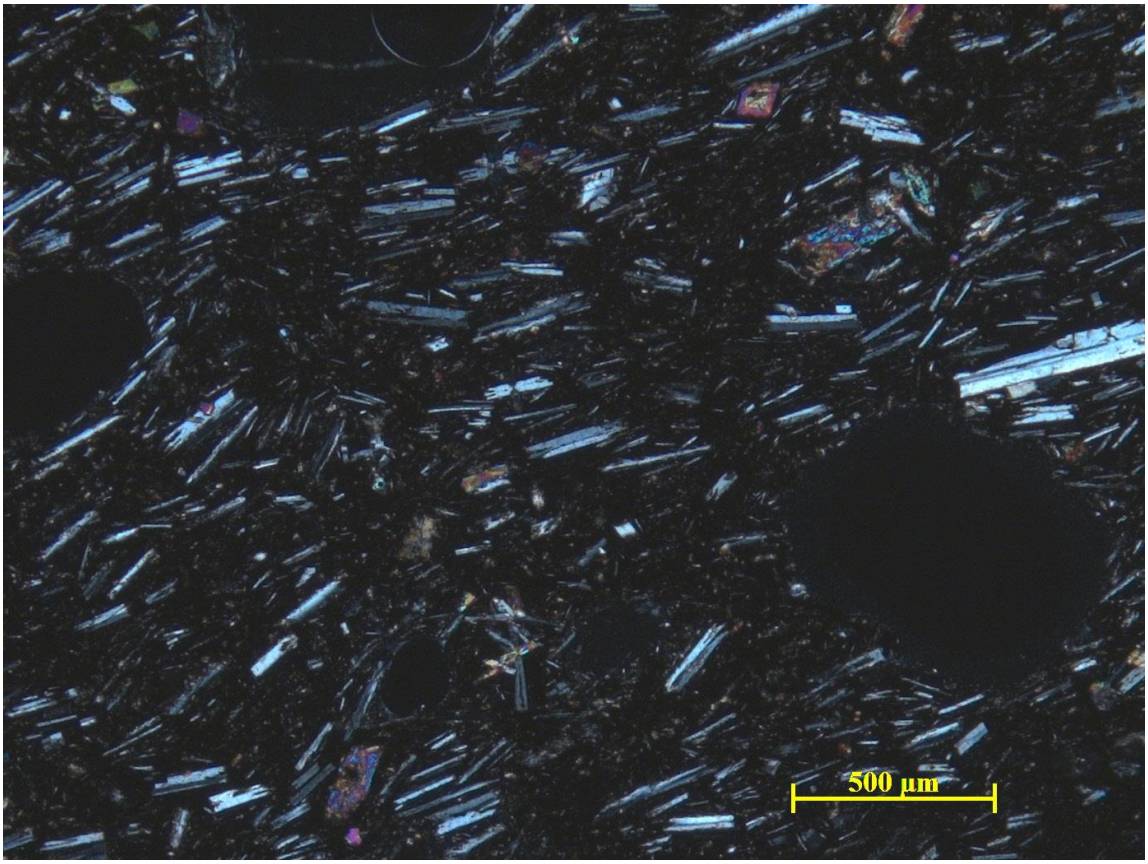

Figure 9. A photomicrograph of thin section view of sample Qyb7-1 (6.8 ka) showing the vesicular nature of the Northwest Rift Zone lavas. (View is in XPL).

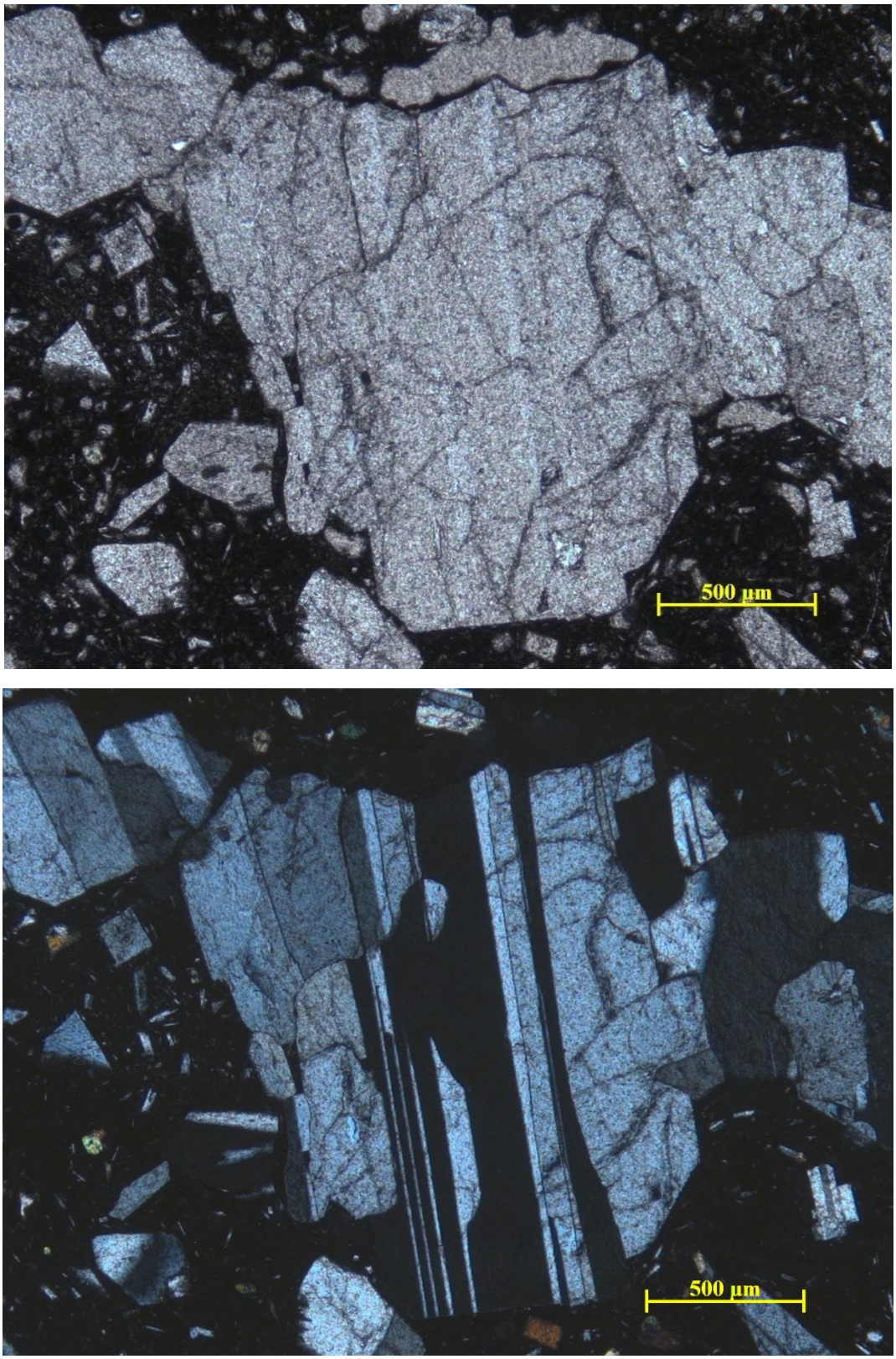

Figure 10. A photomicrograph of thin section view of sample Qba-3PB (188 ka) showing a characteristic plagioclase feldspar phenocryst. (Above: PPL, Below: XPL).

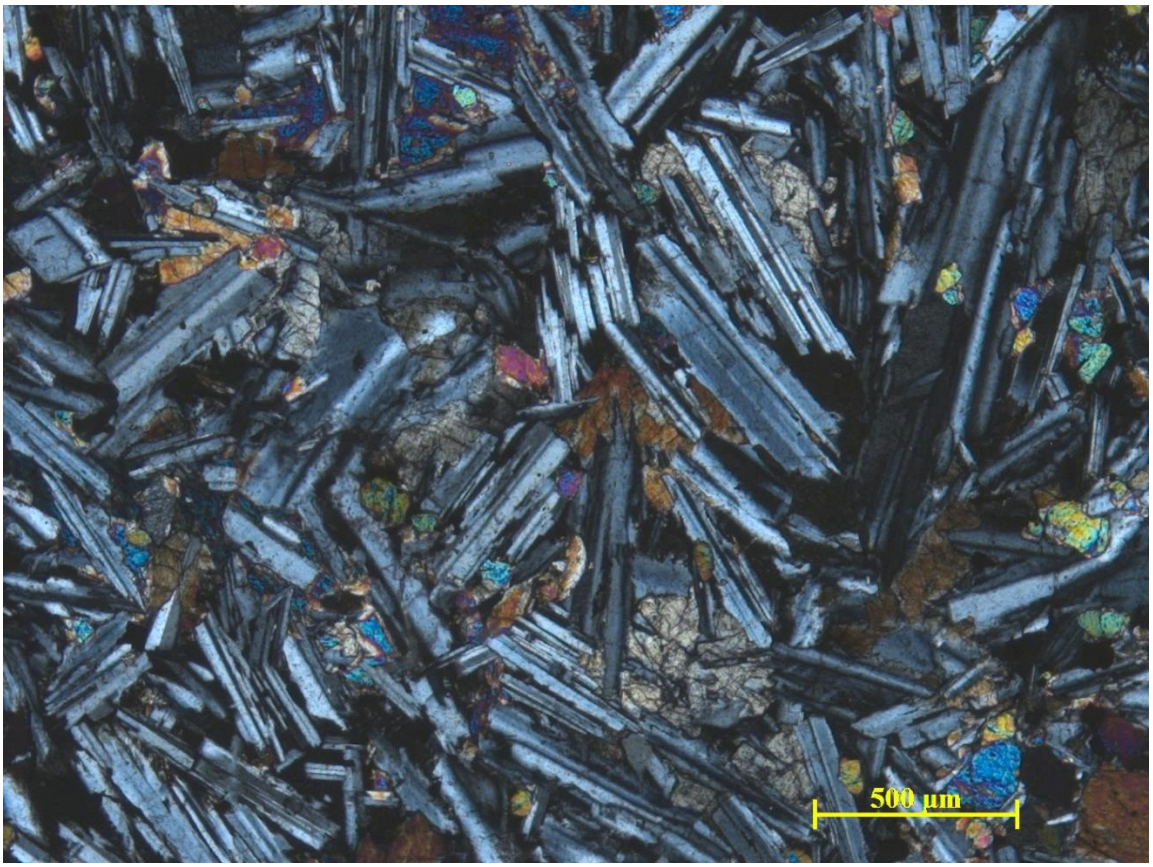

Figure 11. A photomicrograph of thin section view of sample LTBB-3 (75 ka) showing a crystalline network of plagioclase, pyroxene and olivine. (View is in XPL).

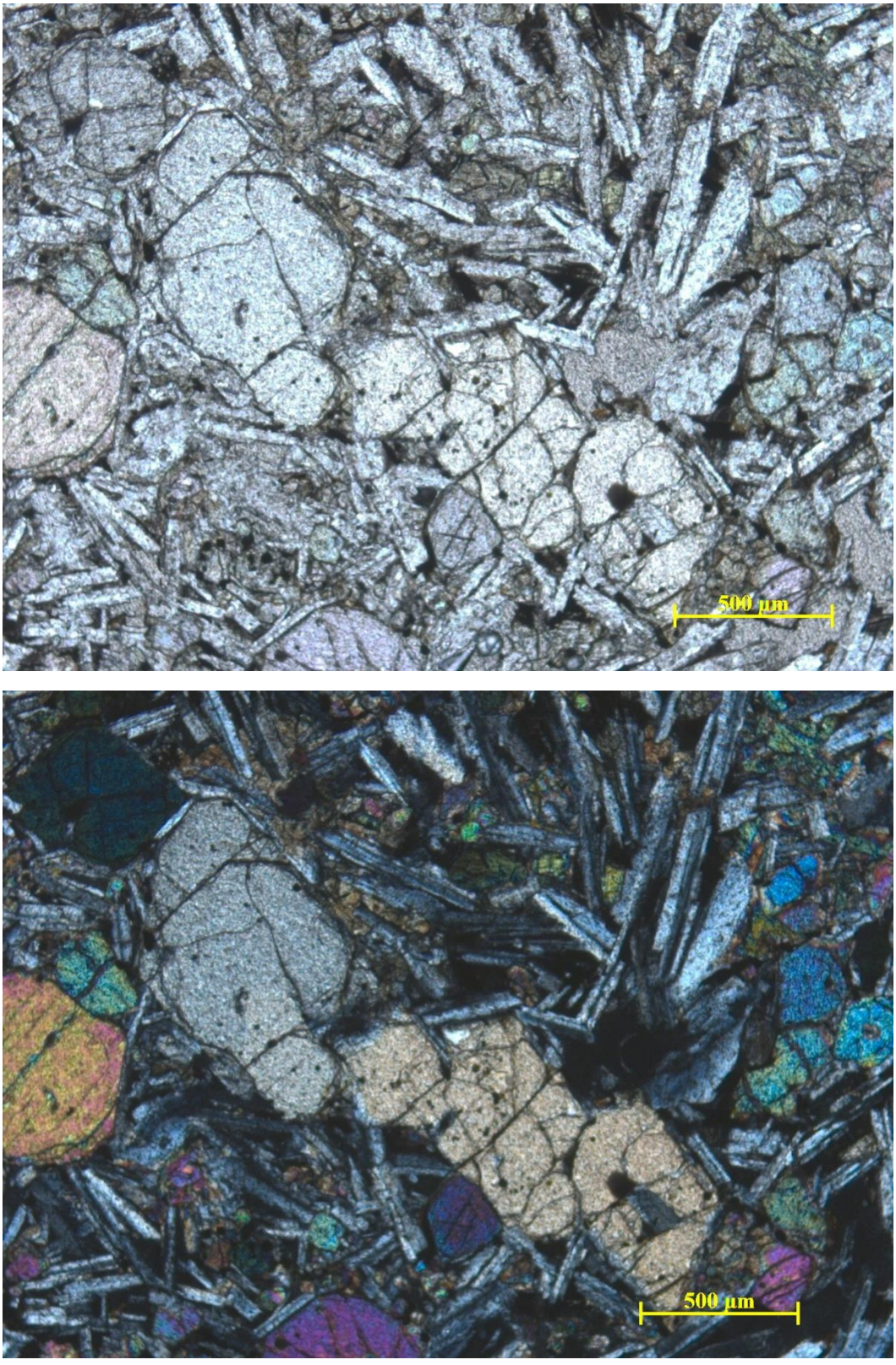

Figure 12. A photomicrograph of thin section view of sample LTBB-4 (75 ka) showing characteristic orthopyroxene and clinopyroxene. (Above: PPL, Below: XPL).

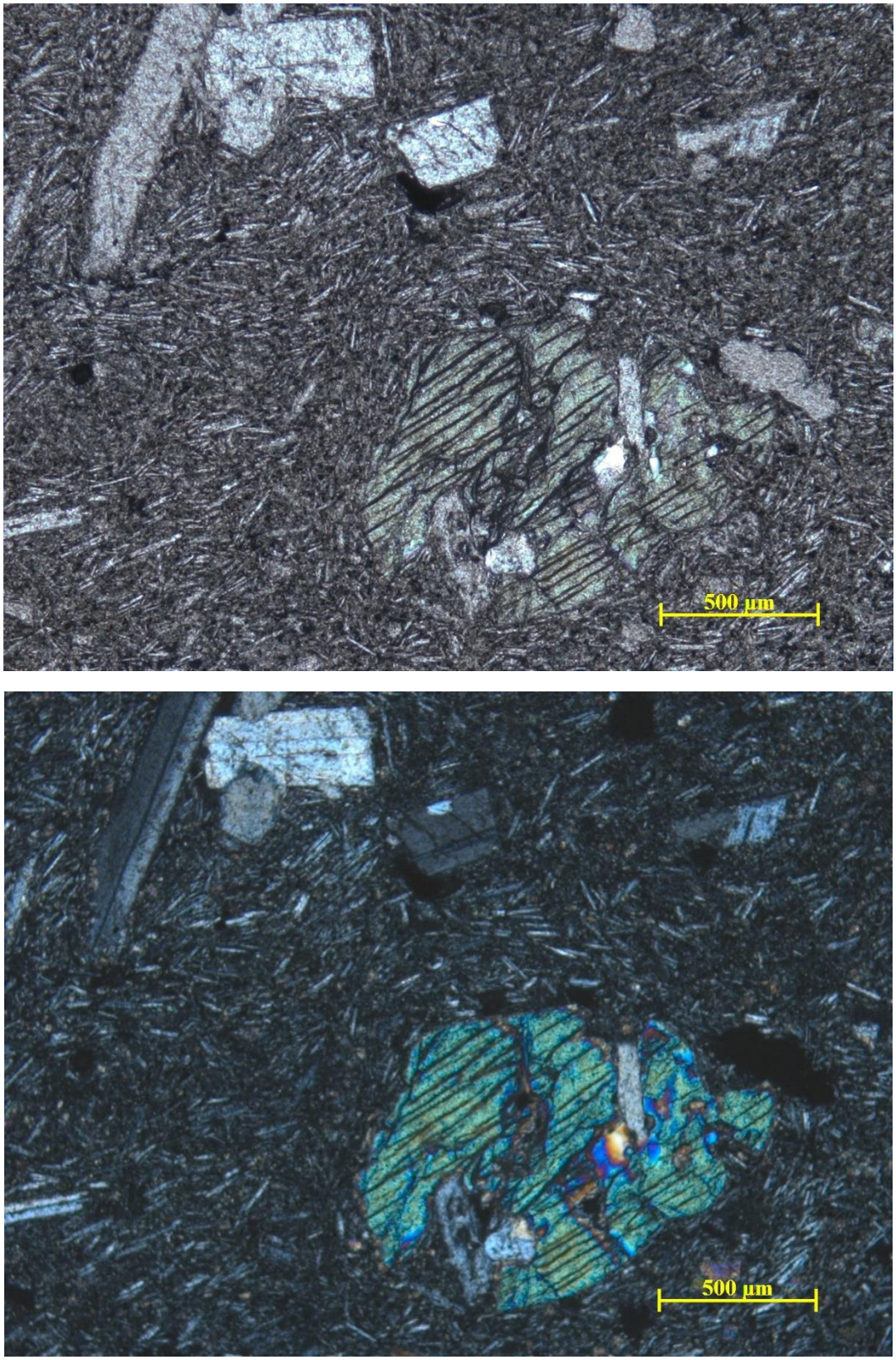

Figure 13. A photomicrograph of thin section view of sample Qbcp-1 showing characteristic clinopyroxene along with plagioclase. (Above: PPL, Below: XPL).

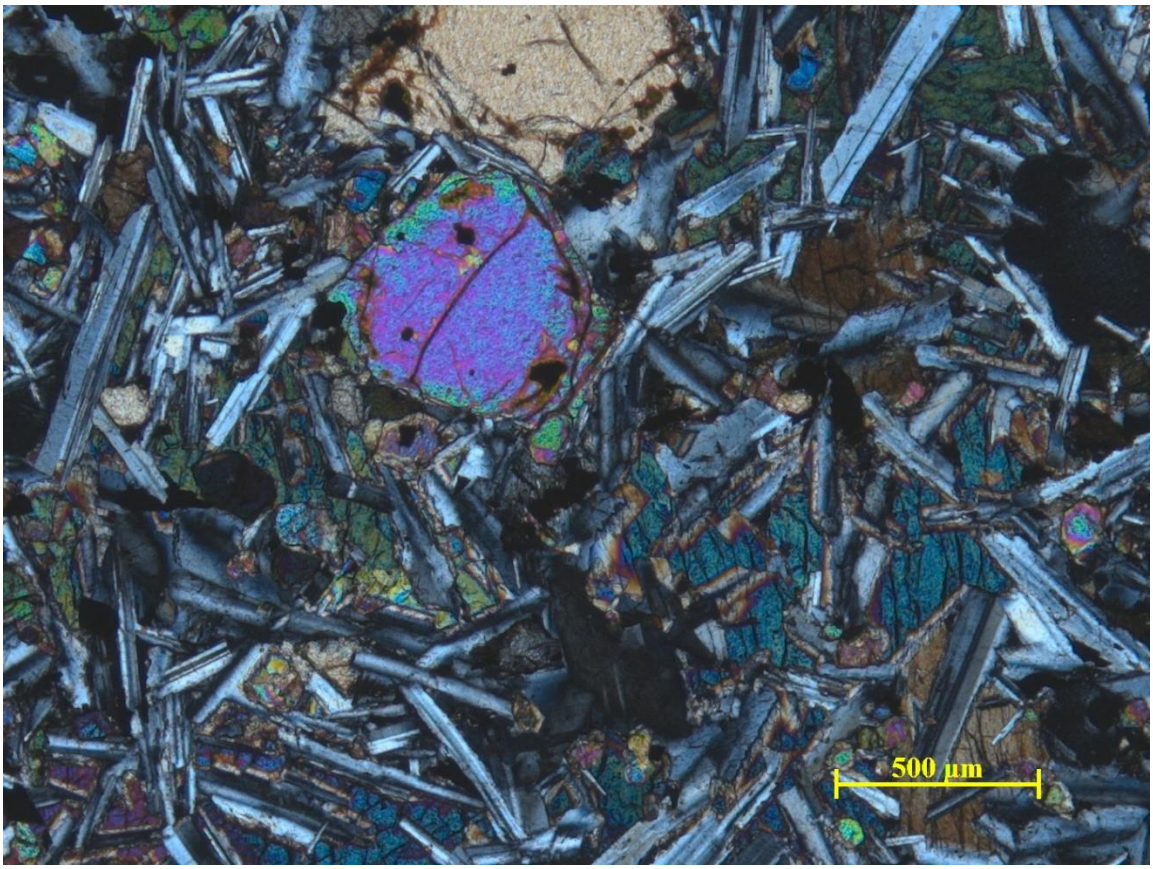

Figure 14. A photomicrograph of thin section view of sample CRGB-3 (350 ka) showing characteristic olivine along pyroxene and plagioclase. (View is in XPL).

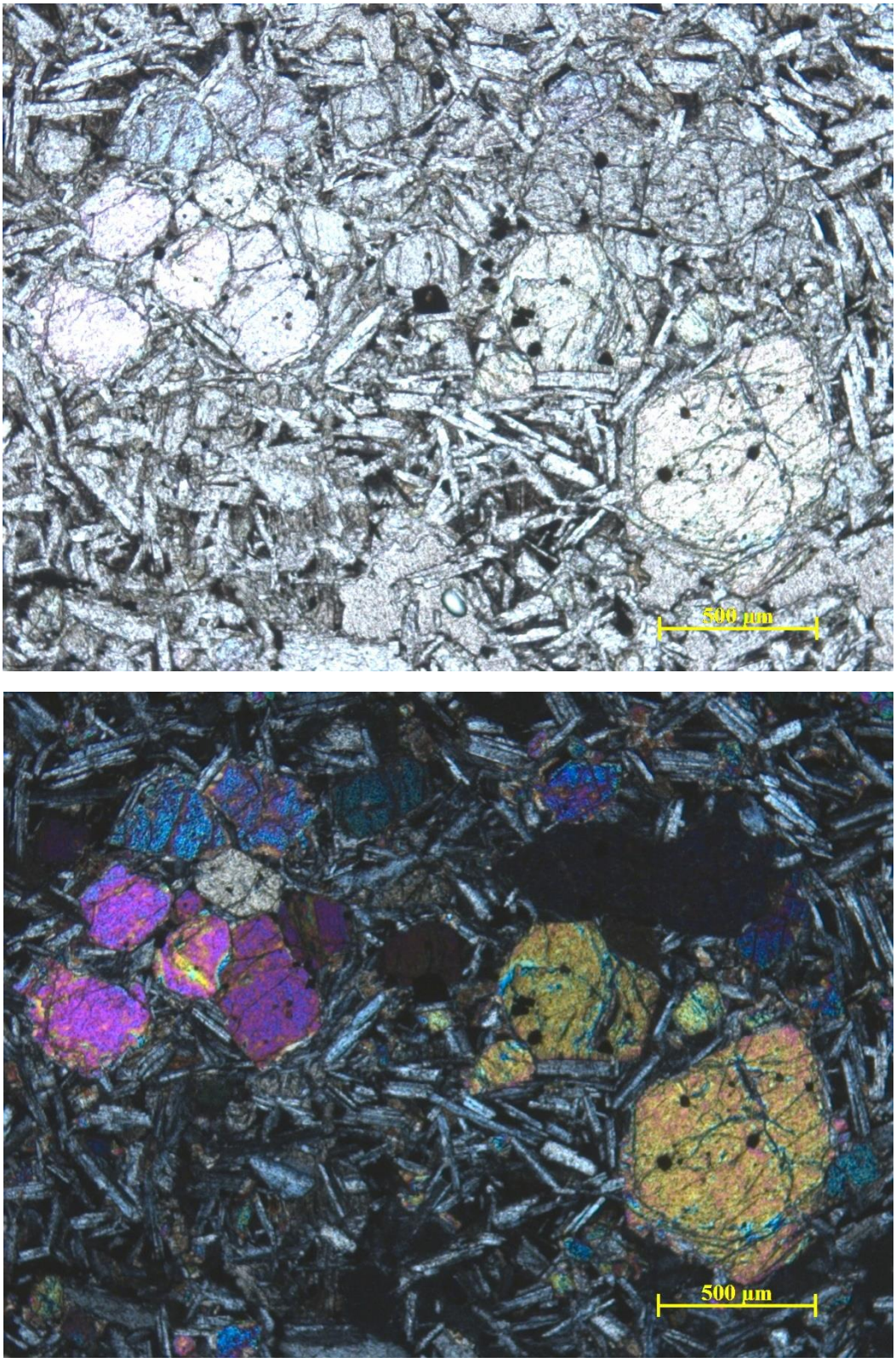

Figure 15. A photomicrograph of thin section view of sample Qba-1 (700 ka) showing characteristic olivine clusters along with plagioclase. (Above: PPL, Below: XPL).

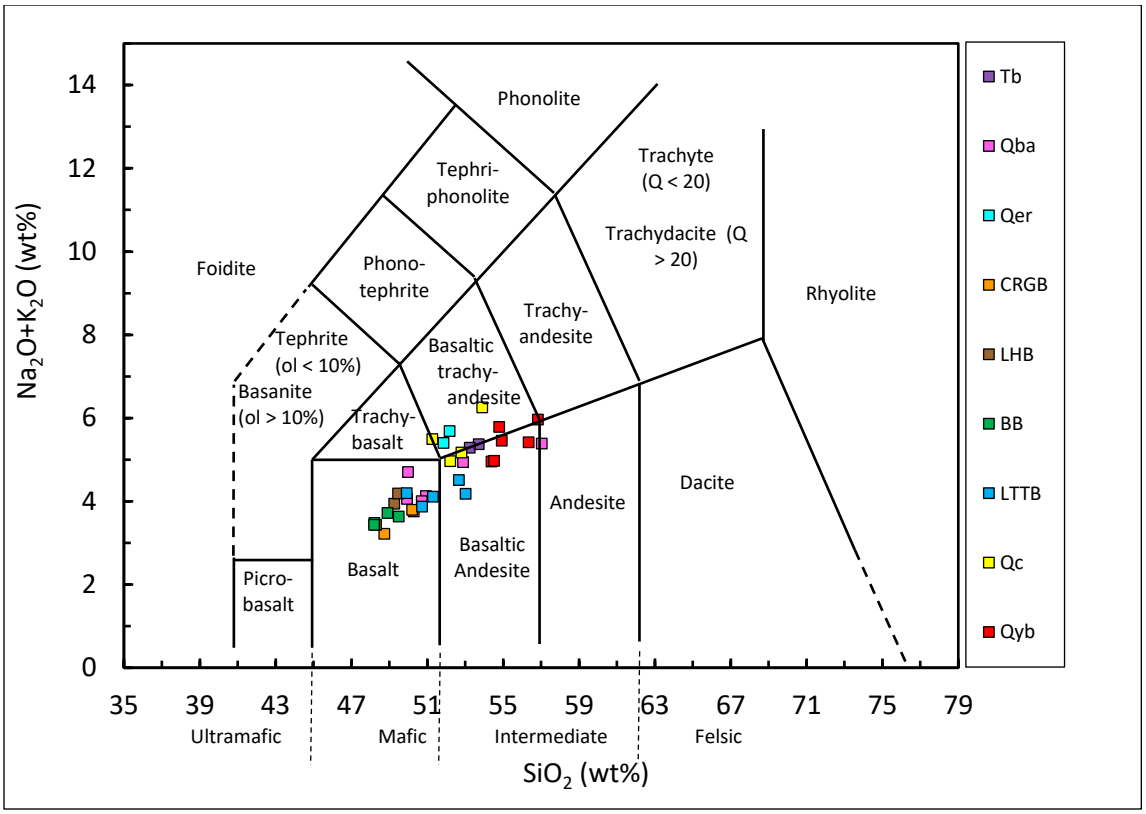

Figure 16. Classification of samples in a Total Alkali Silica (TAS) diagram after (Le Bas et al., 1986; Le Maitre et al., 2002; Winter, 2010). Key describes volcanic units plotted from Newberry Volcano. Major elements values are normalized.

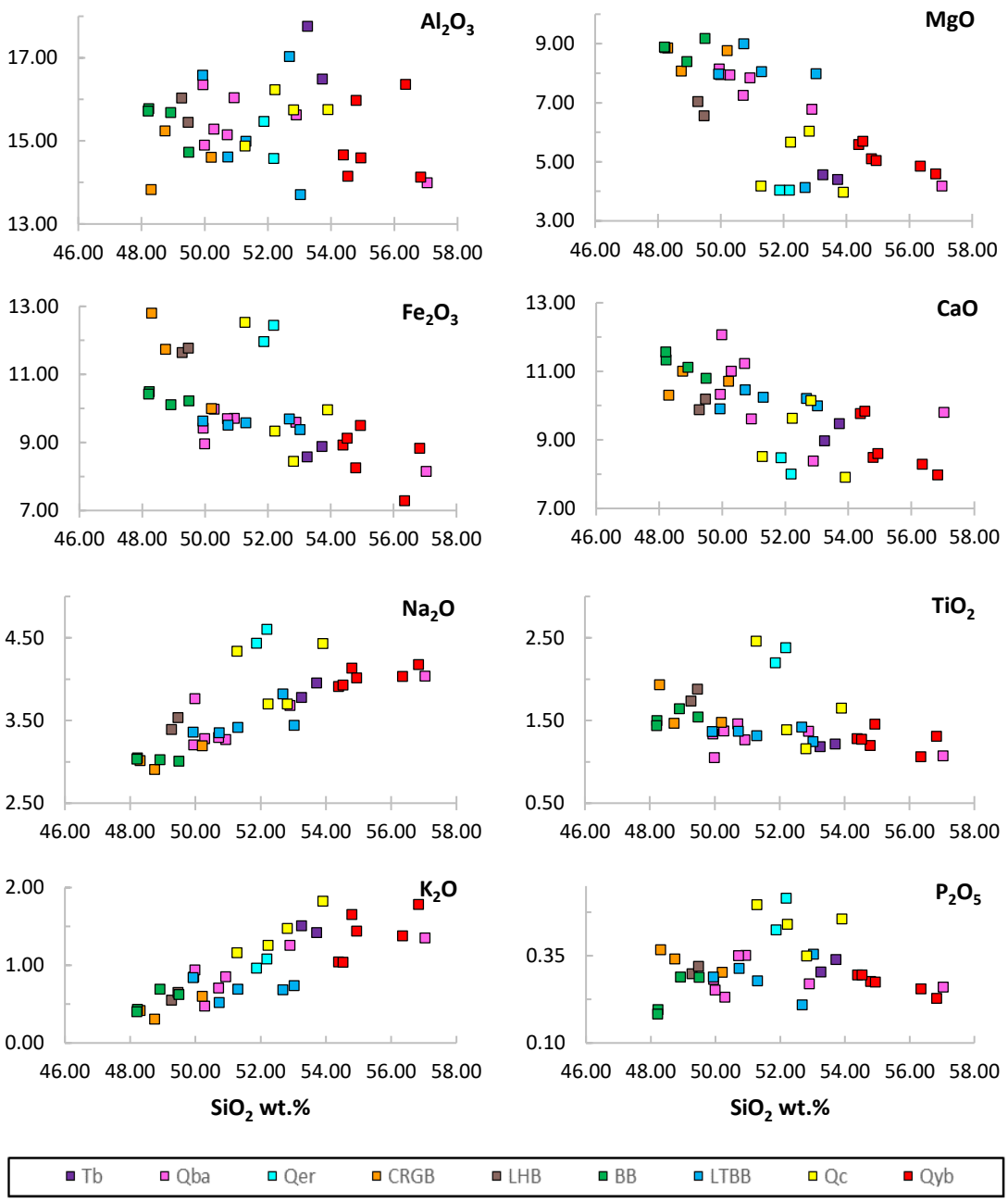

Figure 17. Variation diagrams of major elements (wt %) vs. SiO_2 of samples. Key describes volcanic units plotted from Newberry Volcano. Major element values are normalized.

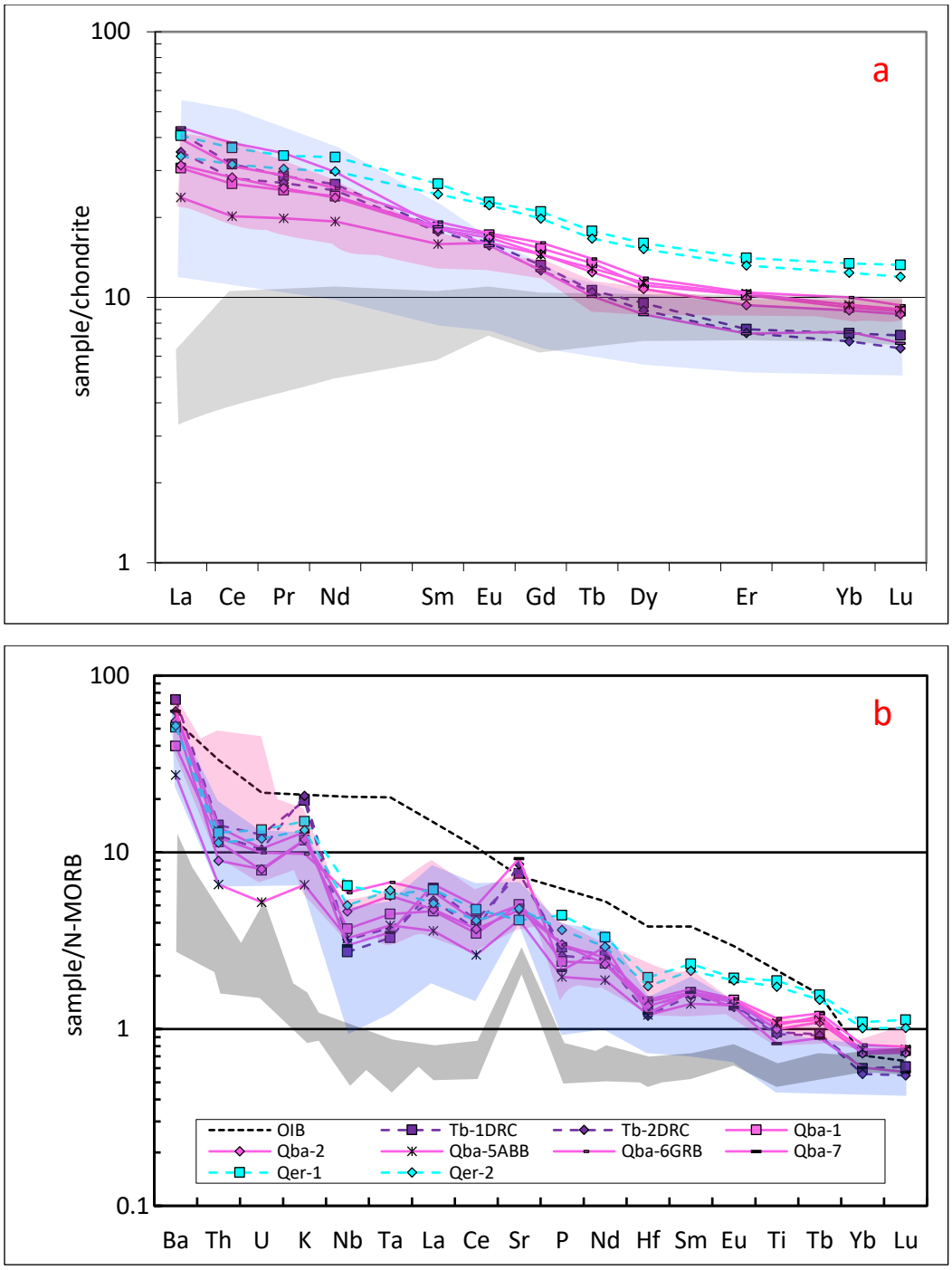

Figure 18. (a) Chondrite normalized REE plots for collected samples that predate Newberry Volcano. Ages span 7.6 Ma to 600 ka. and **(b)** N-MORB normalized multi-element plots for the same samples. Calc-alkaline basalts from Medicine Lake Volcano (red field) (Donnelly-Nolan et al., 2008). High alumina olivine tholeiites from Medicine Lake Volcano (gray field) (Donnelly-Nolan et al., 2008). Cascade arc basalts (blue field) (Bacon et al., 1997). Mafic samples are indicated with solid line; intermediate samples are indicated with dotted line. Chondrite normalization factors based on Leedy Chondrite (Masuda et al., 1973). N-MORB normalization factors based on MORB normalizing factors (Sun and McDonough, 1989).

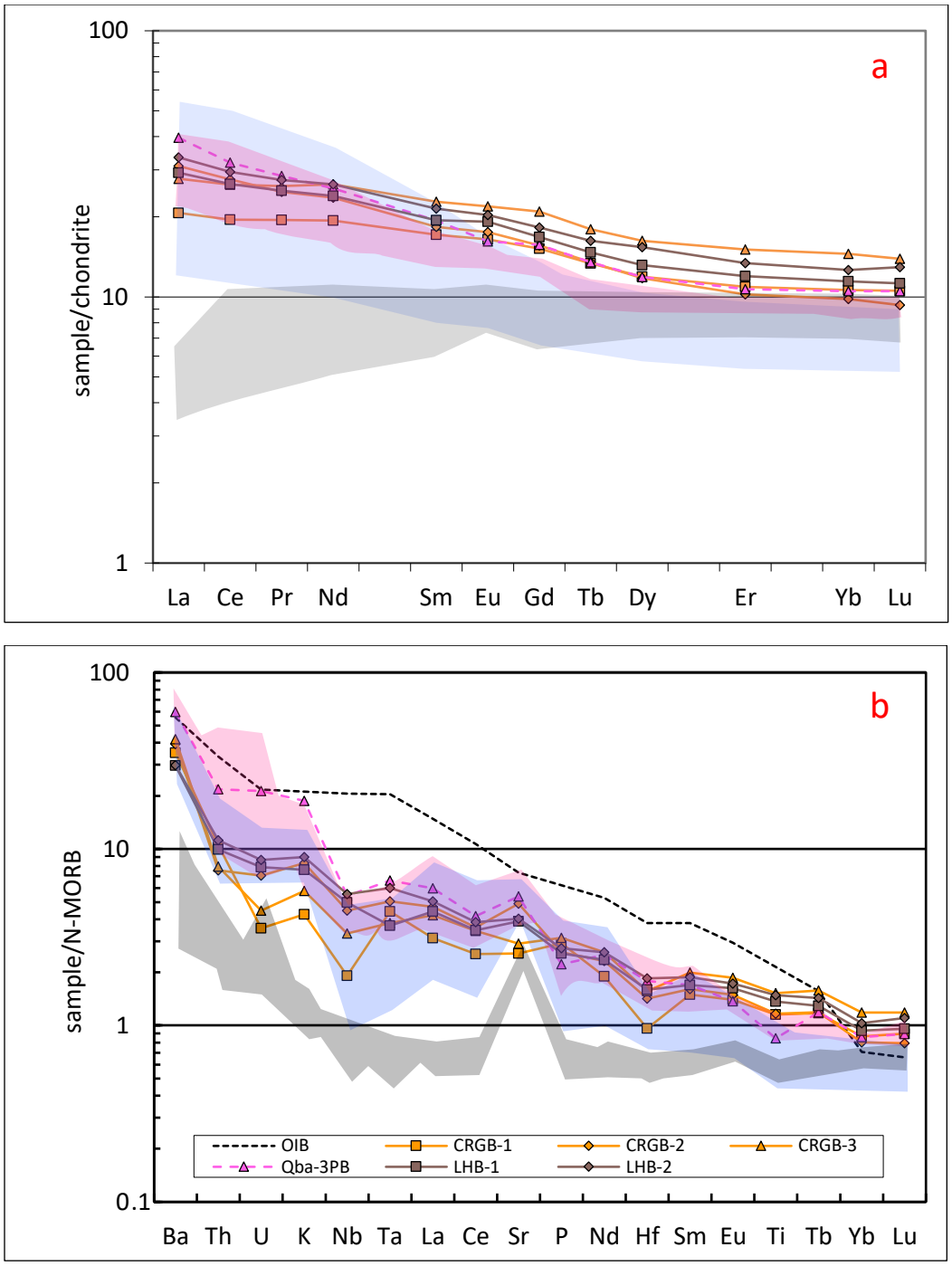

Figure 19. (a) Chondrite normalized REE plots for collected samples from the early stage of Newberry Volcano. Ages span 350 ka to 90 ka. and **(b)** N-MORB normalized multi-element plots for the same samples. Calc-alkaline basalts from Medicine Lake Volcano (red field) (Donnelly-Nolan et al., 2008). High alumina olivine tholeiites from Medicine Lake Volcano (gray field) (Donnelly-Nolan et al., 2008). Cascade arc basalts (blue field) (Bacon et al., 1997). Mafic samples are indicated with solid line; intermediate samples are indicated with dotted line. Chondrite normalization factors based on Leedy Chondrite (Masuda et al., 1973). N-MORB normalization factors based on MORB normalizing factors (Sun and McDonough, 1989).

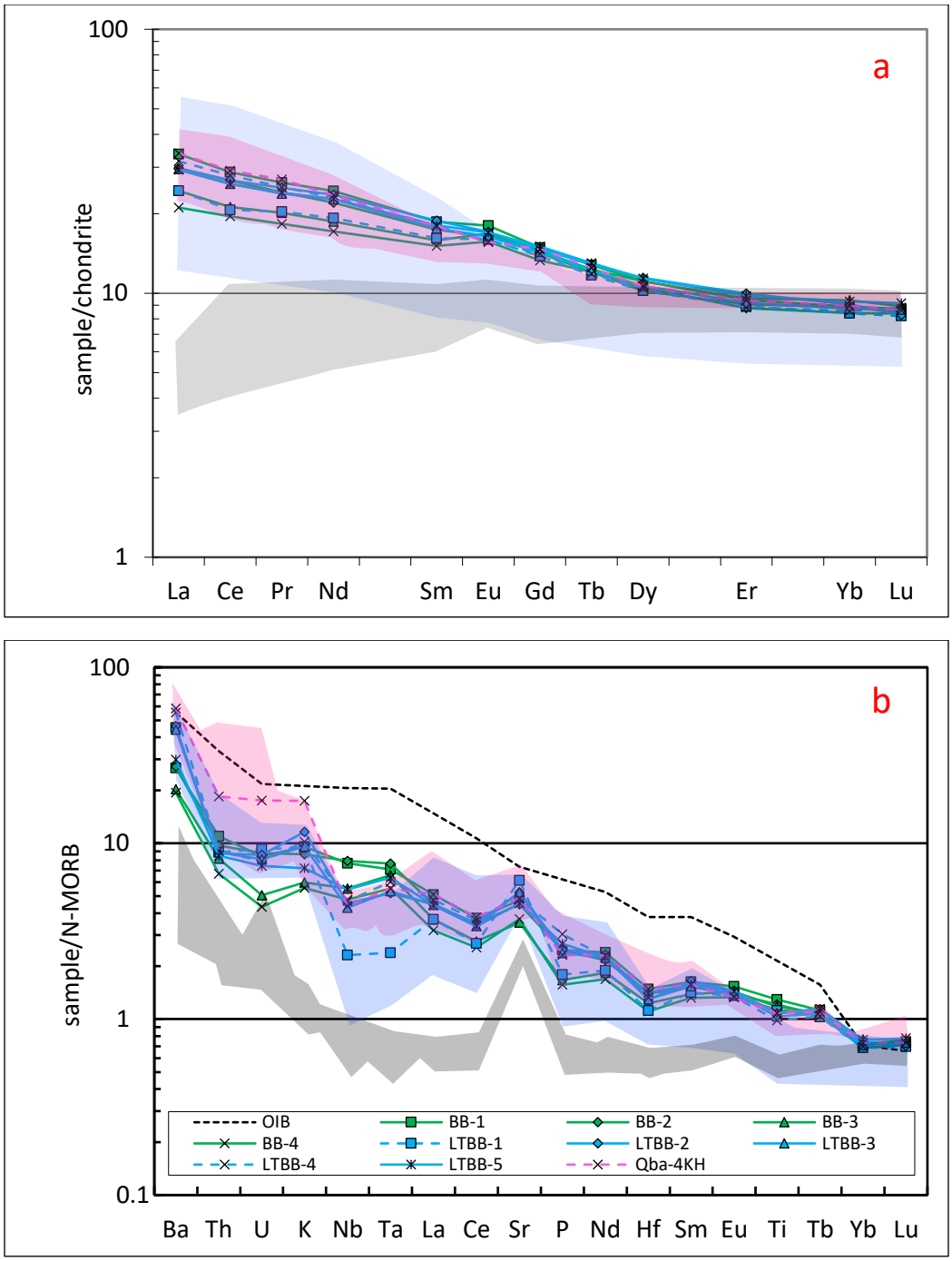

Figure 20. (a) Chondrite normalized REE plots for collected samples from the mid stage of Newberry Volcano. Ages span 78 ka to 39 ka. and **(b)** N-MORB normalized multi-element plots for the same samples. Calc-alkaline basalts from Medicine Lake Volcano (red field) (Donnelly-Nolan et al., 2008). High alumina olivine tholeiites from Medicine Lake Volcano (gray field) (Donnelly-Nolan et al., 2008). Cascade arc basalts (blue field) (Bacon et al., 1997). Mafic samples are indicated with solid line; intermediate samples are indicated with dotted line. Chondrite normalization factors based on Leedy Chondrite (Masuda et al., 1973). N-MORB normalization factors based on MORB normalizing factors (Sun and McDonough, 1989).

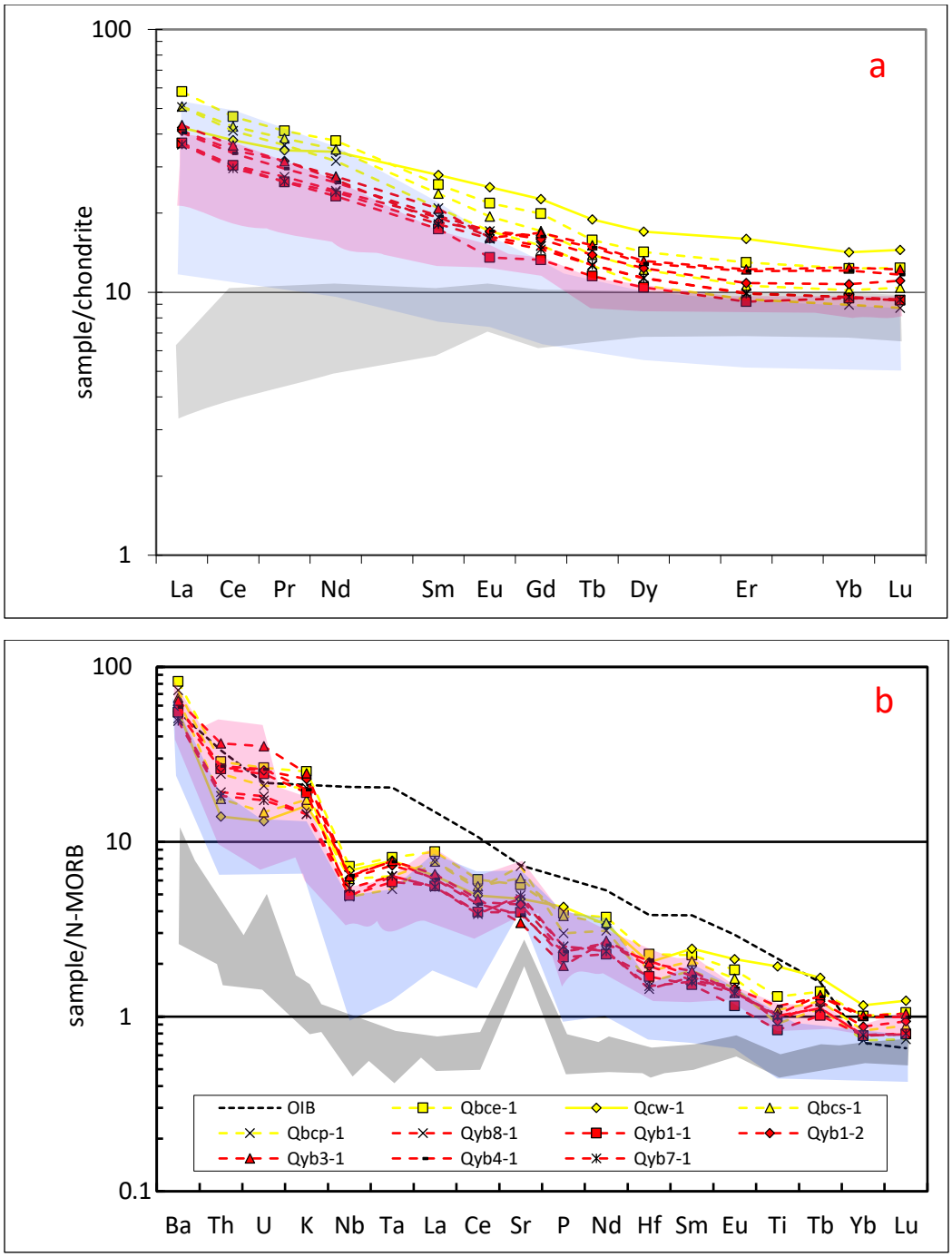

Figure 21. (a) Chondrite normalized REE plots for collected samples from the late stage of Newberry Volcano. Ages span 11.2 ka to 6.8 ka. and **(b)** N-MORB normalized multi-element plots for the same samples. Calc-alkaline basalts from Medicine Lake Volcano (red field) (Donnelly-Nolan et al., 2008). High alumina olivine tholeiites from Medicine Lake Volcano (gray field) (Donnelly-Nolan et al., 2008). Cascade arc basalts (blue field) (Bacon et al., 1997). Mafic samples are indicated with solid line; intermediate samples are indicated with dotted line. Chondrite normalization factors based on Leedy Chondrite (Masuda et al., 1973). N-MORB normalization factors based on MORB normalizing factors (Sun and McDonough, 1989).

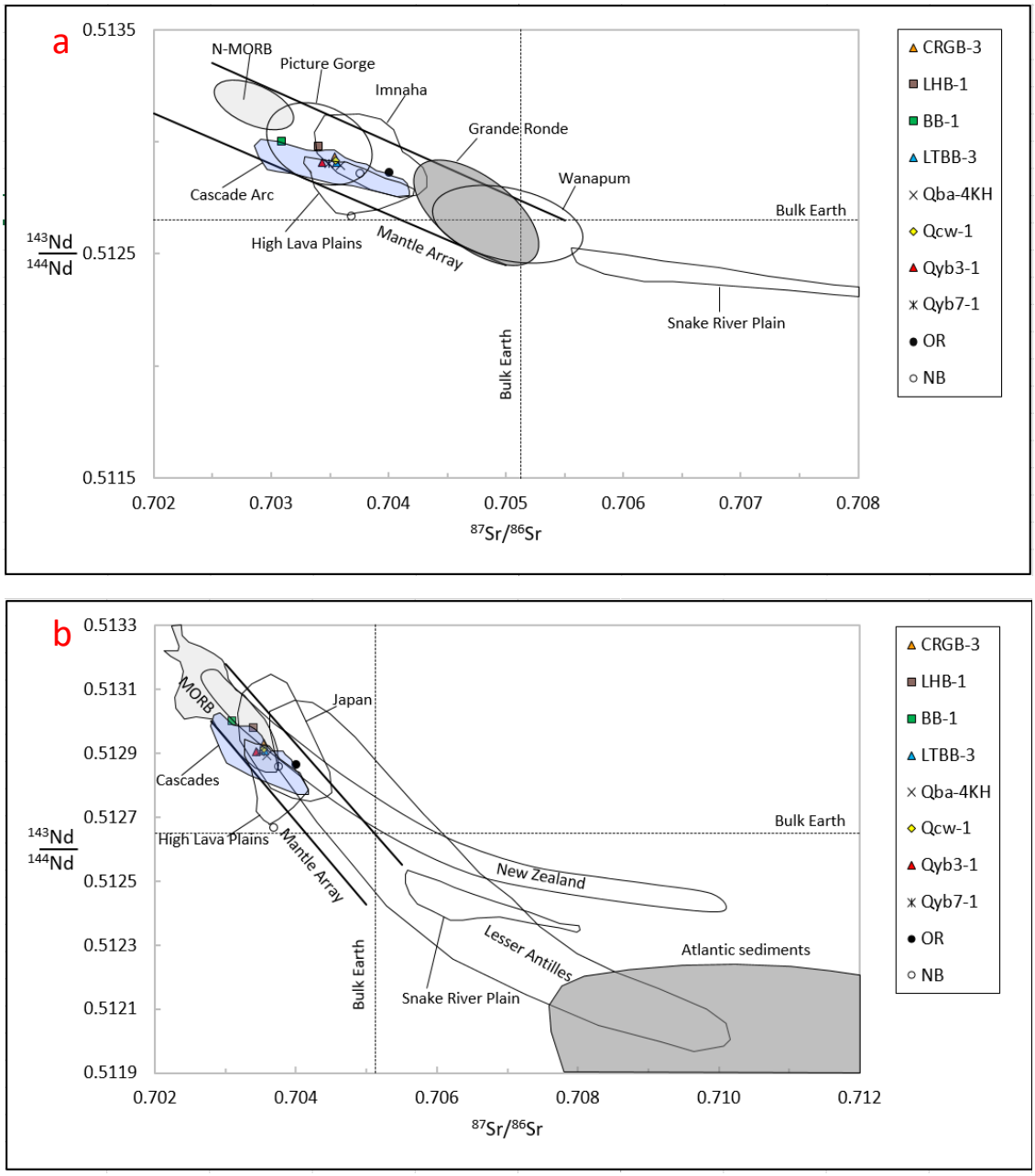

Figure 22. (a) A $^{87}Sr/^{86}Sr$ versus $^{143}Nd/^{144}Nd$ variation diagram showing data from eight Newberry Volcano samples and CRBG data from (McDougall, 1976; Carlson et al., 1981; Carlson, 1984; Hooper, 1988; Brandon et al., 1993; Hooper et al., 1993). Cascade data from (Bacon et al., 1997; Mitchell and Asmerom, 2011). Data from HLP, SRP, two other Newberry samples (NB) and one Owyhee Plain sample (OR) from (Graham et al., 2009). (After Winter, 2010). **(b)** A $^{87}Sr/^{86}Sr$ versus $^{143}Nd/^{144}Nd$ variation diagram showing the same data for Newberry samples, Cascades, HLP, and SRP compared with some island-arc volcanics. (After Gill, 1981; Arculus and Powell, 1986; Wilson, 1989; McCulloch and Bennett, 1994; Winter, 2010). Atlantic sediment data from (White et al., 1985). MORB data from (Schilling et al., 1983). Mantle array data from (Zindler et al., 1982; Menzies, 1983).

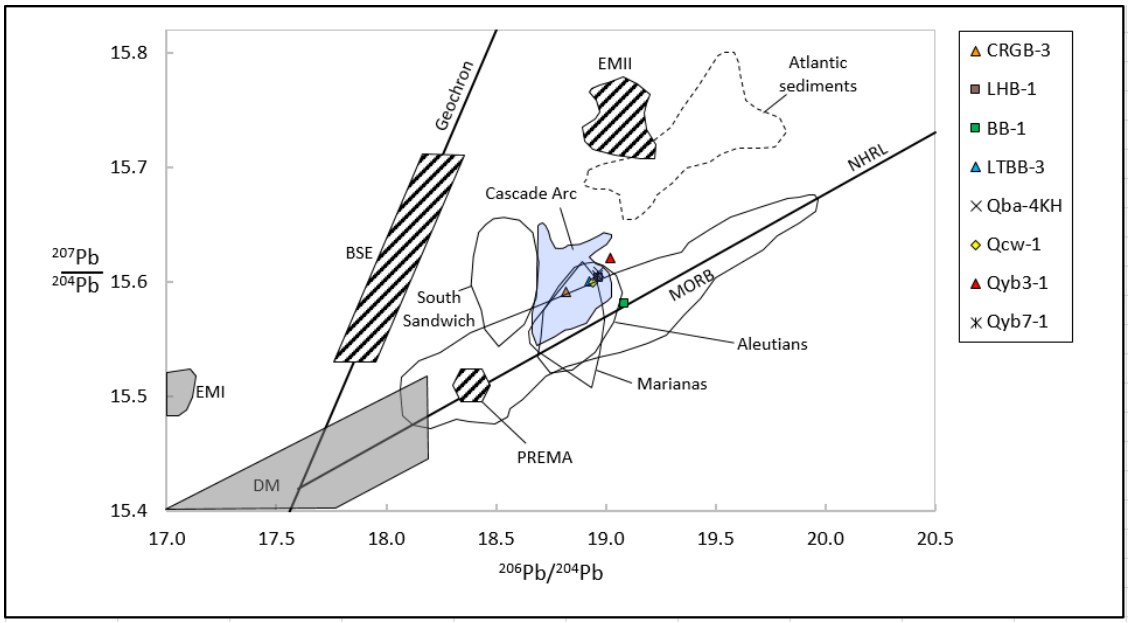

Figure 23. A $^{207}Pb/^{204}Pb$ versus $^{206}Pb/^{204}Pb$ variation diagram showing data from eight Newberry Volcano samples compared with oceanic island-arc volcanics. Cascade data from (Bacon et al., 1997). Isotopic reservoirs and the NHRL (Hart, 1984) are included. Geochron shows the evolution of $^{207}Pb/^{204}Pb$ and $^{206}Pb/^{204}Pb$ in a homogenous reservoir. (After Staudigel et al., 1984; Hamelin et al., 1986; Zindler and Hart, 1986; Wilson, 1989; Winter, 2010). Data for DM, HIMU, EMI, EMII and BSE from (Rollinson, 1993). Sediment data sources in (Wilson, 1989).

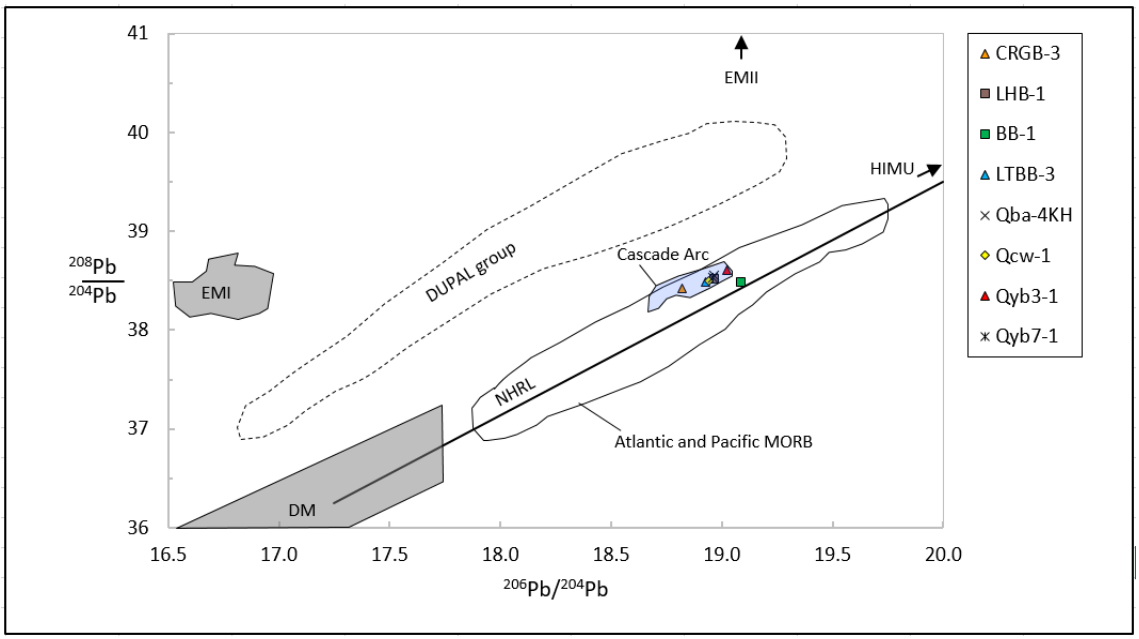

Figure 24. A $^{208}Pb/^{204}Pb$ versus $^{206}Pb/^{204}Pb$ variation diagram showing data from eight Newberry Volcano samples. Cascade data from (Bacon et al., 1997). Included are EMI, EMII, the DUPAL group, the MORB array, the NHRL (Dupré, B. and Allègre, C. J., 1983; Hart, 1984; Vidal et al., 1984; Hamelin, B. and Allègre, C. J., 1985), DM and HIMU. (After Staudigel et al., 1984; Hamelin et al., 1986; Zindler and Hart, 1986; Wilson, 1989; Winter, 2010). Data for DM, HIMU, EMI and EMII from (Rollinson, 1993).

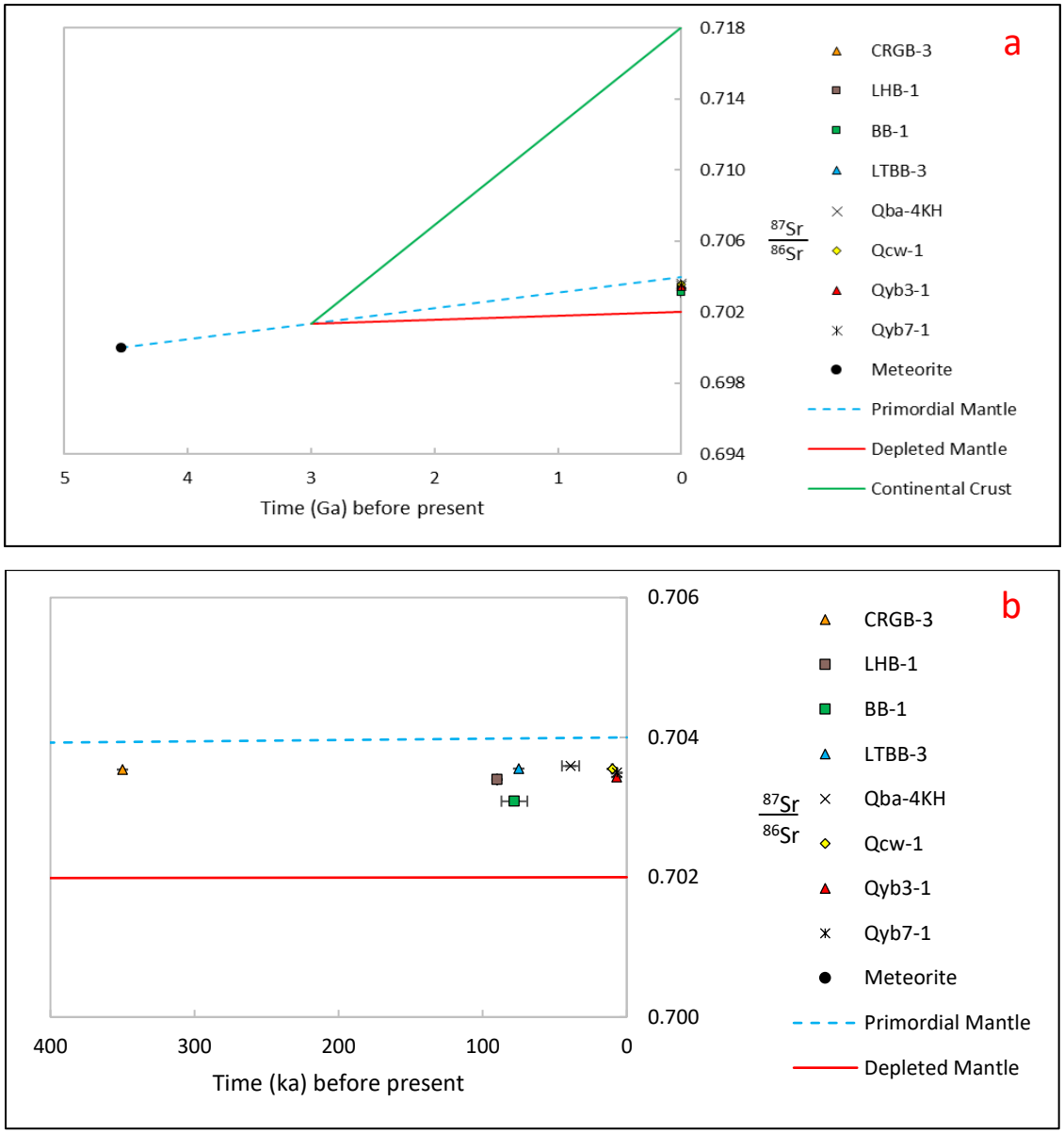

Figure 25. (a) Evolution of Rb and Sr isotopes of the Earth's upper mantle with a large scale melting event of continental crust at 3.0 Ga. (After Wilson, 1989; Winter, 2010). **(b)** 400 ka scale of the same isotopic evolution with Newberry samples plotted.

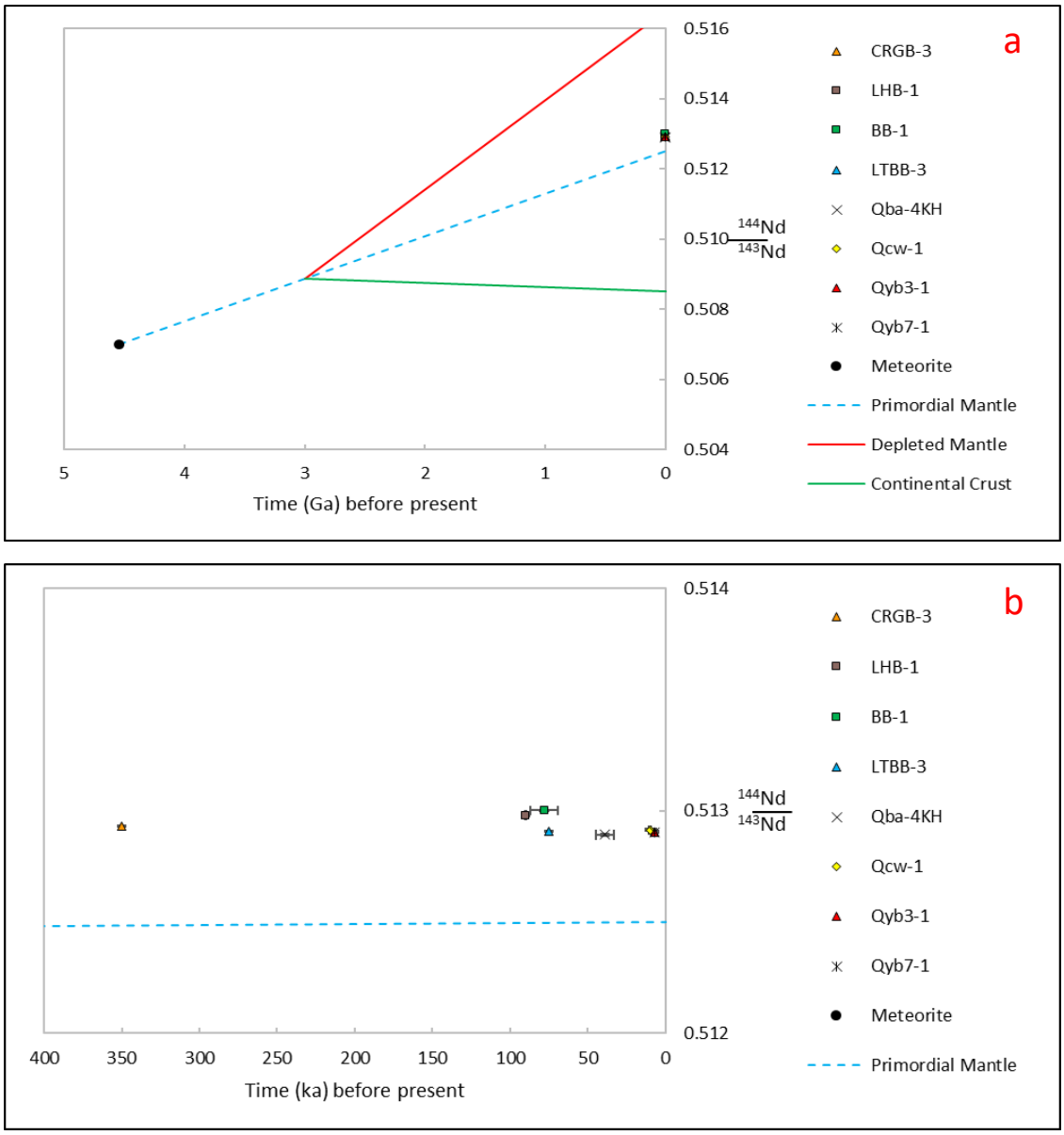

Figure 26. (a) Evolution of Sm and Nd isotopes of the Earth's upper mantle with a large scale melting event of continental crust at 3.0 Ga. (After Wilson, 1989; Winter, 2010). **(b)** 400 ka scale of the same isotopic evolution with Newberry samples plotted.

Table 1. Whole-rock Geochemistry of rocks at Newberry Volcano, OR

Sample	**LTBB-1**	**LHB-1**	**LHB-2**	**Tb-1DRC**	**Tb-2DRC**	**LTBB-2**	**LTBB-3**
Latitude (N)	43°56'48"	43°56'15"	43°56'39"	43°55'05"	43°55'45"	43°57'21"	43°58'47"
Longitude (W)	121°15'46"	121°11'16"	121°11'24"	121°00'28"	121°00'52"	121°02'59"	121°05'38"
Classification	basaltic and	basalt	basalt	basaltic trachyand	basaltic trachyand	basalt	basalt
Age (ka)	75	90	90	7.61±0.08 Ma	7.61±0.08 Ma	75	75
Major Elements							
SiO_2 (wt%)	51.62	49.28	51.30	54.25	50.84	50.88	51.75
TiO_2	1.39	1.73	1.95	1.23	1.13	1.39	1.33
Al_2O_3	16.68	16.03	16.01	16.64	16.95	16.89	15.12
Fe_2O_3	9.50	11.64	12.20	8.96	8.19	9.81	9.66
MnO	0.15	0.18	0.20	0.13	0.12	0.16	0.15
MgO	4.04	7.04	6.80	4.44	4.35	8.12	8.12
CaO	9.99	9.87	10.56	9.56	8.56	10.08	10.33
Na_2O	3.74	3.39	3.66	3.99	3.60	3.42	3.44
K_2O	0.67	0.55	0.67	1.43	1.44	0.85	0.70
P_2O_5	0.21	0.30	0.33	0.34	0.29	0.29	0.28
Total	97.98	100.01	103.69	100.98	95.46	101.89	100.87
Trace Elements							
Sc (ppm)	29.80	32.39	35.18	22.14	20.47	27.12	28.86
V	237.64	239.41	269.06	210.49	194.67	211.77	214.03
Cr	71.68	72.95	76.82	54.51	53.94	186.93	194.23
Co	29.13	44.49	46.53	30.55	29.12	41.87	40.29
Ni	21.09	68.88	71.59	40.04	44.14	144.33	142.48
Ga	19.14	18.55	19.54	19.31	18.39	18.01	17.54
Rb	7.48	8.02	8.18	16.56	14.21	10.75	10.09
Sr	553.70	350.31	362.22	681.82	770.22	473.10	472.52
Y	22.85	29.50	34.03	20.20	18.79	25.06	23.95
Zr	91.03	139.68	163.37	108.14	93.30	112.95	111.53
Nb	5.39	11.57	12.94	6.35	7.46	10.61	10.00
Cs	0.25	0.24	0.22	0.48	0.35	0.35	0.30
Ba	285.87	186.84	187.89	460.57	394.68	291.16	278.67
La	9.24	11.07	12.64	15.63	13.35	11.26	11.17
Ce	20.19	25.93	28.82	30.94	27.37	26.12	25.34
Pr	3.06	3.76	4.13	4.30	4.04	3.77	3.58
Nd	13.79	17.16	18.98	19.05	18.08	16.91	16.29
Sm	3.72	4.46	4.94	4.18	4.07	4.33	4.04
Eu	1.38	1.66	1.76	1.39	1.36	1.48	1.42
Gd	4.30	5.22	5.67	4.11	3.92	4.58	4.47
Tb	0.69	0.87	0.96	0.63	0.62	0.76	0.72
Dy	3.99	5.13	6.00	3.70	3.48	4.46	4.16
Ho	0.84	1.11	1.28	0.75	0.68	0.88	0.86
Er	2.27	3.05	3.41	1.93	1.87	2.54	2.35
Tm	0.34	0.46	0.53	0.30	0.26	0.36	0.34
Yb	2.09	2.85	3.14	1.82	1.70	2.26	2.18
Lu	0.32	0.44	0.50	0.28	0.25	0.32	0.34
Hf	2.29	3.27	3.78	2.76	2.44	2.64	2.66
Ta	0.31	0.48	0.79	0.43	0.50	0.69	0.70
Pb	4.95	6.72	7.47	13.91	9.77	4.89	5.00
Th	1.07	1.19	1.34	1.71	1.49	1.05	1.07
U	0.44	0.37	0.41	0.59	0.49	0.40	0.38

Table 1. (cont.) **Whole-rock Geochemistry of rocks at Newberry Volcano, OR**

Sample	**Qba-1**	**Qba-2**	**LTBB-4**	**Qba-3PB**	**BB-1**	**BB-2**	**Qer-1**
Latitude (N)	43°59'23"	44°01'15"	43°59'00"	44°03'44"	43°03'54"	44°02'16"	43°42'07"
Longitude (W)	121°06'33"	121°08'02"	121°06'01"	121°17'05"	121°18'24"	121°18'29"	121°23'08"
Classification	basalt	basalt	basaltic and	andesite	basalt	basalt	basaltic trachyand
Age (ka)	700±100	700±100	75	188±42	78±9	78±9	600±100
Major Elements							
SiO_2 (wt%)	51.11	51.07	51.93	57.33	49.84	49.92	52.38
TiO_2	1.37	1.27	1.22	1.08	1.67	1.55	2.39
Al_2O_3	16.73	16.08	13.42	14.06	15.97	14.85	14.62
Fe_2O_3	9.64	9.73	9.18	8.18	10.29	10.30	12.48
MnO	0.15	0.14	0.15	0.14	0.16	0.15	0.19
MgO	8.33	7.87	7.81	4.20	8.55	9.25	4.05
CaO	10.56	9.63	9.78	9.84	11.32	10.88	8.02
Na_2O	3.28	3.28	3.37	4.05	3.08	3.03	4.62
K_2O	0.87	0.85	0.72	1.36	0.70	0.63	1.09
P_2O_5	0.29	0.35	0.35	0.26	0.29	0.29	0.52
Total	102.32	100.27	97.92	100.50	101.88	100.86	100.35
Trace Elements							
Sc (ppm)	29.60	29.28	28.90	26.88	30.69	31.16	35.58
V	203.97	198.39	198.75	176.28	207.72	208.37	335.08
Cr	232.18	249.61	250.15	87.24	211.67	276.76	7.49
Co	41.19	38.24	38.06	27.31	45.18	46.33	31.87
Ni	133.20	134.81	132.02	25.67	145.15	181.10	7.94
Ga	17.20	16.90	16.78	18.84	17.38	16.99	19.37
Rb	10.95	11.16	11.03	27.85	10.19	9.74	13.86
Sr	456.29	424.48	434.60	484.37	424.86	405.53	371.31
Y	26.07	24.27	23.64	27.23	24.20	23.25	35.98
Zr	115.92	120.66	122.61	144.63	131.26	124.72	168.88
Nb	8.58	10.79	10.94	12.62	17.94	18.49	15.06
Cs	0.35	0.31	0.33	1.07	0.24	0.19	0.33
Ba	251.20	348.86	348.54	375.96	168.44	172.07	321.24
La	11.59	11.88	11.96	14.97	12.73	11.21	15.34
Ce	26.09	27.58	27.29	31.20	28.06	26.10	35.66
Pr	3.79	3.87	3.79	4.27	3.94	3.62	5.13
Nd	17.19	16.99	16.46	18.29	17.47	15.77	24.16
Sm	4.25	4.15	4.14	4.46	4.29	4.00	6.16
Eu	1.49	1.45	1.37	1.40	1.56	1.42	1.98
Gd	4.76	4.52	4.39	4.88	4.63	4.42	6.53
Tb	0.79	0.73	0.70	0.79	0.75	0.71	1.05
Dy	4.32	4.19	4.08	4.63	4.34	4.09	6.23
Ho	0.92	0.85	0.87	0.99	0.90	0.86	1.31
Er	2.60	2.38	2.25	2.73	2.41	2.24	3.58
Tm	0.37	0.36	0.35	0.42	0.36	0.34	0.53
Yb	2.28	2.22	2.13	2.62	2.22	2.09	3.34
Lu	0.34	0.33	0.34	0.41	0.34	0.32	0.51
Hf	2.92	2.77	2.71	3.66	3.04	2.86	4.01
Ta	0.59	0.75	0.79	0.87	0.94	1.01	0.76
Pb	7.01	6.20	6.36	8.56	3.95	6.83	6.35
Th	1.37	1.07	1.08	2.61	1.32	1.16	1.55
U	0.37	0.38	0.37	1.00	0.40	0.41	0.63

Table 1. (cont.) **Whole-rock Geochemistry of rocks at Newberry Volcano, OR**

Sample	**Qer-2**	**Qbce-1**	**Qcw-1**	**Qbcs-1**	**Qbcp-1**	**Qyb-1-1**	**BB-3**
Latitude (N)	43°42'08"	43°43'20"	43°43'41"	43°44'23"	43°43'09"	44°54'52"	43°54'40"
Longitude (W)	121°21'56"	121°11'42"	121°11'39"	121°11'51"	121°14'34"	121°21'29"	121°23'30"
Classification	basaltic trachyand	basaltic trachyand	trachybasalt	basaltic and	basaltic and	basaltic and	basalt
Age (ka)	600±100	11.16±1.2	10±0.5			7.02±0.14	78±9
Major Elements							
SiO_2 (wt%)	52.10	53.93	51.69	51.46	52.82	51.28	51.46
TiO_2	2.20	1.65	2.48	1.36	1.15	0.96	1.60
Al_2O_3	15.53	15.76	15.00	15.99	15.74	14.89	16.83
Fe_2O_3	12.01	9.96	12.62	9.19	8.44	6.63	11.19
MnO	0.18	0.16	0.20	0.15	0.14	0.13	0.17
MgO	4.05	3.97	4.20	5.58	6.04	4.41	9.46
CaO	8.51	7.91	8.58	9.48	10.14	7.54	12.09
Na_2O	4.45	4.43	4.37	3.64	3.70	3.67	3.25
K_2O	0.97	1.83	1.17	1.24	1.47	1.25	0.46
P_2O_5	0.43	0.46	0.50	0.43	0.35	0.23	0.21
Total	100.44	100.05	100.80	98.54	99.99	91.00	106.70
Trace Elements							
Sc (ppm)	36.77	29.96	37.18	27.82	28.05	23.28	34.19
V	316.29	250.52	333.82	204.60	202.30	154.11	222.90
Cr	17.64	38.93	19.33	99.59	101.66	94.43	223.01
Co	32.11	26.64	33.07	30.97	31.01	25.71	50.58
Ni	12.27	12.67	9.77	57.17	45.69	49.65	147.81
Ga	19.54	19.29	19.82	18.63	18.50	16.69	17.48
Rb	10.96	30.84	14.42	17.95	24.59	32.44	6.60
Sr	433.19	511.20	424.86	556.81	651.00	354.38	319.07
Y	33.78	33.14	38.46	27.89	24.41	24.24	25.19
Zr	145.75	193.79	171.24	165.33	140.54	142.63	103.87
Nb	11.66	16.80	15.91	14.26	11.28	11.49	12.88
Cs	0.32	0.95	0.19	0.61	0.73	1.18	0.09
Ba	327.69	519.49	351.17	419.02	463.27	346.19	127.86
La	12.84	21.93	15.98	19.26	19.16	13.98	9.24
Ce	30.89	45.49	36.97	41.66	40.16	29.66	20.73
Pr	4.57	6.18	5.21	5.78	5.44	3.94	3.03
Nd	21.32	27.02	24.54	25.04	22.59	16.60	13.38
Sm	5.62	5.92	6.43	5.46	4.81	4.01	3.65
Eu	1.92	1.89	2.18	1.68	1.48	1.18	1.46
Gd	6.16	6.20	7.03	5.32	4.69	4.14	4.50
Tb	0.98	0.93	1.12	0.82	0.74	0.68	0.72
Dy	5.93	5.55	6.64	4.76	4.13	4.07	4.33
Ho	1.25	1.17	1.41	0.93	0.85	0.88	0.91
Er	3.36	3.31	4.07	2.71	2.40	2.35	2.43
Tm	0.49	0.48	0.54	0.39	0.35	0.36	0.38
Yb	3.08	3.07	3.54	2.54	2.23	2.37	2.34
Lu	0.46	0.48	0.56	0.40	0.34	0.36	0.35
Hf	3.58	4.67	4.18	3.73	3.25	3.47	2.52
Ta	0.81	1.07	1.03	0.84	0.71	0.78	0.87
Pb	7.34	7.83	6.93	4.23	8.85	6.75	3.22
Th	1.36	3.44	1.67	2.11	2.93	3.14	0.98
U	0.56	1.24	0.62	0.69	0.98	1.15	0.24

Table 1. (cont.) **Whole-rock Geochemistry of rocks at Newberry Volcano, OR**

Sample	**Qyb-1-2**	**BB-4**	**Qba-4KH**	**Qyb-3-1**	**Qba-5ABB**	**Qyb-8-1**	**Qyb-7-1**
Latitude (N)	43°55'45"	43°55'46"	43°52'58"	43°52'51"	43°51'53"	43°48'53"	43°49'07"
Longitude (W)	121°24'32"	121°24'46"	121°18'09"	121°18'18"	121°23'16"	121°17'07"	121°17'19"
Classification	basaltic trachyand	basalt	basaltic and	basaltic trachyand	basalt	basaltic and	basaltic and
Age (ka)	7.02±0.14	78±9	39±6	7		7.21±0.15	6.81±0.13
Major Elements							
SiO_2 (wt%)	54.53	49.89	50.22	56.94	50.53	53.70	54.51
TiO_2	1.19	1.49	1.30	1.31	1.38	1.26	1.27
Al_2O_3	15.90	16.26	14.83	14.15	15.35	14.48	14.14
Fe_2O_3	8.21	10.78	9.11	8.84	10.02	8.81	9.11
MnO	0.14	0.17	0.15	0.16	0.16	0.16	0.16
MgO	5.07	9.19	6.43	4.59	7.98	5.51	5.69
CaO	8.45	11.96	7.95	7.99	11.05	9.64	9.82
Na_2O	4.11	3.13	3.49	4.18	3.29	3.86	3.93
K_2O	1.64	0.42	1.19	1.79	0.47	1.03	1.04
P_2O_5	0.27	0.19	0.26	0.23	0.23	0.29	0.29
Total	99.51	103.48	94.94	100.18	100.47	98.74	99.97
Trace Elements							
Sc (ppm)	26.96	35.26	23.63	29.84	32.42	30.92	31.74
V	177.66	218.36	189.79	206.29	220.92	208.30	216.20
Cr	102.58	229.49	202.31	53.04	194.68	108.94	112.06
Co	28.95	49.23	34.73	30.09	42.73	31.23	32.38
Ni	51.39	141.86	129.06	24.19	110.43	42.89	44.12
Ga	18.09	17.07	17.12	18.35	16.92	18.06	18.21
Rb	32.50	6.16	19.50	44.98	7.61	21.38	21.54
Sr	393.93	333.88	438.15	309.82	372.66	423.77	445.34
Y	28.21	23.99	24.10	31.44	25.79	25.58	25.51
Zr	160.43	94.32	120.99	160.52	102.40	123.97	128.85
Nb	14.44	11.14	10.19	14.75	7.59	11.40	12.64
Cs	1.15	0.08	0.78	1.72	0.18	0.73	0.77
Ba	378.69	122.13	367.89	404.71	172.40	320.19	309.48
La	15.55	7.98	12.81	16.36	8.98	13.79	13.80
Ce	33.98	19.11	28.42	35.33	19.72	29.65	28.94
Pr	4.73	2.75	4.05	4.73	2.97	4.13	3.96
Nd	19.21	12.29	16.82	19.77	13.80	17.45	17.23
Sm	4.26	3.48	4.13	4.78	3.65	4.43	4.18
Eu	1.48	1.36	1.35	1.40	1.39	1.41	1.38
Gd	4.95	4.14	4.57	5.24	4.51	4.66	4.53
Tb	0.82	0.71	0.74	0.89	0.76	0.75	0.75
Dy	4.82	3.98	4.15	5.13	4.43	4.41	4.43
Ho	1.02	0.85	0.88	1.13	0.94	0.92	0.92
Er	2.77	2.32	2.40	3.12	2.63	2.54	2.52
Tm	0.44	0.35	0.37	0.49	0.38	0.39	0.37
Yb	2.67	2.21	2.23	3.09	2.33	2.38	2.39
Lu	0.43	0.33	0.33	0.47	0.35	0.36	0.36
Hf	3.98	2.26	3.03	4.16	2.47	2.94	3.06
Ta	0.97	0.73	0.73	1.03	0.51	0.84	0.84
Pb	8.08	2.81	5.24	7.10	2.82	5.15	6.50
Th	3.19	0.81	2.21	4.39	0.79	2.30	2.19
U	1.20	0.20	0.82	1.65	0.25	0.86	0.81

Table 1. (cont.) **Whole-rock Geochemistry of rocks at Newberry Volcano, OR**

Sample	**Qba-6GRB**	**Qba-7**	**Qyb-4-1**	**CRGB-1**	**CRGB-2**	**CRGB-3**	**LTBB-5**
Latitude (N)	43°50'36"	43°54'33"	43°53'42"	44°15'06"	44°16'21"	44°19'38"	44°21'43"
Longitude (W)	121°21'41"	121°15'30"	121°15'52"	121°03'22"	121°09'48"	121°06'04"	121°17'12"
Classification	basalt	basalt	basaltic and	basalt	basalt	basalt	basalt
Age (ka)				350	350	350	75
Major Elements							
SiO_2 (wt%)	51.55	51.56	53.85	43.95	51.25	49.80	51.44
TiO_2	1.48	1.08	1.42	1.32	1.51	1.99	1.39
Al_2O_3	15.39	15.36	14.30	13.74	14.90	14.25	14.81
Fe_2O_3	9.85	9.24	9.31	10.58	10.19	13.19	9.64
MnO	0.16	0.15	0.15	0.17	0.16	0.19	0.16
MgO	7.37	8.20	4.94	7.28	8.95	9.13	9.11
CaO	11.41	12.44	8.42	9.92	10.92	10.62	10.60
Na_2O	3.35	3.88	3.93	2.62	3.26	3.10	3.40
K_2O	0.72	0.97	1.41	0.28	0.61	0.43	0.53
P_2O_5	0.36	0.26	0.27	0.31	0.31	0.38	0.32
Total	101.64	103.14	98.01	90.14	102.06	103.08	101.39
Trace Elements							
Sc (ppm)	32.79	32.37	29.45	32.61	30.12	40.09	29.11
V	229.07	205.26	211.54	239.62	218.02	303.80	201.01
Cr	176.98	123.86	81.98	218.09	256.24	278.16	245.72
Co	38.12	40.44	30.59	42.73	43.91	53.25	44.69
Ni	67.08	71.57	31.97	128.86	178.75	174.17	183.35
Ga	17.80	17.26	18.12	16.41	17.35	18.18	16.86
Rb	10.13	11.18	31.38	5.54	8.26	6.91	9.43
Sr	452.50	830.13	344.74	230.26	440.07	261.92	409.00
Y	27.19	19.79	30.82	27.92	27.20	38.25	25.37
Zr	127.23	101.23	169.02	82.85	121.67	124.46	129.40
Nb	13.75	6.93	14.97	4.45	10.42	7.74	12.74
Cs	0.25	0.27	1.10	0.15	0.23	0.18	0.25
Ba	382.72	396.34	371.59	221.29	247.68	263.75	188.49
La	14.91	16.46	15.32	7.82	11.73	10.51	11.09
Ce	30.44	37.22	33.04	19.04	26.99	25.80	25.27
Pr	4.31	5.24	4.44	2.92	3.73	3.91	3.61
Nd	18.46	21.25	18.74	13.85	16.89	18.97	16.29
Sm	4.43	4.24	4.49	3.93	4.22	5.24	4.16
Eu	1.51	1.36	1.48	1.43	1.52	1.90	1.47
Gd	4.99	3.93	5.09	4.73	4.86	6.51	4.67
Tb	0.82	0.59	0.87	0.79	0.80	1.06	0.77
Dy	4.61	3.36	5.03	4.65	4.58	6.33	4.44
Ho	0.94	0.73	1.09	1.02	0.98	1.33	0.93
Er	2.66	1.86	3.07	2.78	2.61	3.85	2.49
Tm	0.39	0.29	0.45	0.42	0.37	0.57	0.37
Yb	2.49	1.84	3.01	2.64	2.45	3.61	2.32
Lu	0.36	0.26	0.45	0.41	0.36	0.54	0.36
Hf	3.00	2.52	4.26	1.97	2.91	3.21	2.89
Ta	0.89	0.46	1.02	0.58	0.67	0.50	0.84
Pb	3.82	9.18	10.02	11.89	4.08	3.04	3.22
Th	1.45	1.66	3.26	1.26	0.91	0.95	1.02
U	0.47	0.49	1.22	0.17	0.33	0.21	0.35

Table 2. Summary of ages and locations of samples from Newberry Volcano

Sample	Feature	Road location	Radiometric date	Reference
LTBB-1	Basalt of Lava Top Butte	NF-1810	75 ka	Champion et al., 2004
LHB-1	Basalt of Lunabess Hill	NF-1819	90 ka	Jensen et al., 2009
LHB-2	Basalt of Lunabess Hill	NF-1819	90 ka	Jensen et al., 2009
Tb-1DRC	Basalt of Dry River Canyon	U. S. 20	7.61±0.08 Ma	Fiebelkorn et al., 1983
Tb-2DRC	Basalt of Dry River Canyon	U. S. 20	7.61±0.08 Ma	Fiebelkorn et al., 1983
LTBB-2	Basalt of Lava Top Butte	U. S. 20	75 ka	Champion et al., 2004
LTBB-3	Basalt of Lava Top Butte	U. S. 20	75 ka	Champion et al., 2004
Qba-1	Quaternary basalt	U. S. 20	700±100 ka	Jensen et al., 2009
Qba-2	Quaternary basalt	U. S. 20	700±100 ka	Jensen et al., 2009
LTBB-4	Basalt of Lava Top Butte	U. S. 20	75 ka	Champion et al., 2004
Qba-3PB	Pilot Butte Flow	Pilot Butte trail	188±42 ka	Donnelly-Nolan et al., 2004
BB-1	Basalt of Bend	U. S. 97	78±9 ka	Champion et al., 2004
BB-2	Basalt of Bend	U. S. 97	78±9 ka	Champion et al., 2004
Qer-1	McKay Butte Flow	NF-21	600±100 ka	McKee et al., 1976
Qer-2	McKay Butte Flow	NF-21	600±100 ka	McKee et al., 1976
Qbce-1	East Lake Resort Flow	NF-21	11.16±1.2 ka	Linneman 1990
Qcw-1	Basalt of Crater Wall	NF-300	10±0.5 ka	Linneman 1990
Qbcs-1	Basalt of Sheep's Rump	Newberry Crater trail	-	-
Qbcp-1	Paulina Lake Flow	Paulina Lakeshore Loop trail	-	-
Qyb-1-1	Lava Butte Flow	Trail of the Molten Lands	7.02±0.14 ka	Chitwood et al., 1977 Robinson et al., 1981
BB-3	Basalt of Bend	NF-9702	78±9 ka	Champion et al., 2004
Qyb-1-2	Lava Butte Flow	Black Rock trail	7.02±0.14 ka	Chitwood et al., 1977 Robinson et al., 1981
BB-4	Basalt of Bend	NF-9702	78±9 ka	Champion et al., 2004
Qba-4KH	Klawhop Butte Flow	NF-350	39±6 ka	Donnelly-Nolan et al., 2000
Qyb-3-1	Mokst Butte Flow	NF-380	7 ka	McKay et al., 2009
Qba-5ABB	Abbott Butte Flow	NF-9720	-	-
Qyb-8-1	Lava Cast Forest Flow	Lava Cast Forest trail	7.21±0.15 ka	Peterson et al., 1969
Qyb-7-1	Forest Road Flow	NF-9720	6.81±0.13 ka	Peterson et al., 1969
Qba-6GRB	Grade Butte Flow	NF-9720	-	-
Qba-7	Quaternary basalt	NF-1810	-	-
Qyb-4-1	South Kelsey Flow	NF-800	-	-
CRGB-1	Basalt of Crooked River Gorge	OR-126	350 ka	Jensen et al., 2009
CRGB-2	Basalt of Crooked River Gorge	OR-126	350 ka	Jensen et al., 2009
CRGB-3	Basalt of Crooked River Gorge	OR-370	350 ka	Jensen et al., 2009
LTBB-5	Basalt of Lava Top Butte	Lower Bridge Way	75 ka	Champion et al., 2004

Table 3. Summary of ICP-MS Reproducibility Experiment

	BB-1			BCR-2					
	Average*	STDEV	%RSD	BCR-2**	+/-	Average*	STDEV	%RSD	Accuracy
SiO_2 (wt%)	49.84	1.64	3.28	54.10	0.80	52.95	2.22	4.20	-2.13
TiO_2	1.67	0.09	5.59	2.26	0.05	2.39	0.14	5.83	5.61
Al_2O_3	15.97	0.54	3.35	13.50	0.20	13.70	0.43	3.17	1.49
Fe_2O_3	10.29	0.53	5.14	13.80	0.20	13.93	0.76	5.48	0.97
MnO	0.16	0.01	5.58	0.20	0.01	0.19	0.02	9.87	-3.14
MgO	8.55	0.56	6.50	3.59	0.05	3.84	0.29	7.65	6.92
CaO	11.32	0.63	5.53	7.12	0.11	7.67	0.43	5.60	7.70
Na_2O	3.08	0.15	4.87	3.16	0.11	3.18	0.21	6.51	0.53
K_2O	0.70	0.05	6.90	1.79	0.05	1.92	0.15	8.00	7.21
P_2O_5	0.29	0.02	7.15	0.35	0.02	0.36	0.03	7.36	4.28
Total	101.88	3.87	3.80	99.87	-	100.13	4.32	4.32	0.26
Sc (ppm)	30.69	1.70	5.53	33.00	2.00	34.32	1.98	5.76	4.00
V	207.72	10.22	4.92	416.00	14.00	412.13	22.71	5.51	-0.93
Cr	211.67	11.09	5.24	18.00	2.00	27.27	1.17	4.28	51.49
Co	45.18	2.43	5.38	37.00	3.00	39.14	2.22	5.67	5.77
Ni	145.15	7.22	4.97	12.00	-	14.55	0.68	4.69	21.26
Ga	17.38	0.58	3.33	23.00	2.00	20.76	0.89	4.28	-9.72
Rb	10.19	0.72	7.08	48.00	2.00	48.94	3.32	6.78	1.97
Sr	424.86	23.28	5.48	346.00	14.00	349.47	19.59	5.61	1.00
Y	24.20	1.30	5.38	37.00	2.00	35.64	1.98	5.56	-3.67
Zr	131.26	8.03	6.12	201.00	16.00	182.14	11.66	6.40	-9.38
Nb	17.94	2.47	13.75	13.07	-	13.17	1.83	13.87	0.74
Cs	0.24	0.06	23.12	1.10	0.10	1.22	0.11	9.15	10.58
Ba	168.44	9.48	5.63	683.00	28.00	710.63	49.63	6.98	4.04
La	12.73	0.77	6.03	25.00	1.00	26.10	1.80	6.88	4.39
Ce	28.06	1.55	5.52	53.00	2.00	52.86	2.77	5.25	-0.26
Pr	3.94	0.20	5.10	6.80	0.30	6.98	0.45	6.49	2.59
Nd	17.47	0.93	5.32	28.00	2.00	29.29	1.94	6.61	4.61
Sm	4.29	0.22	5.19	6.70	0.30	6.68	0.38	5.64	-0.35
Eu	1.56	0.10	6.17	2.00	0.10	1.91	0.16	8.55	-4.52
Gd	4.63	0.25	5.32	6.80	0.30	6.81	0.42	6.18	0.09
Tb	0.75	0.04	5.42	1.07	0.04	1.08	0.06	5.39	0.98
Dy	4.34	0.21	4.81	6.35	-	6.28	0.33	5.22	-1.12
Ho	0.90	0.04	4.82	1.33	0.06	1.32	0.07	5.29	-0.74
Er	2.41	0.13	5.36	3.63	-	3.56	0.20	5.48	-1.86
Tm	0.36	0.02	6.75	0.54	-	0.54	0.04	7.18	0.80
Yb	2.22	0.11	4.96	3.38	0.20	3.35	0.18	5.42	-0.86
Lu	0.34	0.02	5.29	0.51	0.02	0.51	0.03	6.05	0.47
Hf	3.04	0.19	6.26	4.80	0.20	4.78	0.33	6.95	-0.39
Ta	0.94	0.30	32.37	0.80	-	0.85	0.08	9.06	6.78
Pb	3.95	1.27	32.08	11.00	2.00	15.02	2.28	15.16	36.56
Th	1.32	0.16	11.87	6.20	0.70	5.97	0.42	7.00	-3.65
U	0.40	0.02	5.76	1.69	0.19	1.73	0.11	6.41	2.56

*. n=8, **. values reported by USGS (Wilson, 1997)

Table 4. Isotopic analyses of key samples at Newberry Volcano

Sample	LHB-1	LTBB-3	BB-1	Qcw-1	Qba-4KH	Qyb-3-1	Qyb-7-1	CRGB-3
Classifi-cation	basalt	basalt	basalt	trachybasalt	basaltic and	basaltic trachyand	basaltic and	basalt
Age (ka)	90	75	78±9	10±0.5	39±6	7	6.81±0.13	350
Isotopes								
$^{87}Sr/^{86}Sr$	0.703398	0.703554	0.703088	0.703549	0.703592	0.703433	0.703494	0.703540
$^{143}Nd/^{144}$ Nd*	0.512980	0.512907	0.513001	0.512914	0.512892	0.512905	0.512903	0.512931
$^{206}Pb/^{204}$ Pb**	18.967	18.927	19.083	18.939	18.966	19.022	18.962	18.820
$^{207}Pb/^{204}$ Pb**	15.583	15.581	15.561	15.580	15.589	15.601	15.585	15.571
$^{208}Pb/^{204}$ Pb**	38.518	38.491	38.491	38.503	38.556	38.609	38.531	38.426

*. Standard normalized, 100 ratios collected

**. Tl added for mass bias, 100 ratios collected

Table 5. Analytical precision of isotopic analyses

Sample	LHB-1	LTBB-3	BB-1	Qcw-1	Qba-4KH	Qyb-3-1	Qyb-7-1	CRGB-3
Uncertainties								
$^{87}Sr/^{86}Sr$ Error (±2σ)	0.000004	0.000003	0.000003	0.000005	0.000004	0.000004	0.000004	0.000004
$^{206}Pb/^{204}Pb$ Std Err (±1σ)	0.001315	0.000951	0.002087	0.000642	0.000638	0.000535	0.000595	0.001318
$^{207}Pb/^{204}Pb$ Std Err (±1σ)	0.001099	0.000831	0.001604	0.000525	0.000539	0.000457	0.000521	0.001122
$^{208}Pb/^{204}Pb$ Std Err (±1σ)	0.002741	0.002081	0.004002	0.001352	0.001309	0.001183	0.001338	0.002786
$^{143}Nd/^{144}Nd$ Std Err (±1σ)	0.000003	0.000004	0.000003	0.000003	0.000004	0.000003	0.000003	0.000003

Table 6. Isotopic standard analyses and analytical precision

Sample	NBS987 ($^{87}Sr/^{86}Sr$)	Shinetsu JNDi-1 ($^{143}Nd/^{144}Nd$)	NBS981 ($^{206}Pb/^{204}Pb$)	NBS981 ($^{207}Pb/^{204}Pb$)	NBS981 ($^{208}Pb/^{204}Pb$)
Ratio Value (Observed)	0.710244[a]	0.512081[b]	16.9292[c]	15.4828[c]	36.6699[c]
Ratio Value (Accepted)	0.710340*	0.512115*	16.9406*	15.4970*	36.7184*
Std Err in abs (±1σ)	0.000004**	0.000003	0.0009	0.0013	0.0033

a. n=2, b. n=3, c. n=4

*. values reported by (Moore et al, 1982; May et al., 2000; Tanaka et al., 2000; Yuan et al., 2016)

**. reported as ±2σ